



GUSTAVO DE ALMEIDA ANDOLPHO

**INVESTIGATING PNICTOGEN BONDS: IMPACT ON
MOLECULAR INTERACTIONS AND NMR PARAMETERS**

LAVRAS – MG

2026

GUSTAVO DE MANEIDA ANDOLPHO

**INVESTIGATING PNICTOGEN BONDS: IMPACT ON MOLECULAR
INTERACTIONS AND NMR PARAMETERS**

A thesis submitted to Federal University of Lavras, as partial fulfillment of the requirements of Graduate Program in Agrochemistry, Chemistry/Biochemistry field of study, for the degree of Doctor of Philosophy.

Advisor
Prof. Dr. Teodorico de Castro Ramalho

**LAVRAS – MG
2026**

**Ficha Catalográfica elaborada pelo Sistema de Geração
de Ficha Catalográfica da Biblioteca Universitária da UFLA, com
dados informados pelo(a) próprio(a) autor(a).**

Andolpho, Gustavo A..

Investigating pnictogen bonds : Impact on molecular interactions and NMR
parameters / Gustavo A. Andolpho. - 2026.

136 p. : il.

Orientador: Teodorico C. Ramalho

Tese (Doutorado) - Universidade Federal de Lavras, 2026.

Bibliografia.

1. Pnictogen bonds. 2. Organophosphorus. 3. Quantum computing. 4. NMR
parameters. 5. Acetylcholinesterase. I. Ramalho, Teodorico C.. II. Universidade
Federal de Lavras. III. Título.

GUSTAVO DE ALMEIDA ANDOLPHO

**INVESTIGATING PNICTOGEN BONDS: IMPACT ON MOLECULAR
INTERACTIONS AND NMR PARAMETERS**

**INVESTIGANDO AS INTERAÇÕES DE PNICTOGÊNIO: IMPACTO EM
INTERAÇÕES MOLECULARES E PARÂMETROS RMN**

A thesis submitted to Federal University of Lavras, as partial fulfillment of the requirements of Graduate Program in Agrochemistry, Chemistry/Biochemistry field of study, for the degree of Doctor of Philosophy.

Approved on March 16, 2026.

DSc. Adélia J. A. Aquino	Texas Tech University
DSc. Atualpa Albert Carmo Braga	USP
DSc. Mateus Puggina de Freitas	UFLA
DSc. Osvaldo Andrade Santos Filho	IPPN/UFRJ

Advisor
Prof. Dr. Teodorico de Castro Ramalho

**LAVRAS – MG
2026**

*A todos que me apoiaram e acreditaram em mim,
em especial ao meu avô Edival (in memoriam).*

Dedico

ACKNOWLEDGEMENTS

I especially thank my wife, Camilla, for believing in me even when I didn't believe in myself. Thank you for all the love, friendship, and companionship. Without you, none of this would be possible!

I also thank my parents, Edilaine and Pedro, my brother, João Pedro, my grandparents, Edival (*in memoriam*), Maria de Lourdes e Marilene, and my aunts, uncles, and cousins for all the love, emotional and financial support, and for always believing in me.

I thank Professor Teodorico for all the support, teachings, and trust during these years of partnership. I thank Professor Adelia for the confidence in welcoming me to Texas Tech and showing me new paths.

All my friends from Lavras and Rio Claro, for the moments of relaxation, fun, and all the companionship.

To all my colleagues from the Computational Chemistry Laboratory – MOLECC.

I am grateful to everyone in the Brazilian group in Lubbock, who welcomed me warmly and helped me a lot during the months I spent there.

I am grateful to the Federal University of Lavras – UFLA, the Department of Chemistry - DQI, and the Postgraduate Program in Agrochemistry at UFLA for the structure provided and the opportunity to pursue my doctorate.

I also thank Texas Tech University for hosting me during my sandwich program.

This study was financed in part by the coordenação de aperfeiçoamento de pessoal de nível superior – Brasil (CAPES) – finance code 001. O presente trabalho foi realizado com apoio do fundação de amparo à pesquisa de minas gerais (FAPEMIG). And to the other institutions that enabled this work to be carried out: CNPq, FINEP, and INCTDefesa.

To the other friends and colleagues who, in one way or another, supported me.

Thank you very much!

RESUMO

A natureza das interações não covalentes tem sido objeto de intenso debate na literatura recente, questionando-se a predominância do modelo puramente eletrostático em favor de uma contribuição orbital significativa. Neste contexto, esta tese investigou a natureza das ligações de pnictogênio (PnB) e seu impacto em dois sistemas reais de alta relevância: a inibição da enzima acetilcolinesterase (AChE) por compostos organofosforados e o design de moléculas para computação quântica via Ressonância Magnética Nuclear (RMN). Utilizando a Teoria do Funcional da Densidade (DFT) aliada a ferramentas de análise topológica e de decomposição de energia (AIM, NBO e EDA), demonstrou-se que as interações envolvendo átomos de fósforo (e selênio) possuem um componente orbital determinante para suas propriedades físico-químicas. No sistema biológico, a formação da ligação PnB entre agentes de guerra química (como Sarin e VX) e o sítio ativo da AChE revelou-se crucial para o mecanismo de inibição, sugerindo novos caminhos para o desenvolvimento de antídotos mais eficientes. No âmbito tecnológico, a modulação de interações intramoleculares P···P e P···Se em derivados de naftaleno permitiu o ajuste fino dos parâmetros de RMN (deslocamento químico e constante de acoplamento), viabilizando o design racional de qubits moleculares que satisfazem os critérios de DiVincenzo. Os resultados unificam a compreensão dessas interações, propondo que a manipulação do caráter covalente em ligações não-covalentes é uma estratégia poderosa tanto para a química medicinal quanto para a engenharia de materiais quânticos.

Palavras-chave: ligações de pnictogênio; organofosforados; computação quântica; parâmetros de RMN; acetilcolinesterase; DFT.

ABSTRACT

The nature of non-covalent interactions has been the subject of intense debate in recent literature, questioning the predominance of the purely electrostatic model in favor of a significant orbital contribution. In this context, this thesis investigated the nature of pnictogen bonds (PnB) and their impact on two highly relevant real systems: the inhibition of the enzyme acetylcholinesterase (AChE) by organophosphorus compounds and the design of molecules for quantum computing via Nuclear Magnetic Resonance (NMR). Using Density Functional Theory (DFT) combined with topological analysis and energy decomposition tools (AIM, NBO, and EDA), it was demonstrated that interactions involving phosphorus (and selenium) atoms have an orbital component that is decisive for their physicochemical properties. In the biological system, the formation of the PnB bond between chemical warfare agents (such as Sarin and VX) and the active site of AChE proved crucial to the inhibition mechanism, suggesting new avenues for the development of more efficient antidotes. In the technological field, the modulation of intramolecular P \cdots P and P \cdots Se interactions in naphthalene derivatives has allowed the fine tuning of NMR parameters (chemical shift and coupling constant), enabling the rational design of molecular qubits that satisfy DiVincenzo's criteria. The results unify the understanding of these interactions, proposing that manipulating the covalent character in non-covalent bonds is a powerful strategy for both medicinal chemistry and quantum materials engineering.

Keywords: pnictogen bonds; organophosphorus; quantum computing; NMR parameters; acetylcholinesterase; DFT.

INDICADORES DE IMPACTO

Os resultados obtidos nesta tese apresentam impactos diretos nas esferas científica e tecnológica, com desdobramentos potenciais para a saúde pública e inovação industrial. **Impacto Científico e Tecnológico:** A pesquisa gerou a publicação de dois artigos em periódicos internacionais de alto impacto, contribuindo para o avanço do conhecimento na fronteira da Química Computacional:

Avanço na Química Medicinal e Defesa: O estudo sobre a inibição da acetilcolinesterase fornece uma nova compreensão mecanística sobre a ação de armas químicas organofosforadas. Este conhecimento é fundamental para o design de novos reativadores enzimáticos (oximas) mais eficazes, impactando diretamente a área de defesa química e toxicologia.

Inovação em Computação Quântica: A proposta de novos qubits moleculares baseados em interações de pnictogênio oferece uma rota química para superar desafios de escalabilidade em computadores quânticos de RMN. A capacidade de "sintonizar" parâmetros de hardware através de engenharia molecular representa um avanço tecnológico significativo para o processamento de informação.

Alinhamento com os Objetivos de Desenvolvimento Sustentável (ODS) da ONU: O trabalho está alinhado com os seguintes objetivos:

- ODS 3 (Saúde e Bem-Estar): Ao contribuir para o entendimento de mecanismos de toxicidade e desenvolvimento de antídotos para agentes neurotóxicos.
- ODS 9 (Indústria, Inovação e Infraestrutura): Ao propor novas tecnologias moleculares para a computação de alto desempenho, fomentando a inovação científica.

Áreas Temáticas da Política Nacional de Extensão: Os impactos desta pesquisa classificam-se primordialmente nas áreas de Tecnologia e Produção e Saúde, consolidando a colaboração internacional com grupos de pesquisa e fortalecendo a pós-graduação *Stricto sensu* da UFLA.

IMPACT INDICATORS

The results obtained in this thesis have direct impacts in the scientific and technological spheres, with potential ramifications for public health and industrial innovation. Scientific and Technological Impact: The research led to the publication of two articles in high-impact international journals, contributing to the advancement of knowledge at the frontier of Computational Chemistry:

Advances in Medicinal Chemistry and Defense: The study on acetylcholinesterase inhibition provides a new mechanistic understanding of the action of organophosphorus chemical weapons. This knowledge is fundamental for the design of new, more effective enzyme reactivators (oximes), directly impacting the field of chemical defense and toxicology.

Innovation in Quantum Computing: The proposal for new molecular qubits based on pnictogen interactions offers a chemical route to overcome scalability challenges in NMR quantum computers. The ability to “tune” hardware parameters through molecular engineering represents a significant technological advance for information processing.

Alignment with the UN Sustainable Development Goals (SDGs): The work is aligned with the following goals:

- SDG 3 (Good Health and Well-Being): By contributing to the understanding of toxicity mechanisms and the development of antidotes for neurotoxic agents.
- SDG 9 (Industry, Innovation, and Infrastructure): By proposing new molecular technologies for high-performance computing, fostering scientific innovation.

Thematic Areas of the National Extension Policy: The impacts of this research are primarily classified in the areas of Technology and Production and Health, consolidating international collaboration with research groups and strengthening UFLA's *Stricto sensu* graduate program.

LIST OF ABBREVIATIONS

ACh	Acetylcholine
AchE/hAChE	Human Acetylcholinesterase
AIM	Atoms-in-Molecules
AO	Atomic Orbital
ASM	Activation Strain Model
BCP	Bond Critical Point
CAPES	Coordenação de Aperfeiçoamento de Pessoal de Nível Superior
ChB	Chalcogen Bond
CNPq	Conselho Nacional de Desenvolvimento Científico e Tecnológico
CWA	Chemical Warfare Agents
DFT	Density Functional Theory
DSO	Diamagnetic Spin-Orbit
EDA	Energy Decomposition Analysis
FAPEMIG	Fundação de Amparo à Pesquisa do Estado de Minas Gerais
FC	Fermi Contact
FINEP	Financiadora de Estudos e Projetos
GA	Tabun
GB	Sarin
GD	Soman
GF	Cyclosarin
GGA	Generalized Gradient Approximation
GIAO	Gauge-Including Atomic Orbitals
GP	2-[fluoro(methyl)phosphoryl]oxy-1,1-dimethylcyclopentane
HB/H-Bond	Hydrogen Bond
HF	Hartree-Fock
HK	Hohenberg-Kohn
HOMO	Highest Occupied Molecular Orbital
INCTDefesa Biológica	Instituto Nacional de Ciência e Tecnologia em Defesa Química e
J/SSCC	Spin-Spin Coupling Constant
KS	Kohn-Sham
LDA	Local Density Approximation

LUMO	Lowest Unoccupied Molecular Orbital
MEP	Molecular Electrostatic Potential
MO	Molecular Orbital
NAO	Natural Atomic Orbitals
NBO	Natural Bond Orbital
NCI	Non-covalent Interactions or Non-covalent Index
NHO	Natural Hybrid Orbitals
NLMO	Natural (semi-)Localized Molecular Orbitals
NMR	Nuclear Magnetic Resonance
ODS (SDG) Goals)	Objetivos de Desenvolvimento Sustentável (Sustainable Development Goals)
ONU (UM)	Organização das Nações Unidas (United Nations)
OP	Organophosphorus
OPCW	Organization for the Prohibition of Chemical Weapons
PnB	Pnictogen Bond
PSO	Paramagnetic Spin-Orbit
QIP	Quantum Information Processing
QM/MM	Quantum Mechanics/Molecular Mechanics
Qubit	Quantum bit
RDC	Reduced Density Gradient
SD	Spin-Dipole
TB	Tetrel Bond
UFPA	Universidade Federal de Lavras
VX	Venomous Agent X
XB	Halogen Bond
ZORA	Zeroth-Order Regular Approximation

SUMÁRIO

1 FIRST PART	14
1.1 INTRODUCTION	14
1.2 THEORETICAL REFERENCE	16
1.2.1 Non-Covalent Interactions.....	16
1.2.2 Pnictogen Bond	18
1.2.3 Acetylcholinesterase Enzyme.....	20
1.2.3.1 AChE inhibition by chemical warfare agents.....	22
1.2.4 Quantum Computation	25
1.2.4.1 Intramolecular Interactions and NMR parameters	27
1.2.4.2 NMR for quantum computation	29
1.2.5 Computational Chemistry	30
1.2.5.1 Density Functional Theory - DFT	30
1.2.5.2 Atoms-in-Molecules	34
1.2.5.3 Natural Bond Orbital	34
1.2.5.4 Non-covalent Index	36
1.2.5.5 Energy Decomposition Analysis	37
1.2.5.6 Computational NMR spectroscopy	39
2 SECOND PART	41
Article 1 - Pnictogen bond-driven control of the molecular interaction between organophosphorus and acetylcholinesterase enzyme.....	42
Article 2 - Intramolecular Pnictogen Bonds as Key Determinants for NMR Quantum Computation Parameters	69
3 THIRD PART	93
3.1 FINAL REMARKS	93
REFERENCES	95
APPENDIX 1 - LIST OF PUBLICATIONS	108
APPENDIX 2 – ARTICLE 1 SUPPORTING INFORMATION	111
APPENDIX 3 – ARTICLE 2 SUPPORTING INFORMATION	126

1 FIRST PART

1.1 INTRODUCTION

An important part of chemistry is the study of bonds and interactions between atoms and molecules. The field of chemical interactions is very important for various systems, and can help stabilize them, lead to the formation of chemical bonds, or even repulsive interactions. One of the main types of interactions present in chemistry are non-covalent bonds (NCI), where we can highlight the famous hydrogen bond, where there is a strong interaction between a hydrogen atom with a positive dipole and an electronegative atom, such as fluorine, oxygen or nitrogen. Other NCIs include the halogen bond, which involves a group 17 atom as an electron density acceptor, the chalcogen bond, involving an element of group 16, and the pnictogen bond, with an element of group 15.

The nature of non-covalent bonds has been the subject of discussion in the literature in recent years. The most accepted explanation in recent years has been that of the σ -hole, where a Lewis acid has a positively charged region opposite the axis of the bond between the atom that gives the interaction its name, the pnictogen for example, and its direct ligand, this region, called the σ -hole, accepts the electronic density of a Lewis base, which has electronic density available, either charged or via its lone pair. This explanation considers both sides of the interaction as charged points or surfaces, leading to the understanding that non-covalent bonds are governed by a purely electrostatic character.

In recent years, researchers have pointed out that this explanation may be flawed since, from a molecular orbital perspective, the orbital component of the interaction's energy is important, in some cases being more important than the electrostatic component. As a result, the very name given to this type of interaction may be incorrect, since, with an important orbital energy component in the interaction, it resembles a covalent bond, making it meaningless to call them non-covalent bonds, and more appropriate to call them inter(intra)-molecular covalent interactions.

However, considering the pnictogen bond (PnB), this new perspective on the nature of the bond has been shown in model systems, with the Lewis acid having a halogen attached to the pnictogen, making it more available to interact, and the Lewis base being a halogen anion, thus more available to interact. It is therefore important to understand whether the orbital nature of the pnictogen interaction remains important in real systems, where an unforced Lewis base

and acid interact via PnB. An important example of this type of real system comes from organophosphorus (OP) compounds.

The importance of OPs is due to their wide application, mainly as agrochemicals, some of which are very well known, such as chlorpyrifos, parathion or methyl-parathion. In addition, they are also used as plastic stabilizers, antioxidants and a not so good application, as chemical warfare agents. In the latter, where OPs are also called nerve agents, we can highlight some well-known compounds, such as Sarin, Soman and VX. The structure of OP compounds used as agrochemicals and as chemical warfare agents is very similar and their ambiguous use is due to the OP's property of interacting with the enzyme acetylcholinesterase (AChE), inhibiting its activity.

This enzyme is very important for humans and is responsible for the transmission of nerve impulses. Its inhibition, via OPs, occurs through the binding of the organophosphorus to the serine residue present in the active site of AChE, preventing AChE from performing its function of breaking down acetylcholine into acetate and choline and, consequently, preventing neurotransmission. When inhibited, AChE cannot perform this function, leading to an accumulation of acetylcholine in the synaptic cleft, which can lead to various situations, such as confusion, respiratory failure and, sometimes, death. There have been some studies into the development of oximes, which are compounds capable of resuscitating AChE, allowing the enzyme to return to its regular activity; however, these oximes are not 100% effective.

Considering this, the AChE-OP system is a good alternative real system for studying the nature of the pnictogen interaction, which in this case will lead to the formation of the bond between the phosphorus atom of the OP compound and the oxygen of the serine present in the active site of acetylcholinesterase. This system is still very important, since a significant number of agrochemicals are organophosphorus compounds, and their incorrect and uncontrolled use can lead to poisoning by OPs, and chemical warfare agents are unfortunately still used.

Another real system where this type of interaction can be observed and is extremely important is in molecules for quantum computing. In recent years, the demand for quantum computers has been steadily rising as they have the potential to solve complex problems that have challenged society for decades. At the same time, artificial intelligence is becoming an integral part of daily life, further driving the need for advanced computing power. To meet this demand, research has focused on overcoming the main challenge of scalability, leading scientists to continuously explore more efficient ways to build large-scale quantum processors using techniques such as Nuclear Magnetic Resonance (NMR).

For a molecule to be applicable as a qubit in Quantum Information Processing (QIP), it must fulfill specific criteria regarding its magnetic properties. Crucially, the candidate molecule must possess spin 1/2 nuclei and exhibit a large difference between the chemical shifts of these nuclei, alongside a high value of spin-spin coupling constants (J or SSCC). These NMR parameters are of great importance because they determine the system's ability to transfer information and implement quantum gates effectively in an organized and scalable manner.

It is well established that these NMR parameters are highly sensitive to the intermolecular or intramolecular interactions occurring within the molecule. Consequently, the nature and strength of these interactions is a crucial factor in analyzing the behavior of these molecules in NMR. Modulating these intramolecular forces through molecular design serves as an effective strategy to tune the spectroscopic properties, thereby enhancing the potential of chemical systems to function as robust qubits.

In this context, the present work employs computational strategies to investigate the nature and impact of pnictogen bond within these two distinct real scenarios. By analyzing both the AChE-OP enzymatic system and the intramolecular interactions in potential qubit candidates, we aim to determine the nature of the PnB in these systems. Furthermore, this study seeks to establish a direct correlation between the fundamental nature of the pnictogen bond and the properties of interest, specifically the inhibition mechanism of acetylcholinesterase and the tuning of NMR parameters for quantum computing, thereby validating the relevance of understanding the nature of inter or intramolecular interactions in complex chemical systems.

1.2 THEORETICAL REFERENCE

1.2.1 Non-Covalent Interactions

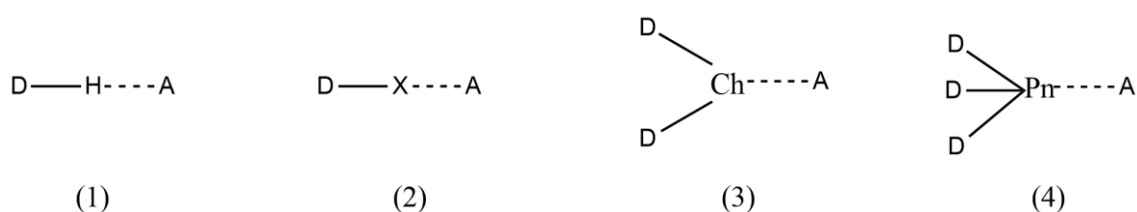
Before studying non-covalent interactions, it is important to define that covalent bonds involve the sharing of electrons to form an electron pair (Moeller et al., 1980). This bond arises from the attraction between nuclei for the same electron, and is only formed when the bonded atoms have a lower energy than the separate atoms (Moeller et al., 1980). Although this definition is part of our chemical knowledge, remembering it is important for understanding non-covalent interactions and the alternative terms to this name that appear in the literature.

Moving on to non-covalent interactions, which unlike covalent bonds, do not share electrons, involve the interaction of molecules or within a molecule. These interactions are classified as electrostatic, π -effects, van der Waals forces and hydrophobic effects (Mahmudov

et al., 2020; Mahmudov, Gurbanov, et al., 2019; Mahmudov, Kopylovich, et al., 2019). This type of interaction is present in several areas, such as the structural properties of proteins and nucleic acids, and is also of great importance in organic synthesis and the design of drugs and materials (Černý & Hobza, 2007; Scheiner, 2013; Wolters & Bickelhaupt, 2012).

This work will focus on electrostatic interactions, including the hydrogen bond (H-bond), halogen bond (XB), chalcogen bond (ChB) and pnictogen bond (PnB) (Figure 1), which will be discussed in the following sections. The usual explanation for these interactions comes from the σ -hole model, where a positively charged region, called a sigma-hole, interacts with a negatively charged region, a Lewis base, considering a pure electrostatic model (Mahmudov et al., 2020; Politzer et al., 2017; Politzer & Murray, 2013).

Figure 1 — Schematic representation of (1) H-bond, (2) halogen bond, (3) chalcogen bond, and (4) pnictogen bond.



Source: From the author (2026).

In the structures shown in Figure 1, atoms D and A are more electronegative than the central atom. According to the σ -hole model, the lone pair of A interacts with the σ antibonding orbital of the bond between D and the central atom, whether it is H, X, Ch or Pn.

However, new publications point out that this model is flawed, since it considers these two centers as charged points or surfaces, ignoring the orbital interaction that is present in the interactions (Politzer et al., 2008, 2013, 2019). Regarding this, De Azevedo and collaborators in 2021 pointed out that the best name for this type of interaction should be intermolecular covalent bonds (de Azevedo Santos et al., 2023; de Azevedo Santos, Hamlin, et al., 2021a, 2021b).

Despite the ongoing debate regarding their physical nature and nomenclature, the role of these interactions in biological processes is indisputable and paramount. In the biological realm, non-covalent forces are the primary determinants of the three-dimensional architecture of macromolecules, stabilizing the secondary and tertiary structures of proteins, and the double helix of DNA (Adhav & Saikrishnan, 2023; Cai et al., 2025; Hashemi et al., 2026; Hosseini Faradonbeh et al., 2025; Shotonwa & Olasunkanmi, 2023). Furthermore, they govern the dynamics of molecular recognition, acting as the driving force behind ligand-receptor binding

and the formation of enzyme-substrate complexes (Adhav & Saikrishnan, 2023; Cai et al., 2025; Hashemi et al., 2026; Hosseini Faradonbeh et al., 2025). In this context, while hydrogen bonds have historically been the focus, recent evidence suggests that other types of interactions, such as halogen and pnictogen bonds, play a pivotal role in the selectivity and stability of bioactive molecules within enzymatic active sites.

1.2.2 Pnictogen Bond

The first step is to define what pnictogens are. These elements are part of group 15, Nitrogen, Phosphorus, Arsenic, Antimony and Bismuth. The name of this family comes from the German and Greek terminology for suffocating substance, a characteristic attributed to nitrogen, leading to the family name (Girolami, 2009). The first time that this type of interaction was reported in the literature was in 1978, when Hill and coworkers observed the PnB using NMR studying ortho-carbaborane derivative (Hill & Silva-Trivino, 1978). Since then, some studies involving the pnictogen bond were published (Klinkhammer & Pyykko, 1995; Moilanen et al., 2009; Murray et al., 2007; Zahn et al., 2011), however, only in the early 2010 did a couple of papers raise the importance of this type of bond in the design of new compounds, leading the scientific community to study of the pnictogen bond (Scheiner, 2011a, 2011c; Zahn et al., 2011).

The term pnictogen bond arises from the characteristic of the pnictogen atom can act as electron donor, since these atoms have lone pairs of electrons. It donates electron density to an atom with electron deficiency, which can be a positively charged atom, a π -electron system or other electron-deficient regions (Bauzá et al., 2015; Scheiner, 2023). Pnictogens atoms (Pn-atom) present relatively different characteristics due the difference of electronegativity as one moves down in the group. This can allow the pnictogen atom to act as a Lewis acid or base, depending of the specie that it is interacting. Lights elements, such as Nitrogen, trend to act as Lewis base, when heavier elements, such as Bismuth, present a predominant Lewis acid characteristic (Norman, 1997; Wolters & Bickelhaupt, 2012).

This decrease in the electronegativity leads to a more positivity charge in the pnictogen atom, allowing an electrostatic interaction of the Pn-atom and a Lewis base (de Azevedo Santos et al., 2023; de Azevedo Santos, Hamlin, et al., 2021a; Wolters & Bickelhaupt, 2012). The mechanism of this interaction is similar to other non-covalent bonds, such as HB, ChB or XB, where the electrostatic interaction occurs between the σ^* orbital of the Pn-D bond, i.e., the σ -hole, and a Lewis base, via its electron density of a lone pair or π -electrons (Bauzá et al., 2015;

Politzer et al., 2017). There are two main aspects that determine the stability of a σ -hole interaction on the donation side, the first one is the polarizability of the Pn-atom, that increases when the size of the Pn increase, and, therefore, the strength of the interaction increases (Bauzá et al., 2015). The second factor that determines the stability is the electron-withdrawing potential of the covalently bonded substituents, with more electron-withdrawing the substituent the stronger the σ -hole interaction (Scheiner, 2011a, 2011c). On the Lewis base side, the better is the capacity of donate electron density, more stable will be the complex (Scheiner & Adhikari, 2011).

Nonetheless, as previously mentioned, the σ -hole model considers both Lewis acid and base, as point charges or a charged surface, ignoring the fact that the orbital interaction plays a significant role in the interaction strength. This leads to a focus on understanding the importance of this component in model systems containing non-covalent interactions. Some papers published in the last few years by professor Bickelhaupt group point out that not just the pnictogen bond, but also the chalcogen bond, halogen bond and, even hydrogen bond, have an important covalent component on the bond energy, being sometimes more important than the electrostatic component in a molecular orbital perspective (de Azevedo Santos et al., 2022, 2023; de Azevedo Santos, Hamlin, et al., 2021a; Larrañaga et al., 2021; Wolters & Bickelhaupt, 2012). Considering these results, the researchers suggest that the name of non-covalent interactions is inadequate, and that these interactions are better represented by the name of inter(intra)-molecular covalent interactions (de Azevedo Santos et al., 2023; de Azevedo Santos, Hamlin, et al., 2021a).

Besides these controversies and new studies on the nature of the PnB, several studies have appeared in recent years on the importance, application and presence of the pnictogen bond in various areas. Among them, we can highlight its presence in biological systems, where, in 2016, Tripathi collaborators found, using computational techniques, PnB between nitrogen atoms present in amino acids (G. Tripathi et al., 2016). In the next years, a few other studies considering biological studies emerged, with an emphasis on transmembrane transportation and drug delivery (Humeniuk et al., 2021; Lee et al., 2019; Rosli et al., 2020). The presence of the PnB in organic systems was also investigated in the literature, highlighting its presence in the aromaticity and antiaromaticity of compounds with Pn atoms (Karabıyık et al., 2015; Trujillo et al., 2017), and the interactions between Pn atoms and some organic compounds, such as azides and cyclohexane (Bursch et al., 2021; Schiavo et al., 2021).

There are also publications that have studied the technological application of Pn bonds, with their presence identified and studied in semiconductors (Shieh & Li, 2019), in

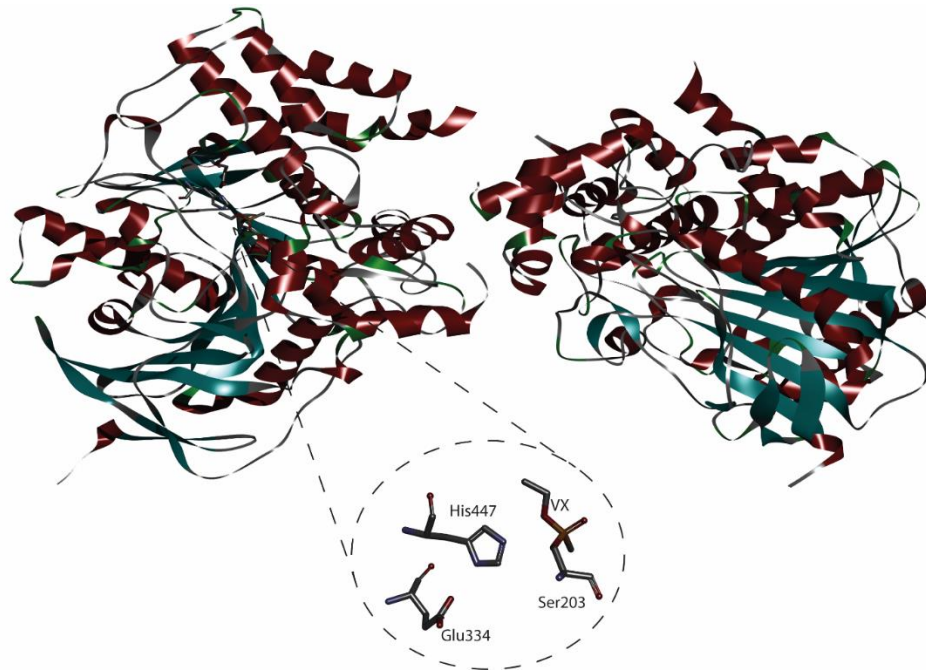
photoluminescence (Smith et al., 2004), and as a gas sensor (Yan & Wei, 2022). This type of bond is also present in nuclear fuels, in the Pn-U interaction (Atkinson et al., 2018). However, most of the work involving PnB is related to catalysis, stabilization and formation of complexes and the nature of the interaction. In catalysis, the interaction is found as an important part of several types of reactions, such as brevetoxin-type cyclization (Gini et al., 2020; Paraja et al., 2020), Reissert-type substitution (Li et al., 2020) or enantioselective hydrogenation (Zhang et al., 2021). In complexes, PnB is responsible for the stability of complexes, mainly involving compounds with antimony (Pomogaeva et al., 2021; Radha et al., 2019; Rodrigues & Gabbai, 2021) and arsenic (Dube et al., 2012; Fanfrlík & Hnyk, 2018), and this bond has also been reported in the formation of complexes using Pn atoms (Esrafilí et al., 2015; Tondro & Roohi, 2019). Finally, some studies on the nature of pnictogen bonds can be highlighted, where the interaction of different Pn compounds with hydrogen gas (Grabowski et al., 2013), the N-N interaction between substituted NH₃ (Scheiner, 2011b), interactions involving Bi (Gehlhaar et al., 2022) have been reported. We can also highlight work studying the general nature of these interactions, comparing them with other non-covalent interactions (De Vleeschouwer et al., 2021; George et al., 2014; Gomila & Frontera, 2021; Legon, 2017).

Despite being present in specific and very important areas, such as organophosphorus compounds (OP), the literature about PnB is still scarce, especially when we consider the orbital nature of this interaction. The following sessions will present more details about OPs, especially their use as agrochemicals and chemical warfare agents, and their relationship with the acetylcholinesterase enzyme.

1.2.3 Acetylcholinesterase Enzyme

The human Acetylcholinesterase (AChE) enzyme has a general α/β hydrolase globular fold (Figure 2). Each monomer contains one catalytic center composed of two compartments: the catalytic site, along with the anionic site that accommodates the positively charged quaternary nitrogen moiety of Acetylcholine (ACh) (Hörnberg et al., 2007). It is shown that the catalytic triad (Ser203-Glu334-His447) is at the bottom of the active site, surrounded by relevant structural attributes for catalytic activity: the acyl pocket (residues Phe295, Phe297 and Phe338), the oxyanion hole (Gly121, Gly122 and Ala204), and the choline binding site (Trp86 and Tyr337) (Hörnberg et al., 2007).

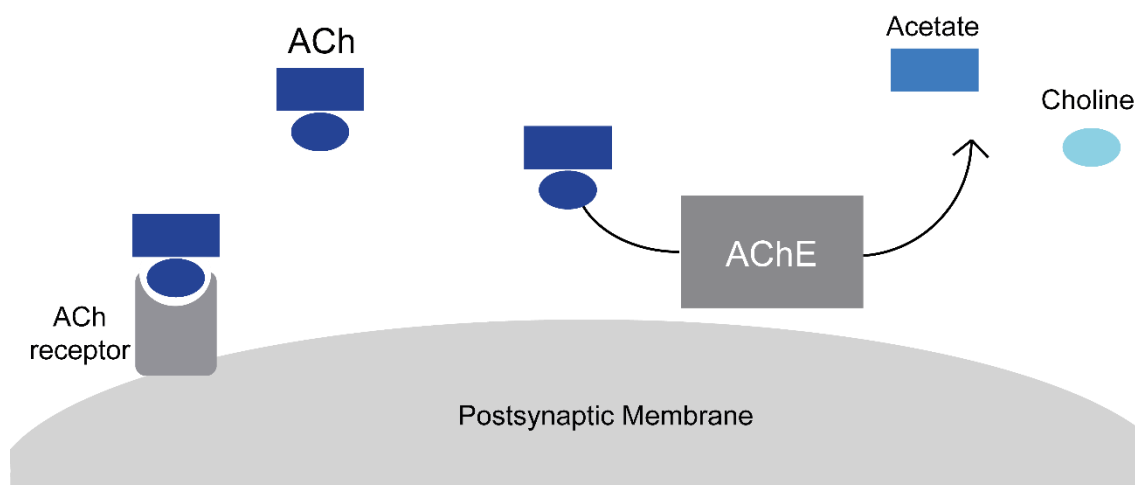
Figure 2 — Representation of the three-dimensional structure of hAChE (PDB code = 6CQZ). The catalytic residues and VX are highlighted in the dashed cycle.



Source: From the author (2026).

The AChE enzyme is a serine protease that finalizes the transmission of nerve impulses at cholinergic synapses by the hydrolysis of the ACh neurotransmitter (Soreq & Seidman, 2001). ACh-mediated neurotransmission is essential for nervous system function (Soreq & Seidman, 2001). ACh binds to the postsynaptic receptor, transmitting the information. After propagating the message, the ACh molecule disconnects itself from the postsynaptic receptor and returns to the synaptic cleft, where it undergoes AChE-catalyzed hydrolysis, giving rise to acetate and choline (Figure 3) (Soreq & Seidman, 2001). Regarding neurodegenerative diseases, there are currently some potential central nervous system targets to treat neurodegenerative disorders. In this line, it is important to mention that the drug molecular targets include neurotransmitter receptors and enzymes within neurotransmitter synthetic or degradative pathways, such as in AChE. Other existing drug molecular targets highlight, for instance, the monoamine oxidase that intracellularly metabolizes catecholamine neurotransmitters and the catechol-O-methyltransferase that extracellularly metabolizes catecholamine neurotransmitters (Youdim & Buccafusco, 2005).

Figure 3 — Schematic representation of ACh hydrolysis catalyzed by AChE.



Source: From the author (2026).

The AChE enzyme is broadly distributed throughout the body, standing out because it is the main cholinesterase in the human brain (Saeed et al., 2014; Schwarz et al., 2014). Cholinesterase inhibitors have been employed in the treatment of many disorders such as Alzheimer's disease, Parkinson's disease, dementia, myasthenia gravis, among others, along with applications in the treatment of glaucoma (Heinig et al., 2000; Pohanka, 2011).

Thus, studying the existence, importance and nature of the pnictogen interactions present in the formation of the OP-AChE bond is extremely important. Understanding the factors that lead to bond formation, and their nature can help to develop more effective oximes or methods to prevent bond formation.

For this, the use of computational chemistry techniques is extremely important. These techniques make it possible to study complex systems in terms of various characteristics, such as bonds, interactions, energy, among others (Corrêa et al., 2021; De Castro et al., 2017; Medimagh et al., 2021; Rasouli et al., 2022). Thus, these techniques are effective tools to be applied to the study of the interactions of the OP-AChE system.

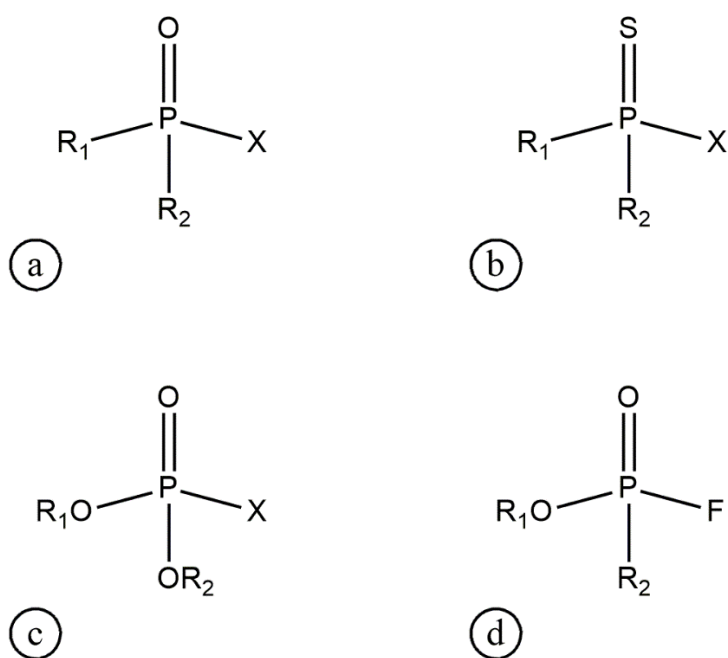
1.2.3.1 AChE inhibition by chemical warfare agents

Organophosphorus compounds are described as an organic compound derived from phosphoric acids and contain at least one C—P bond, however some compounds, such as triphenylphosphate, does not have this C—P bond and are usually classified as an OP compound (Balali-Mood & Abdollahi, 2014). Most OP compounds have the P atom with

oxidation state V, where several known compounds are found, such as parathion, sarin and glyphosate (Watson et al., 2009).

The general structure of an OP is shown in figure 4a, where R1 and R2 are aryl or alkyl radicals and X can be different groups, such as halogens, aliphatic, aromatic, among others. OPs are compounds used worldwide for various purposes, including agrochemicals and chemical warfare agents.

Figure 4 — Basic structures of an (a) organophosphorus, (b) phosphonothiates, (c) organophosphates, and (d) phosphonofluoridate.



Source: From the author (2026).

It is important to highlight that some OPs belong to phosphonothioates class, where oxygen is replaced by sulfur (Figure 4b), such as malathion (Kumar et al., 2016). Another important class in the OPs are the organophosphates, where the R ligands are replaced by an OR ligand (Figure 4c) (Mukherjee & Gupta, 2020). Last, the phosphonofluoridate compounds that have a fluor atom in its structure (Figure 4d), where the major part of chemical warfare agents is included (Mukherjee & Gupta, 2020).

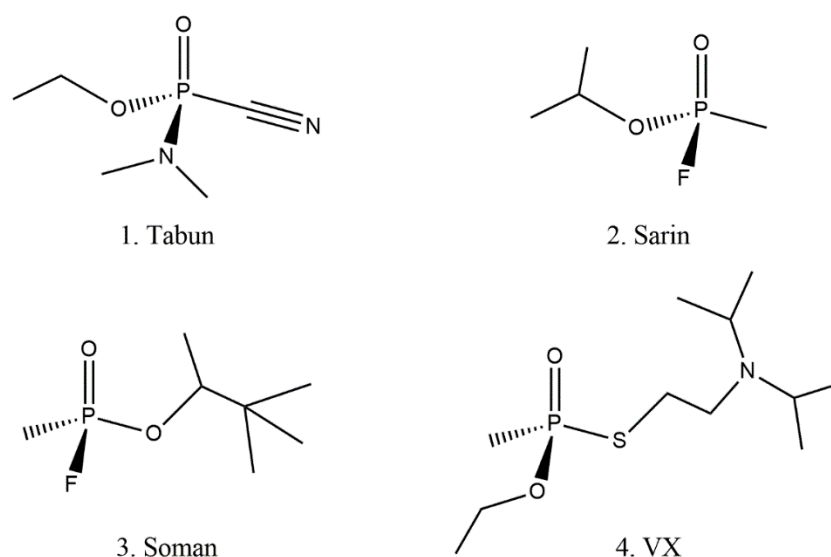
Despite being important as an agrochemical, OPs have a toxic potential, as they are easily absorbed through breathing or through the skin, leading to inhibition of the acetylcholinesterase enzyme, causing a cholinergic crisis, which can lead to death (Figuroa-Villar et al., 2021). This inhibition by the two types of OPs that will be studied in this work will be discussed below.

The use of neurotoxic organophosphorus compounds as chemical warfare agents has become one of the greatest global threats today. (Costa, 2018; Delfino et al., 2009; Ganesan et al., 2010; Mukherjee & Gupta, 2020; Watson et al., 2015; Worek et al., 2020). Chemical warfare is based on the use of substances with toxic properties, which are capable of killing, for mass destruction, besides causing severe damages to the environment (Ganesan et al., 2010). The most remarkable and lethal chemical warfare agents are organophosphorus neurotoxins. Because of its extreme toxicity, even tiny doses can cause seizures and even death. Since ancient times, chemical warfare agents have been employed on multiple occasions in combat. From that point on, there was a greater focus on the creation of neurotoxic agents (Costa, 2018; Mukherjee & Gupta, 2020).

Before World War II, the German army began the development of the first neurotoxic compound as chemical warfare agent, especially tabun (GA), sarin (GB), and soman (GD) (Figure 3) (DELFINO; RIBEIRO; FIGUEROA-VILLAR, 2009; MUKHERJEE; GUPTA, 2020). In the 1950s, neurotoxic OP compounds of the V family were developed, which are more toxic and persistent in the environment, with the first one, called VX (Figure 5), being developed in England (Watson et al., 2009, 2015).

Unfortunately, some countries still do not take part in the OPCW (Organization for the Prohibition of Chemical Weapons), thus chemical weapons can easily be used by terrorist groups. The low cost and ease of manufacture make chemical weapons of interest to terrorist organizations, which is a major concern around the world (Ganesan et al., 2010).

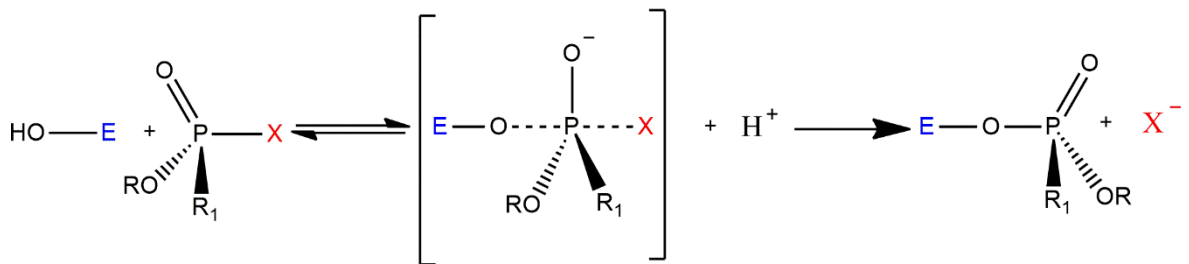
Figure 5 — Chemical structures of the chemical weapons (1) Tabun, (2) Sarin, (3) Soman and (4) VX.



Source: From the author (2026).

The OPs used as chemical warfare agents act as an irreversible inhibitor of AChE. Once they are substrates similar to ACh, the OPs covalently binding in the active site to the serine hydroxyl group (Delfino et al., 2009; Figueroa-Villar et al., 2021; Jacquet et al., 2016; Worek et al., 2020). This leads to a process where the OP is split and the enzyme is phosphorylated (Figure 6). Without AChE available for the ACh hydrolysis, the acetylcholine accumulates in the synaptic cleft (see Figure 3), resulting in an overstimulation of the cholinergic pathways and thus impeding neurotransmission (Jayawardane et al., 2009; Mukherjee & Gupta, 2020; Watson et al., 2009, 2015). The OP poison symptoms are muscle weakness and fasciculations, agitation, miosis, sweating and hypersalivation, severe infections could lead to respiratory failure, confusion, unconsciousness, convulsion and death (Watson et al., 2009, 2015).

Figure 6 — General representation of AChE inhibition by OPs.



Source: From the author (2026).

1.2.4 Quantum Computation

In recent decades, society has witnessed a growing demand for computational power, driven by the need to solve problems of exponential complexity that challenge the limits of classical computing. While traditional computers operate based on classical physics and binary logic, processing information through bits that assume values of 0 or 1, quantum computing emerges as a new technological paradigm (J. B. R. Lino et al., 2017). This field of computer science utilizes the fundamental principles of quantum mechanics, such as superposition and entanglement, to perform operations on data in a fundamentally different way and, for certain classes of problems, exponentially faster (Jones, 2011, 2024; J. B. D. R. Lino & Ramalho, 2019).

The fundamental unit of information in quantum computing is the quantum bit, or qubit. Unlike a classical bit, a qubit can exist in a state of superposition, simultaneously representing values of 0 and 1 with different probability weights (Jones, 2011, 2024). This property allows

a quantum computer to process a vast number of possibilities at the same time, a phenomenon known as quantum parallelism (Jones, 2011, 2024). Furthermore, quantum entanglement allows the state of one qubit to be intrinsically correlated to that of another, regardless of the physical distance between them, which is essential for state teleportation and the execution of complex algorithms such as Shor's algorithm (integer factorization) and Grover's algorithm (unstructured database search) (Anwar et al., 2004; Chae et al., 2024; Jones, 2011, 2024; Vandersypen et al., 2001).

For a physical system to be viable as a quantum computer, it must satisfy a rigorous set of conditions known as the DiVincenzo criteria. These criteria establish that the system must possess: (i) a scalable set of well-characterized qubits; (ii) the ability to initialize the state of the qubits with high fidelity; (iii) decoherence times much longer than the gate operation time; (iv) a universal set of quantum logic gates; and (v) the capability to measure specific qubits individually (Chae et al., 2024; DiVincenzo, 2000; Jones, 2011, 2024; J. B. dos R. Lino et al., 2022). Among the various architectures proposed for the physical implementation of qubits, which include trapped ions, quantum dots, and superconductors, liquid-state Nuclear Magnetic Resonance (NMR) stands out as one of the most successful techniques for experimental demonstrations and Quantum Information Processing (QIP) on a small scale (Chae et al., 2024; Criger et al., 2012; Jones, 2011, 2024; Kaushik & Khaneja, 2025; J. B. D. R. Lino et al., 2020; J. B. D. R. Lino & Ramalho, 2019; J. B. dos R. Lino et al., 2022; J. B. R. Lino et al., 2017; Lino & Ramalho, 2018; Ramanathan et al., 2004; Yamauchi & Yanai, 2024).

In NMR-based quantum computing, qubits are represented by nuclear spins ($I = 1/2$) in molecules in solution. Nuclei such as ^1H , ^{13}C , ^{19}F , ^{31}P , and ^{77}Se are frequently used due to their favorable magnetic properties and ease of manipulation via radiofrequency pulses (J. B. D. R. Lino et al., 2020; J. B. dos R. Lino et al., 2022). In this context, chemistry plays a central role, as the hardware of the quantum computer is, essentially, the molecule itself. The challenge, therefore, lies in rational molecular design: synthesizing compounds that act as efficient quantum processors. To achieve this, the molecule must possess nuclear spins that are spectroscopically distinguishable and capable of interacting with each other in a controlled manner (Criger et al., 2012; Jones, 2011, 2024).

The addressability of qubits is governed by the chemical shift parameter (δ). For logic operations to be applied to a specific qubit without perturbing the others, a large chemical shift difference between the involved nuclei is necessary (Chae et al., 2024; Jones, 2011, 2024; J. B. R. Lino et al., 2017). Meanwhile, communication between qubits, which is required for the creation of multi-qubit logic gates, is mediated by the scalar spin-spin coupling constant (J or

SSCC). A high J value is desirable, as the speed of logic operations is inversely proportional to the magnitude of the coupling; that is, stronger couplings allow for faster computations, minimizing the deleterious effects of decoherence, which tends to destroy quantum information over time (Chae et al., 2024; Jones, 2011, 2024; J. B. D. R. Lino et al., 2020; J. B. dos R. Lino et al., 2022). Thus, the optimization of these NMR parameters through molecular engineering is a critical step for the advancement of this technology.

1.2.4.1 Intramolecular Interactions and NMR parameters

The suitability of a molecule for quantum information processing is strictly dependent on its magnetic properties, which are governed by the local electronic environment surrounding the nuclei (Jimmink et al., 2021; Scheiner et al., 2024; Viesser et al., 2018). As previously established, distinct chemical shifts are required to address qubits individually, and significant scalar couplings are necessary for quantum logic operations (Chae et al., 2024; J. B. D. R. Lino & Ramalho, 2019; J. B. dos R. Lino et al., 2022; J. B. R. Lino et al., 2017). It is well established in the literature that these NMR parameters are highly sensitive to structural variations and electronic perturbations, including those caused by non-covalent interactions, such as pnictogen, chalcogen, and halogen bonds (Criger et al., 2012; Jimmink et al., 2021; Jones, 2011, 2024; Scheiner et al., 2024; Viesser et al., 2018).

These intramolecular interactions can induce profound changes in the electron density distribution and orbital energies of the interacting atoms (Jimmink et al., 2021; Krivdin, 2020; Ramszv, 1950; Scheiner et al., 2024). To understand the influence of these interactions on the chemical shift, one can refer to Ramsey's theory of nuclear shielding (Krivdin, 2020; Ramszv, 1950). Ramsey described the shielding tensor as the sum of diamagnetic and paramagnetic contributions. The diamagnetic term depends on the ground-state electron distribution, while the paramagnetic term involves the mixing of ground and excited states induced by the magnetic field (Krivdin, 2020; Ramszv, 1950). Intramolecular interactions, particularly those involving heavier atoms like phosphorus or selenium, significantly alter the orbital angular momentum and the energy gaps between occupied and virtual orbitals, thereby modulating the paramagnetic contribution and shifting the resonance frequencies (Krivdin, 2020; Rusakov et al., 2015).

This modulation capability is a powerful tool for qubit design. By engineering specific intramolecular interactions, it is possible to tune the chemical shift difference between two nuclei (Alkorta & Popelier, 2023; Dračinský et al., 2018; Ramszv, 1950). A larger $\Delta\delta$ improves

the spectral resolution, ensuring that the radiofrequency pulses intended for one qubit do not accidentally perturb another (Duddeck, 1995; Rusakov et al., 2015; Rusakova & Rusakov, 2020; Zheng et al., 2017). Thus, the presence of a pnictogen or chalcogen bond can be strategically used to increase the distinguishability of qubits, directly satisfying one of the key conditions for effective quantum control.

Similarly, the scalar coupling is physically transmitted through the intervening electrons connecting the two nuclei. The dominant mechanism for this interaction in many systems is the Fermi contact (FC) term, which depends on the s-character of the bonding orbitals and the electron spin density at the nucleus (Alkorta & Popelier, 2023; Dračinský et al., 2018). When an intramolecular interaction brings two NMR-active nuclei closer, or creates a direct orbital pathway between them, as seen in pnictogen bonds where the overlap between lone pairs and antibonding orbitals is significant the efficiency of the spin information transfer is dramatically altered (Michalczyk et al., 2025; Scheiner, 2011a, 2011c, 2013; Scheiner et al., 2024).

This phenomenon is often described as through-space coupling, although, from a molecular orbital perspective, it arises from the direct overlap of orbitals in the interaction region, effectively acting as a bridge for spin communication (Dračinský et al., 2018; J. B. D. R. Lino & Ramalho, 2019; Nordheider et al., 2015; Sanz Camacho et al., 2016). Studies indicate that stronger orbital interactions often lead to a substantial increase in the magnitude of the J-coupling (Rusakova & Rusakov, 2020; Sanz Camacho et al., 2016; Scheiner et al., 2024). This is of utmost importance for quantum computing because, as noted, the gate operation time is inversely proportional to J. A stronger intramolecular interaction that enhances J allows for faster quantum gates, enabling the system to perform more operations within the limited coherence time available (Chae et al., 2024; Jones, 2011, 2024).

Therefore, understanding and controlling these intramolecular forces provides a purely chemical means to engineer superior qubits. By manipulating the strength and nature of pnictogen or chalcogen bonds, for instance, by varying substituents to alter the Lewis acidity/basicity of the interacting centers, chemists can systematically optimize the NMR parameters. This establishes a direct link between the fundamental nature of chemical bonding and the performance of a quantum processor, highlighting the importance of characterizing these interactions not just for structural stability, but for their functional role in quantum information technologies.

1.2.4.2 NMR for quantum computation

Nuclear magnetic resonance (NMR) spectroscopy is intrinsically rooted in quantum mechanics, as it probes the interaction between nuclear spins and external magnetic fields through well-defined quantum states (Chae et al., 2024; Jones, 2011, 2024; J. B. R. Lino et al., 2017; Lino & Ramalho, 2018). Nuclei with non-zero spin angular momentum possess a magnetic moment, which, when placed in an external magnetic field, gives rise to discrete energy levels associated with different spin projections (Rusakova & Rusakov, 2025). Transitions between these levels, induced by electromagnetic radiation in the radiofrequency range, constitute the fundamental physical basis of NMR spectroscopy.

From a quantum mechanical perspective, the nuclear spin represents a natural two-level system, formally equivalent to a quantum bit. In this framework, the spin-up and spin-down states correspond to the logical states $|0\rangle$ and $|1\rangle$, respectively (Chae et al., 2024; Jones, 2011, 2024). This correspondence has positioned NMR as one of the earliest experimental platforms for the implementation and conceptual development of quantum computation, particularly in proof-of-principle demonstrations of quantum algorithms and quantum control protocols (Chae et al., 2024; Jones, 2011, 2024; Kaushik & Khaneja, 2025).

In molecular systems, nuclear spins do not exist in isolation but are embedded in an electronic environment. The interaction between nuclear magnetic moments and the surrounding electron density leads to local magnetic shielding effects, which modify the effective magnetic field experienced by each nucleus (Chae et al., 2024; Rusakova & Rusakov, 2025). These shielding effects, quantified through chemical shifts, encode detailed information about the electronic structure and molecular geometry. From the standpoint of quantum chemistry, chemical shifts arise as response properties of the electronic system to an external magnetic perturbation, directly linking NMR observables to the underlying wavefunction or electron density (Chae et al., 2024; Jones, 2024; Rusakova & Rusakov, 2025; Scheiner et al., 2024; Yamauchi & Yanai, 2024).

The accurate theoretical description of NMR parameters therefore relies on quantum chemical methods capable of capturing the electronic response to magnetic fields (Rusakova & Rusakov, 2025). Approaches based on density functional theory (DFT) have become particularly important due to their favorable balance between accuracy and computational cost, enabling the study of medium- to large-sized molecular systems relevant to quantum information science (Bagno & Saielli, 2007; Das & Merz, 2025; Grunenber, 2010; Rusakova & Rusakov, 2025). In this context, NMR parameters serve not only as spectroscopic

observables but also as sensitive probes of subtle electronic effects, including weak intramolecular interactions and relativistic contributions in systems containing heavier elements.

In the realm of quantum computation, NMR offers a chemically intuitive and experimentally accessible platform for implementing quantum logic operations (Chae et al., 2024; Rusakova & Rusakov, 2025). Radiofrequency pulses can be used to coherently manipulate nuclear spin states, enabling the preparation, control, and readout of quantum states with high precision. Molecular systems containing multiple magnetically active nuclei can thus be viewed as small quantum registers, where individual spins act as qubits and their interactions define the structure of the quantum system (Chae et al., 2024; Jones, 2024; Rusakova & Rusakov, 2025).

Although NMR-based quantum computation faces intrinsic limitations, such as scalability and signal sensitivity at room temperature, it has played a fundamental role in establishing key concepts in quantum information processing (Jones, 2011, 2024; J. B. D. R. Lino & Ramalho, 2019; J. B. dos R. Lino et al., 2022; J. B. R. Lino et al., 2017). Moreover, the chemical tunability of molecular systems allows for rational design strategies aimed at optimizing NMR-relevant quantum properties, such as spin coherence and addressability, through controlled modifications of molecular structure and electronic environment (Jones, 2011, 2024; J. B. D. R. Lino et al., 2020; J. B. dos R. Lino et al., 2022).

Within this framework, quantum chemistry provides essential tools for understanding and predicting how molecular interactions influence NMR parameters that are critical for quantum computation. By linking electronic structure, molecular interactions, and spin dynamics, computational NMR emerges as a powerful approach for guiding the design of molecular architectures with tailored properties for quantum information applications.

1.2.5 Computational Chemistry

1.2.5.1 Density Functional Theory - DFT

Computational methods are useful for improving chemical studies, using equations to study molecules, complexes and several other chemical systems. The quantum mechanics calculations are techniques that use the Schrödinger equations to obtain chemical information. These methods could be divided into two different approaches, the semi-empirical methods, that uses pre-defined values for solving the Schrödinger equation, and the *ab initio* calculation,

that will solve the Schrödinger equation from the beginning, without pre-defined parameters (Cramer, 2013; Jensen, 2017).

The *ab initio* methods are used to solve the Schrödinger equation for systems with more than one electron, using the Hartree-Fock (HF) approximation, however this approach can not consider the electronic correlation of a molecular system (Cramer, 2013; Pessôa et al., 2018). In this sense, merge the post-Hartree-Fock (post-HF) methods were developed to include the electronic correlation in the calculations, nevertheless, these approaches are associated with a significantly higher computational cost. The computational scaling of the Hartree–Fock method increases approximately as N^4 , where N is the number of electrons in the system, on the other hand the post-HF methods are scaled with at least N^5 , N^6 , ..., N^n (Cramer, 2013; Jensen, 2017; Morgon, 2007).

This problem led to the development of DFT, which uses an approximation of the electronic density instead of the wave function as the variable of the Schrödinger equation, i.e., the Thomas-Fermi method (Jensen, 2017). Despite this, it was only in the 1960's, with the Hohenberg-Kohn theorems (HK), that the relation between the electronic and the true ground-state energy of a system was established.

The first theorem aims that an external potential ($V_{ext}(r)$) for the electrons of the system, the one that describes the nuclear interaction with the electrons, is determined solely by the density of the ground state so to describe the dependence on energy of the fundamental state concerning this density, it is enough to show that this density determines the Hamiltonian operator (\hat{H}) of the system and that its integration provides the number of electrons in the system (Equation 1) (Duarte, 2001).

$$\int \rho(r) = N \quad (1)$$

This theorem then establishes that energy can be described in terms of a functional of the electronic density of the fundamental state. To corroborate with this result that a certain density is the density in the fundamental state, Theorem 2 establishes that:

Theorem 2 - The electronic density of the fundamental state can be calculated, in principle, using the variational method, where the total calculated energy of this density ($E[\rho(r)]$) cannot be less than the real energy of the fundamental state (E_0), as shown in Equation 2. The name “functional” comes from the fact that energy depends on a function, which in DFT is density,

which depends on spatial variables, *i.e.*, $E[\rho(\mathbf{r})]$. Based on wave function-based methods, energy is a function of the wave function ($E[\psi(\mathbf{r})]$) (Duarte, 2001).

$$E[\rho(r)] \geq E_0 \quad (2)$$

It is possible to express the energy of the fundamental electronic state according to equation 3, applying the HK theorems.

$$E_0 \leq E[\rho(r)] = T_e[\rho_0] + E_{ee}[\rho_0] + E_{Ne}[\rho_0] \quad (3)$$

where the first term is related to electronic kinetic energy, the second related to electron-electron potential energy and the last one is the electron-nucleus potential energy. However, the HK theorems do not provide enough information for the construction of the density functionalities mentioned above. Only the functional $E_{Ne}[\rho_0]$ is fully known.

In this line, it merges the Kohn-Sham (KS) method, which allows the direct application of the HK theorem in atomic and molecular systems (Duarte, 2001; Kohn, 1965). In this method, the density of a fictional system with electrons that do not interact can be considered as a representation of the density of the fundamental state of a proper system. The kinetic part of the fictitious system is similar to the kinetic part of the HF method, so a correction term is added to the kinetic energy functional (Equation 4).

$$T[\rho] = T_s[\rho] + T_c[\rho] \quad (4)$$

where $T_s[\rho]$ is the kinetic energy of a fictitious system and $T_c[\rho]$ is the kinetic correction due to electron-electron interaction. The contribution of $T_c[\rho]$ is small when compared to $T_s[\rho]$.

The exact density functional is known for the classic Coulomb interaction between two electrons (Equation 5). However, it is also necessary to know the non-classical electron-electron interactions, commonly referred as exchange and correlation interactions.

$$J[\rho] = \iint \frac{\rho x_1 + \rho x_2}{r_{12}} \delta x_1 \delta x_2 \quad (5)$$

where, $J[\rho]$ is the classical Coulomb interaction energy, $\rho(x_1)$ and $\rho(x_2)$ are the electron densities at positions x_1 and x_2 , and r_{12} is the distance between electrons.

In the KS method, the exchange and correlation interactions are inserted into an approximate functional, called the exchange and correlation functional (Equation 6).

$$E_{xc}[\rho] = E_x[\rho] + E_c[\rho] + T_c[\rho] \quad (6)$$

where, $E_{xc}[\rho]$ is the exchange–correlation functional, $E_x[\rho]$ is the exchange energy, $E_c[\rho]$ is the correlation energy, and $T_c[\rho]$ is the kinetic correlation contribution.

Thus, the total electronic energy can be expressed according to equation 7.

$$E_{elect}[\rho] = T_s[\rho] + \int V_{ext}\rho(x) + J[\rho] + E_{xc}[\rho] \quad (7)$$

where, $E_{elect}[\rho]$ is the total electronic energy, $T_s[\rho]$ is the kinetic energy of non-interacting electrons, V_{ext} is the external potential, $J[\rho]$ is the Coulomb energy, and $E_{xc}[\rho]$ is the exchange–correlation energy.

The exact expression for the exchange and correlation functional is not known, so for the use of the KS method, an appropriate determination of the exchange and correlation term is necessary. This term presents the most difficult physical interpretation of DFT. To perform the approximations, the local density approximation (LDA) and the generalized gradient approximation (GGA) are usually used (Duarte, 2001; Jensen, 2017).

The development of this exchange and correlation function has been studied to advance DFT. The first step towards this is the complete understanding of the chemical characteristics of the system to be investigated. Since there are several functionals available for DFT calculations, this understanding provides a better choice for the functional to be employed (Jensen, 2017).

Despite many functionals available, problems still exist and knowing them is important to improve computational investigations. The first problem is known as asymptotic behavior, where chemical properties involving differences in orbital energies, ionization energy, electron-affinity, among others are not adequately described, in molecular systems containing an electron far from the nucleus, which will be shielded by the other electrons, when comparing the experimental values (Jensen, 2017).

Another known problem with DFT is called derivative discontinuity. None of the functionals can properly describe the exchange–correlation potential with the variation in the

number of electrons, a phenomenon that reflects the chemical potential for charge transfer between two systems (Jensen, 2017).

The last problem is called electron correlation, which occurs when there is no total cancellation of the exchange and correlation functional with the corresponding part of Coulomb interactions, causing errors to appear when applied to paramagnetic systems (Jensen, 2017).

These three problems do not occur in the HF method, therefore, the use of hybrid functionals, which consider the HF method to correct the problems with DFT, has been a widely used solution (Jensen, 2017).

1.2.5.2 Atoms-in-Molecules

In the 1990's the atoms-in-molecules theory (AIM), developed by R.F.W. Bader and his group emerged an important approach for analyzing chemical interactions. This method allows the characterization of inter- or intramolecular interactions between two fragments or molecules at the bond critical points (BCP) (Bader, 1985). This analysis uses the electron density to obtain topological parameters related to the interaction.

The topological parameters provided by AIM are useful to study and understanding an interaction and its strength, among these parameters are the electron density ($\rho(r)$) and their Lapacian ($\nabla^2\rho(r)$), kinetic energy density ($G(r)$), potential energy density ($V(r)$) and total energy density ($H(r)= V(r)+ G(r)$) (Boraei et al., 2021; Thomas & Thomas, 2023; M. K. Tripathi & Ramanathan, 2023).

Over time, various quantum chemistry software programs that use DFT have provided the results for AIM analysis. These results include wave function files (wfn-files) that contain the information necessary for obtaining the topological parameters. Among the various software available it is possible to highlight the chemistry packages Gaussian (Frisch et al., 2009) and ORCA (Neese, 2022), that will provide the wfn-files for obtaining the topological parameters using software like AIMAll (Keith, 2019), AIMPAC (Cheeseman et al., 1992) or Multiwfn (Lu & Chen, 2012).

1.2.5.3 Natural Bond Orbital

The natural bond orbital (NBO) is the bonding orbital calculated to have the maximum electron density. The NBOs are part of a sequence that begins in the atomic orbitals (AOs) and leads to the molecular orbitals (MOs). This sequence passes through the so-called natural

atomic orbitals (NAOs), followed by the natural hybrid orbitals (NHOs), which then form NBOs and the natural (semi-)localized molecular orbitals (NLMOs) (Köppel et al., 1998; Weinhold et al., 2016).

This sequence leads to the possibility of writing each valence bonding NBOs (σ_{AB}) in terms of the NHOs, h_a and h_b , for atoms A and B, multiplying by a polarization coefficient c_a and c_b (Equation 8a). These coefficients may be equal for a covalent bond or with one much larger than the other for ionic bond (Weinhold & Landis, 2001). Also, the bonding NBO expressed in equation 8a, need to be paired with a valence antibonding NBO (Equation 8b) to complete the valence space (Weinhold & Landis, 2001).

$$\sigma_{AB} = c_A h_A + c_B h_B \quad (8a)$$

$$\sigma_{AB}^* = c_B h_A + c_A h_B \quad (8b)$$

Where σ_{AB} and σ_{AB}^* correspond to bonding and antibonding molecular orbitals formed from the linear combination of atomic orbitals h_A and h_B , with coefficients c_A and c_B .

In a Lewis perspective, the orbitals represented by equations 8a and 8b, are considered a donor and an acceptor, respectively. These orbitals can also be called Lewis and non-Lewis type NBO, for the donor and acceptor orbital, respectively. The non-Lewis orbital is not occupied by formalism considering an ideal Lewis structure (Weinhold & Landis, 2001).

The energetic contribution related to the $\sigma \rightarrow \sigma^*$ interaction can be described by equation 9, that uses the 2nd-order perturbation theory to estimate the $\sigma_i \rightarrow \sigma_j^*$ interaction (Weinhold & Landis, 2001).

$$\Delta E_{i \rightarrow j^*}^{(2)} = -2 \frac{\langle \sigma_i | \hat{F} | \sigma_j^* \rangle^2}{\varepsilon_{j^*} - \varepsilon_i} \quad (9)$$

where \hat{F} is the effective orbital Hamiltonian and the orbital energies of the NBOs donor and acceptor are $\varepsilon_i = \langle \sigma_i | \hat{F} | \sigma_i \rangle$ and $\varepsilon_{j^*} = \langle \sigma_j^* | \hat{F} | \sigma_j^* \rangle$, respectively. The σ_{AB}^* are usually the most important non-Lewis acceptor orbital, once they can act on resonance stabilization, H-bond, and other acceptor-donor interactions (Weinhold & Landis, 2001).

These natural orbitals are used to obtain the distribution of the electron density in atoms and in bonds paths. NBOs aim to encompass the maximum achievable electron density, ideally nearing 2.000, to yield the most precise representation of the natural Lewis structure of wave

function. A substantial electron density percentage (designated as %- ρ L), frequently exceeding 99% with typical organic molecules, aligns with a reliable depiction of the natural Lewis structure (Weinhold et al., 2016).

The natural bond orbital analysis can be performed by a software called NBO developed by the Theoretical Chemistry Institute at the University of Wisconsin. This software is affiliated to several other quantum chemical software, in some, such as Gaussian, ADF and ORCA, the NBO software is nature include in the program to generate the NBO results, and other, such as NWChem, have an interface to generate NBO archives, that can generate NBO results (Glendening et al., 2013; Weinhold et al., 2016).

1.2.5.4 Non-covalent Index

The non-covalent interaction index, often called as non-covalent interaction (NCI), based on the electron density (ρ) and the reduced density gradient (RDG) to generate a 2D visualization index of the NCI (Equation 10) (Contreras-García et al., 2011; Laplaza et al., 2021).

$$s = \frac{1}{3(3\pi^2)^{1/3}} \frac{|\nabla\rho|}{\rho^{4/3}} \quad (10)$$

where s is the reduced density gradient, ρ the electron density, and $|\nabla\rho|$ the magnitude of the gradient of the electron density.

Regions with small values of reduced density gradient are associated with low electronic densities, the same goes for the reverse behavior (Contreras-García et al., 2011; Laplaza et al., 2021; Thomas & Thomas, 2023).

The main use of NCI is related to the visualization of three-dimensional images of the isosurfaces of the RDG, characterizing the intensity of the interaction according to colors (Laplaza et al., 2021; Thomas & Thomas, 2023). This strength is obtained through the product of the electron density and its second eigenvalue of the Hessian at each point of the isosurface. The sign of the second eigenvalue of the Hessian of the electron density determines the attractive or repulsive character of the region (Contreras-García et al., 2011; Laplaza et al., 2021; Thomas & Thomas, 2023).

1.2.5.5 Energy Decomposition Analysis

Energy Decomposition Analysis (EDA) has established itself as one of the most powerful tools in modern quantum chemistry to interpret the nature of chemical bonding (Alkorta et al., 2020; de Azevedo Santos et al., 2023; de Azevedo Santos, Hamlin, et al., 2021a; de Azevedo Santos, van der Lubbe, et al., 2021; Wolters & Bickelhaupt, 2012, 2015). The fundamental goal of EDA is to bridge the gap between the precise but complex results obtained through Quantum Mechanics (such as total energies and wave functions) and heuristic chemical concepts, such as electrostatic attraction, steric repulsion, and covalency (Wolters & Bickelhaupt, 2015). Among the various proposed schemes, the method developed by Ziegler and Rauk, known as ETS (Extended Transition State), and its modern variations implemented within the Kohn-Sham DFT formalism, stand out for their physical robustness in describing inter- and intramolecular interactions (Bickelhaupt, 1999; Ziegler & Rauk, 1977).

The theoretical foundation of EDA is based on constructing the interaction energy through hypothetical steps connecting isolated fragments to the final supermolecule (Bickelhaupt, 1999; Bickelhaupt & Baerends, 2000; Fernández & Bickelhaupt, 2014; Wolters & Bickelhaupt, 2015). In the context of Kohn-Sham DFT, the total energy of a system is a functional of the electron density $\rho(\mathbf{r})$ and can be expressed as the sum of the kinetic energy of non-interacting electrons, nuclear and inter-electronic interactions, and the exchange-correlation term (E_{xc}). EDA leverages this formalism to decompose the bond energy (ΔE) into two main components, often associated with the Activation Strain Model (ASM): the strain energy and the interaction energy (Bickelhaupt, 1999; Bickelhaupt & Baerends, 2000; Fernández & Bickelhaupt, 2014; Wolters & Bickelhaupt, 2015).

$$\Delta E = \Delta E_{strain} + \Delta E_{int} \quad (11)$$

The strain term, ΔE_{strain} , represents the energy penalty paid to deform the isolated fragments from their equilibrium geometries to the geometry they assume in the final complex, as well as to excite them to the appropriate valence electronic state for bonding. The interaction term, ΔE_{int} , which captures the essence of the chemical bond between the deformed fragments, is decomposed into physically meaningful contributions (Bickelhaupt, 1999; Bickelhaupt & Baerends, 2000; Bickelhaupt & Houk, 2017; Fernández & Bickelhaupt, 2014; Wolters & Bickelhaupt, 2015):

$$\Delta E_{int} = \Delta V_{elstat} + \Delta E_{Pauli} + \Delta E_{OI} + \Delta E_{disp} \quad (12)$$

Each term in this equation reflects a specific stage of bond formation from the perspective of Kohn-Sham orbitals:

Electrostatic interaction (ΔV_{elstat}): Corresponds to the classical (quasi-classical) Coulomb interaction between the unperturbed charge densities of the fragments ρ_A and ρ_B and their respective nuclei. This term is generally attractive and reflects the ionic or electrostatic character of the interaction.

Pauli repulsion (ΔE_{Pauli}): Arises from the requirement that the total wave function of the system obeys the Pauli exclusion principle. When the occupied Kohn-Sham orbitals of the fragments begin to overlap, they must be orthogonalized to ensure the antisymmetry of the wave function. This process removes electron density from the internuclear region, deshielding the nuclei and increasing repulsion. This term is strictly repulsive and is the exact quantum correlate to the concept of steric repulsion.

Orbital interaction (ΔE_{OI}): This term captures the energy stabilization resulting from the relaxation of electron densities and orbital mixing. It encompasses charge transfer (interaction between occupied orbitals of one fragment and virtual orbitals of another, such as HOMO-LUMO) and intra-fragment polarization. ΔE_{OI} is frequently associated with the covalent character of the bond.

Dispersion (ΔE_{disp}): In functionals that do not natively describe London dispersion forces, an empirical or semi-empirical correction term (such as DFT-D3 or D4) is added to account for these long-range attractive interactions, which are crucial for weakly bound systems (Caldeweyher et al., 2020; Grimme et al., 2016).

The sum of the ΔV_{elstat} and ΔE_{Pauli} terms is sometimes referred to as "steric interaction" (ΔE^0), representing the energy the system would have if the electron densities were frozen and merely orthogonalized, without allowing the orbital relaxation that characterizes covalent bond formation (de Azevedo Santos et al., 2023; de Azevedo Santos, Hamlin, et al., 2021a, 2021b; Wolters & Bickelhaupt, 2012, 2015). This detailed decomposition allows for quantifying whether an interaction, such as the pnictogen bond discussed in this work, is dominated by electrostatic forces or possesses a determining orbital component.

1.2.5.6 Computational NMR spectroscopy

Computational NMR spectroscopy has established itself as an indispensable tool for assisting in the interpretation of complex experimental spectra and predicting the magnetic properties of new compounds, being particularly relevant in the design of candidate molecules for qubits (Bagno & Saielli, 2007; Chae et al., 2024; Das & Merz, 2025; Grunenberg, 2010; Rusakova & Rusakov, 2025). The dominant methodology for calculating NMR parameters is DFT, due to its excellent compromise between computational cost and accuracy for medium and large-sized systems, allowing for the virtual screening of diverse molecular architectures (Bagno & Saielli, 2007; Das & Merz, 2025; Grunenberg, 2010; Rusakova & Rusakov, 2025).

The calculation of the chemical shift is based on the determination of the nuclear shielding tensor (σ), which is the second derivative of the system's energy with respect to the external magnetic field and the nuclear magnetic moment (Bagno & Saielli, 2007; Das & Merz, 2025; Grunenberg, 2010; Rusakova & Rusakov, 2025). The standard method for these calculations is GIAO (Gauge-Including Atomic Orbitals). The use of GIAO orbitals is fundamental because it ensures that results are independent of the origin of the coordinate system chosen for the magnetic potential vector, guaranteeing gauge invariance and faster convergence with basis set size (Das & Merz, 2025). Compared with experimental data, the calculated isotropic shielding values are converted into chemical shifts relative to a reference standard, such as tetramethylsilane (TMS) or phosphoric acid, through the relationship $\delta = \sigma_{ref} - \sigma_{calc}$ (Das & Merz, 2025).

For the calculation of spin-spin coupling constants, second-order perturbation theory is employed to evaluate the response of the electron density to nuclear magnetic perturbations (Das & Merz, 2025; Rusakova & Rusakov, 2025). According to Ramsey's formulation, the total coupling J is the sum of four distinct physicochemical contributions: the Fermi contact (FC) term, the paramagnetic spin-orbit (PSO) term, the diamagnetic spin-orbit (DSO) term, and the spin-dipole (SD) term (Bagno & Saielli, 2007; Das & Merz, 2025). The Fermi Contact term, which describes the direct interaction between the nuclear spin and the s-electron density at the nucleus position, is frequently the dominant mechanism for couplings transmitted through bonds (or through space in lone pair interactions) in organic and organophosphorus systems (Bagno & Saielli, 2007; Das & Merz, 2025; Grunenberg, 2010).

The accuracy of these calculations depends critically on the quality of the basis set used. Since the Fermi contact term depends on the electron density exactly at the nucleus position, standard basis sets (designed for valence energy) are often insufficient (Bagno & Saielli, 2007;

Das & Merz, 2025; Grunenberg, 2010). The use of specialized basis sets, which include basis functions with high exponents to better describe the core region, such as modified pcJ-n or cc-pVnZ basis, is highly recommended to obtain reliable J values. The cc-pVnZ, correlation-consistent polarized valence n-zeta, are well known and have been used in many calculations, the polarization-consistent basis sets optimized for spin-coupling constants (pcJ-n), where n indicates the size level of the basis set, were specifically developed for NMR calculations. Furthermore, in systems containing heavy atoms, relativistic effects become non-negligible and must be included, for example, through the zero-order regular approximation (ZORA) to correctly capture spin-orbit couplings (Das & Merz, 2025; J. B. D. R. Lino & Ramalho, 2019; Pascual-Borràs et al., 2015).

2 SECOND PART

Article 1 - Written in accordance with journal standards - Published version	
Article Title:	Pnictogen bond-driven control of the molecular interaction between organophosphorus and acetylcholinesterase enzyme
Autors:	Gustavo A. Andolpho Teodorico C. Ramalho
Journal:	Journal of Computational Chemistry
ISSN	0192-8651
DOI	https://doi.org/10.1002/jcc.27328

Pnictogen Bond-Driven Control of the Molecular Interaction Between Organophosphorus and Acetylcholinesterase Enzyme

Gustavo A. Andolpho and Teodorico C. Ramalho *

*Correspondence to: Teodorico C. Ramalho (E-mail: teo@ufla.br)

ABSTRACT

This study addresses a comprehensive assessment of the interaction between chemical warfare agents (CWA) and acetylcholinesterase (AChE) systems, focus on the intriguing pnictogen-bond interaction (PnB). Utilizing the crystallographic data from the Protein Data Bank pertaining to the AChE-CWA complex involving Sarin (GB), Cyclosarin (GF), 2-[fluoro(methyl)phosphoryl]oxy-1,1-dimethylcyclopentane (GP) and and venomous agent X (VX) agents, the CWA is systematically displaced by increments of 0.1 Å along the P-O bond axis, extending its distance by 4 Å from the original position. The AIM analysis was carried out and consistently revealed the presence of a significant interaction along the P-O bond. Investigating the intrinsic nature of the PnB, the NBO and the EDA analysis unearthed the contribution of orbital factors to the overall energy of the system. Strikingly, this observation challenges the conventional σ -hole explanation commonly associated with such interactions. This finding adds a layer of complexity to understanding of PnB, encouraging further exploration into the underlying mechanisms governing these intriguing chemical phenomena.

Introduction

One of the most significant global risks today is the utilization of neurotoxic organophosphorus chemicals (OP) as chemical warfare agents.¹ Chemical warfare hinges on the deployment of toxic substances capable of causing fatalities, enabling mass destruction, and inflicting substantial harm on the environment.² Neurotoxic organophosphates stand out as the most remarkable and lethal compounds in the realm of chemical warfare.

These OPs act as an Acetylcholinesterase (AChE) inhibitor, leading to a covalent bond between the OP and the serine residue of the active site of AChE. This leads to a scenario where the OP is split and the enzyme is phosphorylated.^{1,2}

Chemical warfare agents have been used as weapons since ancient times. More recently, at the time of the Second World War, new and more lethal compounds were developed for this purpose.³ These include the G-series, which includes compounds such as sarin (GB), soman (GD), cyclosarin (GF), and GP, as well as the more recent V-series, which includes venomous agent X (VX). Figure 1 shows the structure of some of these compounds.

Human Acetylcholinesterase (AChE) is a serine protease that facilitates the hydrolysis of the acetylcholine (ACh) neurotransmitter to complete the transmission of nerve impulses at cholinergic synapses. Neurotransmission mediated by ACh is necessary for the nervous system to work.⁴ ACh

transmits the information by binding to the postsynaptic receptor. Following message transmission, the ACh molecule releases the postsynaptic receptor and returns to the synaptic cleft where it is hydrolyzed by the AChE enzyme, releasing acetate and choline.⁴

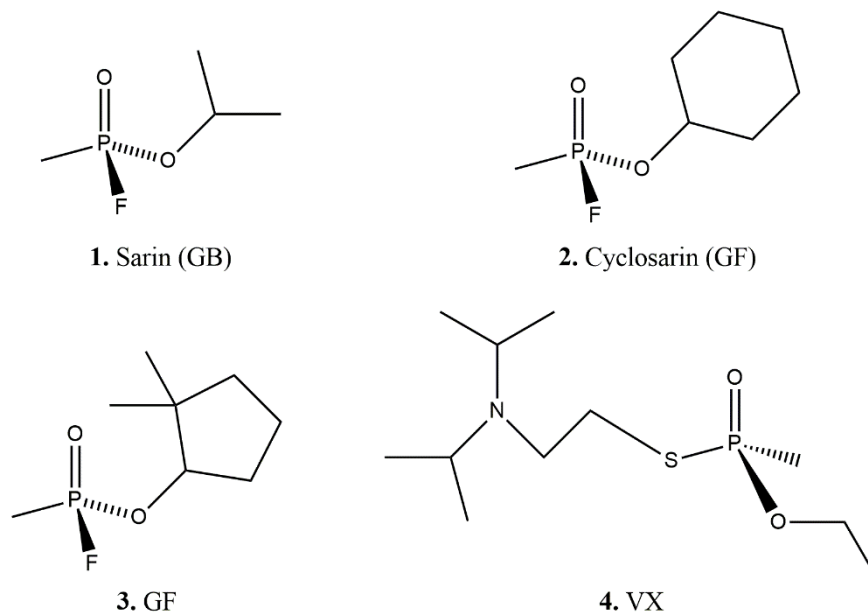


Figure 1. Structure of some organophosphorus chemical warfare agents.

When AChE is inhibited by an external agent, phosphorylated AChE, also known as aged-AChE, is obtained, which loses its biological function and causes an accumulation of acetylcholine in the synaptic cleft since hydrolysis of ACh is not possible. As a consequence, there is an overstimulation of the cholinergic pathway that leads to an interruption of neurotransmission.² The AChE inhibition can lead to muscle weakness and fasciculations, agitation, miosis, sweating, and hypersalivation, severe infections could lead to respiratory failure, confusion, unconsciousness, convulsion, and death.⁵⁻¹¹

The understanding of the interaction that occurs before the bond formation is a research field that can be further explored since the understanding of these interactions can lead to conclusions that lead to improvements in the proposition of agents capable of preventing AChE inhibition. Recent studies point out that the molecular interaction between the phosphorus atom of the OP and the oxygen of the serine can be considered a pnictogen bond (PnB).¹²

The pnictogen bond is the name given to an interaction that occurs between a pnictogen atom, *i.e.*, an element of the group 15 (nitrogen group), acting as Lewis acid, and an atom acting as a Lewis basis.^{12, 13} A model system where a PnB is occurring is presented in Figure 2. As well as other similar interactions, such as chalcogen and halogen bonds, the PnB is usually called a non-covalent interaction due to its electrostatic nature.¹⁴⁻¹⁷ However, understanding the nature of these weak interactions is still an open topic in the literature.¹⁸⁻²⁶

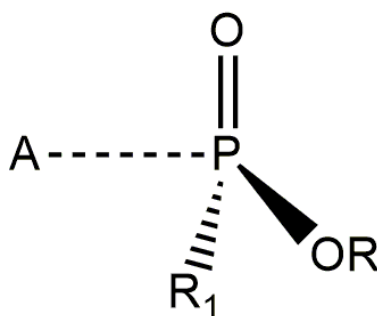


Figure 2. Schematic representation of a PnB in an OP compound. OR and R₁=ligands; A=Lewis basis.

Taking this into consideration, the present study aimed to investigate the Pnictogen Bond (PnB) formation between the organophosphorus (OP) chemical warfare agents and human acetylcholinesterase (AChE). The selected OP agents included the VX agent and the G-Series agents: Sarin (GB), Cyclosarin (GF), and GP. These systems, composed of the OP agents and AChE, were designated as **1**, **2**, **3**, and **4**, corresponding to GB, GF, GP, and VX agents, respectively.

Methods

Preparation of structures and energy calculations

The crystallographic structures of the four systems under study were obtained from the Protein Data Base under the codes 6WUZ, 6WVP, 6WVQ, and 6CQZ, for systems **1**, **2**, **3**, and **4**, respectively.²⁷ To study the molecular interactions between organophosphorus compounds and the protein target the Molegro Virtual Docker software was used.²⁸

Once is well known that the catalytic triad of hAChE, formed by serine-histidine-glutamate, it's responsible for the reactivity in the active site, these three residues were considered for the study of the OP-AChE interaction in the active site.²⁹⁻³¹

Thus, as the OP forms a chemical bond with the Serine residue from the catalytic triad to the inhibition of the enzyme,^{3, 32, 33} it is possible to scale down the system to contain the OP and the serine residue for further DFT calculations, using the Discovery Studio 2021 Software.³⁴ These two reductions in the system are important to make DFT calculations more feasible at a plausible computational cost.

Then, these systems were edited using the GaussView 5.0 software in order to move the OP away to serine to understand the behavior of the interaction that occurs between the P of the OP and the catalytic triad or the O of the serine during the OP approach to the serine. From the P-O distance of the crystallographic structure, the OP was moved away from the initial distance by 0.1 in 0.1 Å until it reached 4.0 Å more than the initial distance. This distance was defined using the energy profile of the systems. Specifically, the distance was truncated once the system reached a stable energy level.

Thus, all the 80 structures (40 OP plus catalytic triad and 40 OP plus serine) from the 4 systems were submitted to DFT single point calculations at B3LYP functional and def2-TZVP basis set using ORCA 5.0.4 package³⁵, this approach was previously used for similar systems.³⁶⁻⁴² In addition to the single-point calculation, wfn-files were obtained for the flowing analysis.

Nature of the molecular interactions

Using the wfn-files, the topological analysis of the Multiwfn 3.7 software⁴³ was used to perform the atoms-in-molecules (AIM) calculations.⁴⁴ From this analysis is possible to obtain the electron densities (ρ) and their Laplacian ($\nabla^2\rho$) at the bond critical points (BCPs), in order to analyze the interactions. Then, the interactions were also analyzed using the non-covalent interaction (NCI) theory⁴⁵ in the Multiwfn 3.7 software and VMD 1.9.3 visualization software.⁴⁶

In the sequence, natural bond orbital (NBO) analysis was applied to obtain the donor-acceptor interactions and the orbital and electronic contributions to the interaction energy. These calculations were performed using the NBO 6.0 program⁴⁷ in the Gaussian09 package⁴⁸ using the same theory level of the single-point calculations.

Then, the AMS2022 package⁴⁹ was used to analyze the energy decomposition analysis (EDA)⁵¹, at the B3LYP|TZ2P theory level. The fragments considered was the OP and the Serine residue. These approaches provide us insights into the composition of the energy at one point along the OP's approach to Serine residue.

Results and Discussion

Interaction between Organophosphorus and Acetylcholinesterase

The crystallographic structure of systems 1-4 were obtained from Protein Data Bank (PDB codes= 6WUZ; 6WVP; 6WVQ and 6CQZ, respectively). The crystallographic orientation for each system was analyzed Figure 3 shows the molecular structure of the four systems and the interactions identified by the docking study.

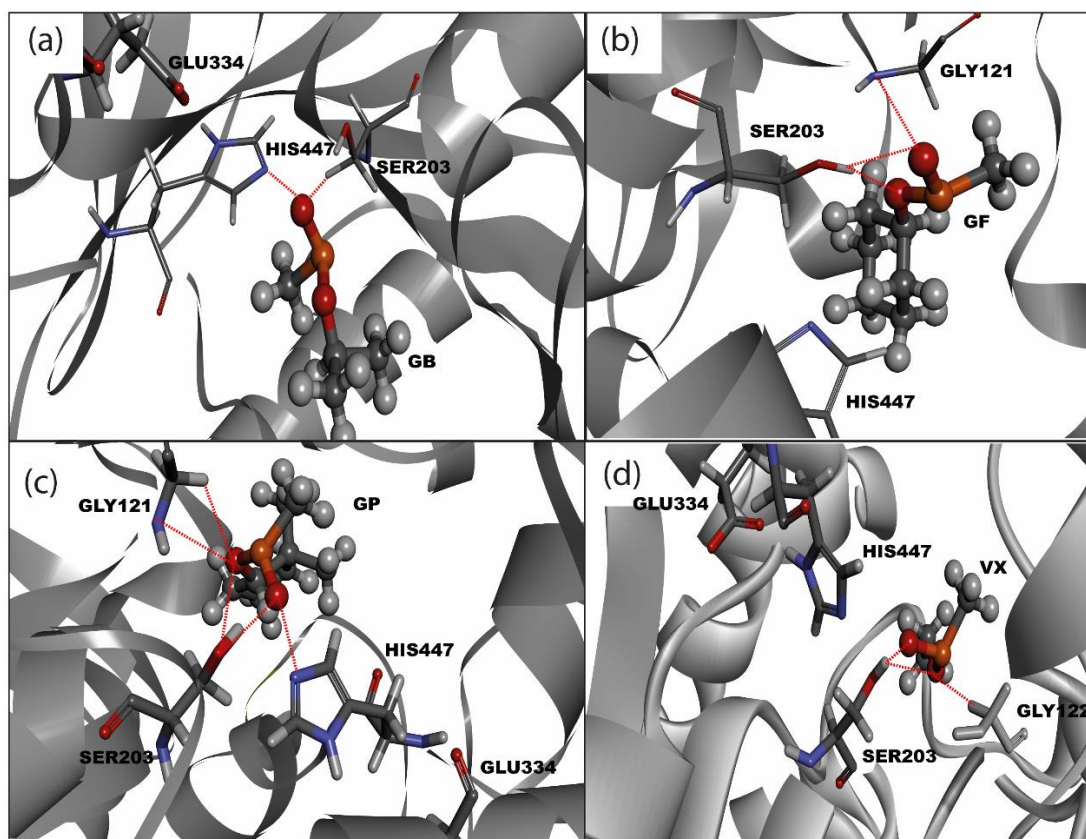


Figure 3. Interactions between OP and AChE active site for systems 1 (a), 2 (b), 3 (c), and 4 (d).

The protein-ligand binding affinity calculations were carried out at the Molecular Mechanics Level. For system 1, where GB is in the active site of AChE, it is possible to observe two hydrogen

bond interactions between the OP and the Serine203 and Histidine447 residues, the binding energy related to these interactions is about -2.50 and -2.41 kcal mol⁻¹, respectively. The pose interaction energy was -40.89 kcal mol⁻¹, indicating a favorable GB—AChE interaction. In system **2**, containing GF at the AChE active site, two H-Bond were observed between the OP and the Ser203 residue, with an interaction of -2.50kcal mol⁻¹ for each one. In addition, a weak H-Bond with Gly121 with an energy of -0.25kcal mol⁻¹ was observed. The interaction energy of GF and AChE was around -60.95kcal mol⁻¹, again indicating a favorable interaction.

Figure 3(c) shows the interactions present in system **3**, where it is possible to note that two H-Bonds are present between GP and Ser203, and one with His447, these three interactions show an interaction energy of 2.50 kcal mol⁻¹. Also, two weak interactions, with interaction energy of -0.91 and -0.32 kcal mol⁻¹, with Gly121 residue. The interaction energy between GP and AChE was around -82.49kcal mol⁻¹.

Finally, the system contains VX as organophosphorus, two H-Bonds can be observed between VX and the Serine203 residue, with interaction energies of -2.50 and -1.05 kcal mol⁻¹, and two weak H-Bonds with Gly122 residue, with interaction energies of -0.93 and -0.11kcal mol⁻¹. The interaction energy between the VX and AChE was -54.18 kcal mol⁻¹.

These results indicate that, as expected, the main interactions that occur between the organophosphorus and the AChE active site are with the serine and histidine residues. While some interactions between the OP and various glycine residues are present, they have very low energy, indicating that they are not significant for the OP-AChE interaction.

It is well-known that the AChE catalytic site is composed of a catalytic triad, which consists of the amino acid residues Serine203, Glutamine334 and Histidine447.^{52, 53} The docking calculation indicates that two of these residues, Ser203 and His447, exhibit significant interaction energy with the organophosphorus. Additionally, there is no identified interaction between OP and Glu334. However, this residue is crucial for the activation of the serine residue to facilitate the S_N² reaction with the OP (or acetylcholine).^{3, 32, 33}

With this in mind, it is possible to scale down the systems, considering the OP and the catalytic triad, for a deeper understanding of the strength and nature of molecular interactions evolved in the AChE active site, more sophisticated QM calculations will be employed.

Non-covalent Interactions at the Organophosphorus-Active Site

The study of the energetic profile of all four systems is important to understand the behavior of the bond/interaction between the OP and the catalytic triad. Our findings are shown in Figure 4.

By analyzing the graphs of Figure 4, it becomes clear that for all systems, there is a decrease in energy as the OP group begins to detach. Following this, the energy gradually increases until it reaches a stable state. Starting from the initial distance and progressing to the energy's lowest point, an evident chemical bond between P-O materializes. The establishment of a consistent energy level indicates the presence of an interaction involving the P-O bond.

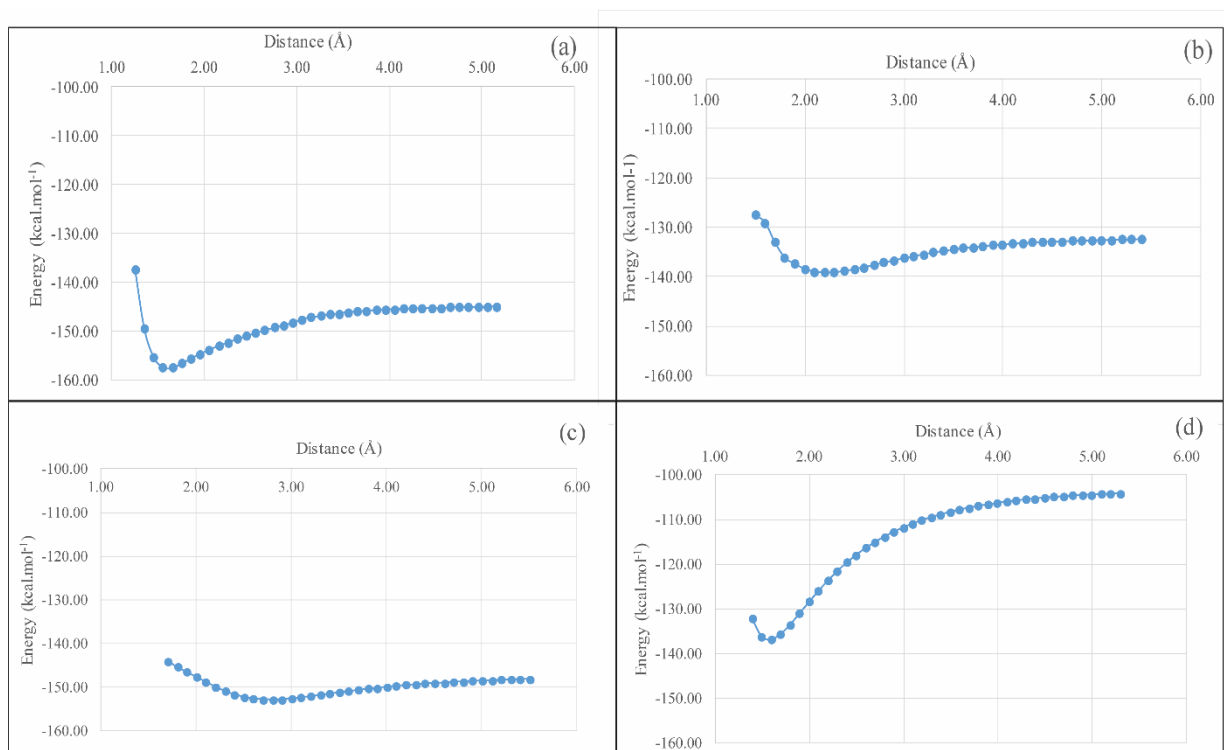


Figure 4. System Energy versus P-O distance for the systems **1** (a), **2** (b), **3** (c), and **4** (d).

It is possible to observe that for systems **1**, **2**, and **4** the energy stabilization and, thus, the indication of the P-O interaction occurs around 3.5Å. In the case of system **3**, stabilization becomes evident at approximately 4.5Å. Despite the noticeable disparity among the systems, it is worth noting that the initial P-O bond distance in the last system is slightly greater than the other three. This observation suggests that the distinction in stabilization energy between the systems is not

significantly substantial. Furthermore, the forthcoming topological analysis will aid in comprehending the interaction between the OP and the active site.

The atoms in molecules (AIM) analysis is widely used as a technique for studying the intra- and intermolecular interactions using the so-called bond critical points (BCP) through diverse parameters such as electron density ($\rho(r)$), Laplacian of the electron density ($\nabla^2\rho(r)$), kinetic energy density ($G(r)$), potential energy density ($V(r)$), and the total electron energy density ($H(r)$).^{36, 37, 54} These parameters, also called topological properties, are important to describe the strength and nature of the interaction.

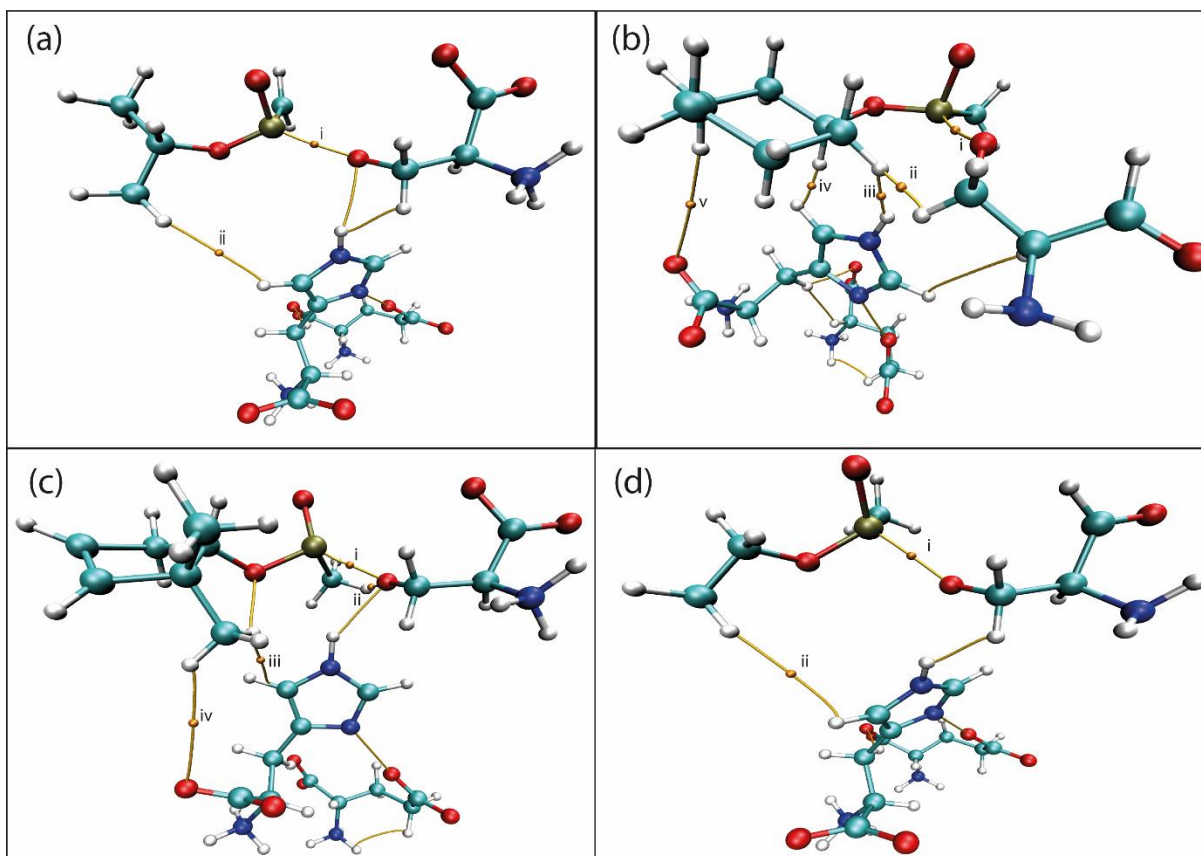


Figure 5. BCP for the systems **1** (a), **2** (b), **3** (c), and **4** (d) where the energetic profile indicates that the P-O bond became an interaction. H= white, C=light blue, N=dark blue, O=red, P=yellow.

Figure 5 presents the systems **1-4** and the BCP at the point where the energetic profile indicates that the P-O bond became an interaction, i.e., the distance between P and O is 2.00 Å for system **1**, 2.11 Å for system **2**, 2.40 Å for system **3**, and 2.26 Å for system **4**.

The topological parameters for each BCP that represents the interactions between OP and active site are presented in Table 1. From these results, it is clear that for all the systems the interaction between the Oxygen from serine and the phosphorus atom from OP is strong, and results in the formation of a chemical bound generating OP-AChE. This bond irreversibly inhibits the AChE enzyme.

Table 1. Partial values of topological parameters for the systems. Electron densities and their Laplacian are described in atomic units.

System	BPC	Electron Densities ($\rho(\mathbf{r})$)	Laplacian Electron Densities ($\nabla^2\rho(\mathbf{r})$)
1	i	0.0609	0.0202
	ii	0.0011	0.0041
2	i	0.0756	0.0407
	ii	0.0451	0.1292
	iii	0.0233	0.0808
	iv	0.0424	0.1192
	v	0.0011	0.0036
3	i	0.0780	0.0722
	ii	0.0691	0.2884
	iii	0.0102	0.0345
	iv	0.0010	0.0034
4	i	0.0507	0.0267
	ii	0.0008	0.0030

As the nature of H-Bond is similar to other non-covalent interactions, we have applied the Popelier and Koch criteria to characterize molecular interactions.⁵⁵⁻⁵⁹ Small positive values of $\nabla^2\rho$ associated with high values of ρ indicate that a strong interaction is occurring.^{60, 61} For all four

systems, the BPC i, which is the interaction pathway between the P and O exhibits a pronounced strength, with System **1** demonstrating the strongest interaction, followed by Systems **4**, **2**, and **3** in descending order of strength.

As anticipated, in all four systems, various other interactions are observed, warranting a thorough discussion. For System **1** an interaction path (path ii) can be observed between hydrogens from GB and histidine. This interaction can be characterized as a repulsive interaction. A similar repulsive interaction can be observed in all the other systems, described by the interaction paths iv, iii, and ii, for systems **2**, **3**, and **4**, respectively.

For systems containing GF and GP (systems **2** and **3**), other interactions can be noticed, for the first one, other two repulsive interactions between hydrogens are present, represented by paths ii and iii, with an interaction between atoms from the OP and serine and histidine, respectively. The final pathway within this system, labeled v, illustrates a fragile interaction between the hydrogen of OP and the oxygen of histidine. An analogous interaction is observed in System **3**, denoted as path iv. In contrast, the second significant interaction observed in this system, designated as BPC ii, is a robust connection involving the hydrogen from OP and the oxygen of serine, which participates in the pnictogen bond. This aspect potentially sheds light on the factors contributing to the comparatively weaker PnB observed in this system.

The significance of the Pnictogen Bond (PnB) toward the overall electron density, as evaluated by the BCP within the region bridging the OP and the active site, highlights this interaction as crucial in this area. This importance is particularly pronounced, with contributions exceeding 98% for systems **1** and **4**, approximately 49% for system **3**, and 40% within system **2**. These values collectively underscore the PnB as the foremost interaction transpiring between the OP and the active site.

From Molecular Interaction to Chemical Bonding: Organophosphorus-Serine Interaction

It is well-known that the catalyst behind the formation of aged-AChE is the reaction resulting in the bonding between the phosphorus from OP and the oxygen from serine.^{3, 32, 33} Keeping this in mind, it is possible to investigate specifically the formation of aged-AChE.

For all four systems, the BCP was selected in the path of the P-O bond, from the original bond length of the crystallographic structure to the final structure. These systems are shown in Figure

6. The topological parameters for the BCP at each distance can be seen in tables S1 to S4 in the supplementary material.

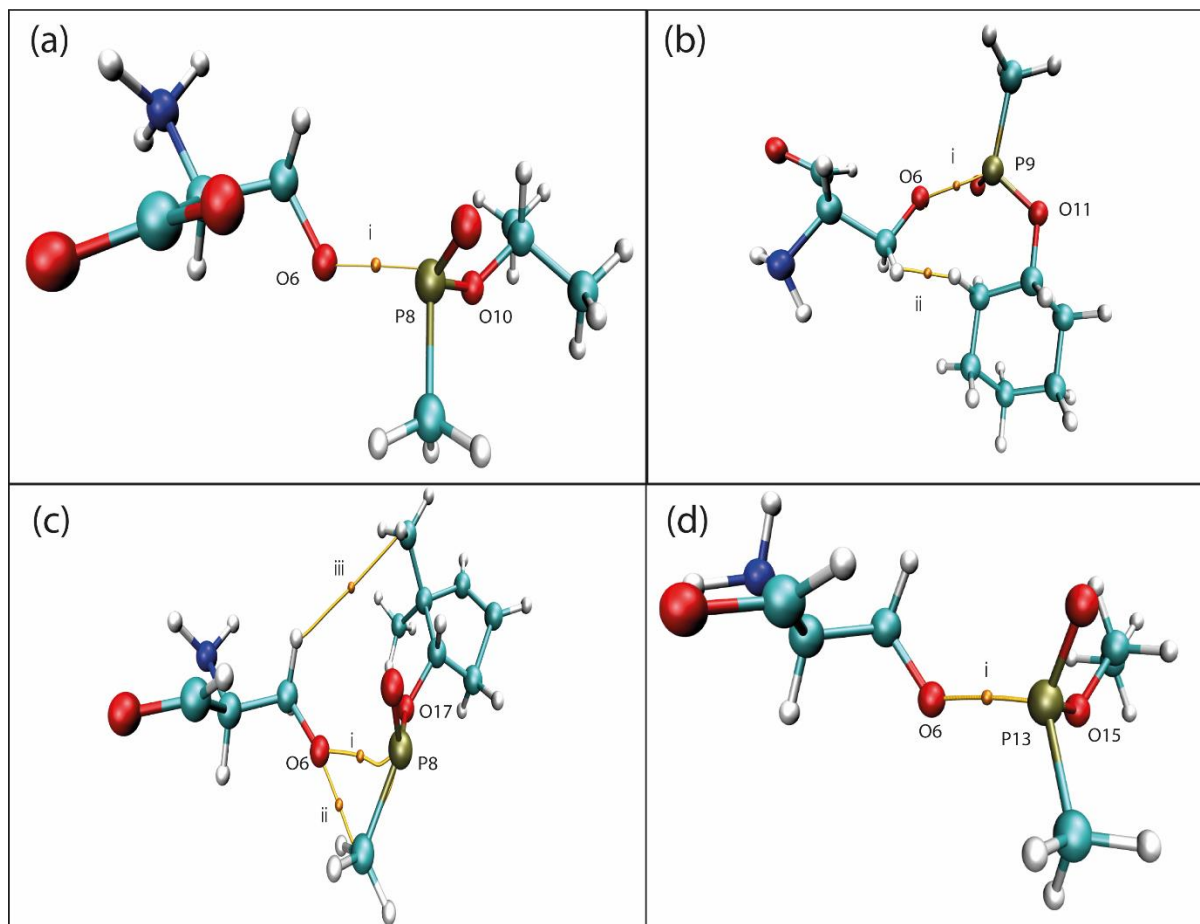


Figure 6. BCP for the systems **1** (a), **2** (b), **3** (c), and **4** (d) where the Laplacian of the electronic density turns slightly positive. H= white, C=light blue, N=dark blue, O=red, P=yellow.

Table 2 presents an overview of the topological parameters for the BCPs where the Laplacian of the electronic density turns slightly positive. This shift signifies the rupture of the P-O bond and indicates the initiation of an interaction between these atoms.

Table 2. Partial values of topological parameters for the systems. Distance in Angstroms, Electron densities and its Laplacian in atomic units.

System	Distance (Å)	Electron Densities ($\rho(r)$)	Laplacian Electron Densities ($\nabla^2\rho(r)$)
1	2.16	0.0897	-0.0231
	2.26	0.0774	0.0036
2	1.90	0.2200	-0.1012
	2.00	0.1754	0.1542
3	2.01	0.0888	-0.0031
	2.11	0.0770	0.0544
4	2.30	0.0307	-0.0066
	2.40	0.0514	0.0269

It is evident for all systems, that the alteration in the P-O interaction's nature is discernibly observed to manifest at approximately 2Å. In the case of GB (system **1**), this shift signifies a transformation from an open-shell to a closed-shell interaction, marked by a 1Å extension in the OP-Ser distance from the crystallographic structure. For GF (system **2**), the shift in interaction nature occurs at a distance 0.40Å beyond the initial OP-Ser distance. This similar behavioral pattern is observed for GP (system **3**). VX, on the other hand, exhibits a parallel behavior to the first system, with the alteration in interaction nature occurring 1Å beyond the crystallographic OP-Ser distance.

The topological parameters describe that the nature of the interaction path is in accordance with the systems containing the active site, indicating a stronger interaction in system **1**, followed by systems **4**, **3**, and **2**. The other BCP observed in system **2** is a repulsive interaction between hydrogens, as well as, the BCP iii of system **3**. The other BCP in system **3**, BCP ii, is related to the interaction between the O from serine and the H from the OP.

Similar to the scenario involving the active site, when solely focusing on serine, the Pnictogen Bond (PnB) emerges as the predominant interaction. It stands alone in Systems **1** and **4**, and accounts for approximately 66% in System **2** and 51% in System **3**. Consequently, delving into

the intrinsic nature of this interaction within these systems represents a pivotal stride in comprehending its significance in AChE inhibition.

Interaction between Organophosphorus and Acetylcholinesterase: Probing the Pnictogen Bond using Natural Orbitals Analysis

With the non-covalent interaction now elucidated, and this interaction indicating a Pnictogen Bond (PnB), a Natural Bond Orbital (NBO) analysis was carried out. This analysis aims to understand the primary interactions involving the phosphorus atoms and the main contributions spanning the 4Å distance from the crystallographic structure. Natural Bond Orbital (NBO) analysis estimates the charge localization between an acceptor and donor orbital, i.e., non-Lewis and Lewis type, respectively. For our systems, this analysis can provide information about the donor/acceptor orbitals of the phosphorus center and its energetic value. The second-order perturbation theory provides the energetic values related to the electron donation from the oxygen of serine to the σ^* of the organophosphorus P—O bond. This donation is responsible for characterizing the Pnictogen Bond. These energy values are presented in Table 3 for the distance of the crystallographic structure and the distance just before the chemical bond occurs.

Table 3. Energy for the donor/acceptor orbital related to the PnB. The number of atoms can be seen in Figure 6.

System	Donor/Acceptor	Distance (Å)	Energy (kcal mol ⁻¹)
1	n_{O6}/σ^*_{P8-O10}	1.26	34.00
		2.26	2.94
2	n_{O6}/σ^*_{P9-O11}	1.50	9.47
		2.00	3.33
3	n_{O6}/σ^*_{P8-O17}	1.71	8.29
		2.11	1.54
4	$n_{O6}/\sigma^*_{P13-O15}$	1.50	10.21

		2.40	1.16
--	--	------	------

A frame of the second-order perturbation energy value for the entire system is presented in the supplementary material (Tables S5 and S6), where it can be seen that the main energy contributions come from donations of σ and π orbitals to its anti-bonding, from system **1**. For system **2** the donor is the lone pair of oxygen and the acceptor is the π^* and σ^* . In systems **3** and **4**, it is possible to observe both cases. Moving to the final structure, *i.e.*, OP and Serine 4Å apart from an initial distance, different from the first stage, the phosphorus core orbitals receive electron density, as well as some π^* and σ^* , and the donations came from the oxygen lone pair.

In addition, Figure 7 shows a representation of these interaction orbitals for system **1** in both moments, *i.e.*, distance equals 1.26 and 2.26 Å. From these results, it is possible to notice that the interactions between the lone pair from the oxygen of serine and the anti-bonding orbital of the P—O bond, although decreasing, remain present when the OP is distanced from serine.

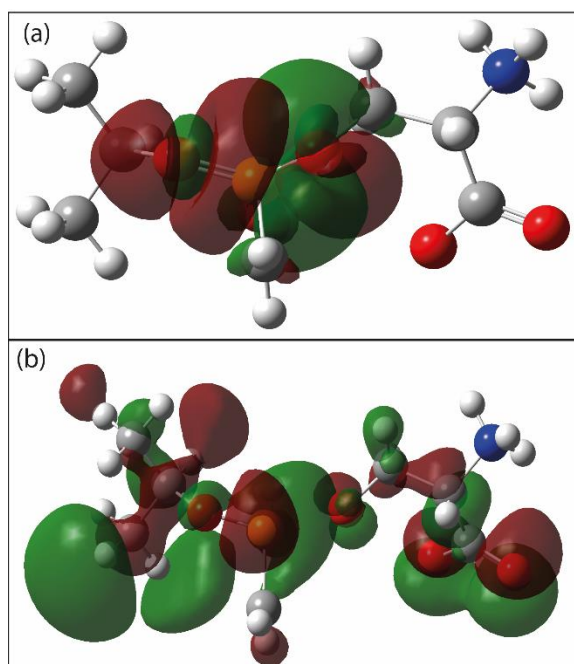


Figure 7. NBOs involved in the interaction of GB—Serine distance at (a) 1.26 and (b) 2.26Å.

For the other three systems a similar behavior can be observed (Figures S1, S2, and S3), with a higher orbital interaction in the crystallographic distance, and a lower, but still significant, interaction when the OP is 1Å further.

We note that the formation of a bond between the phosphorus of an organophosphate and the oxygen of the serine residue within the catalytic triad of AChE, resulting in AChE inhibition, is governed by the pnictogen bond interaction. However, it is important a better understanding of the nature of this interaction, which will be discussed in the following section.

Investigating the nature of Pnictogen Bond between Organophosphorus and Acetylcholinesterase

The initial step in investigating the nature of the Pnictogen Bond (PnB) within these systems involves employing the NCI index. This methodology is used to examine the nature of non-covalent interactions between molecules, thereby offering insights into the physical and chemical attributes of the system. This analysis involves plotting the reduced density gradient (RDG) against the product of the sign of the second Hessian eigenvalue (λ_2) and the electron density (ρ).⁴⁵ The RDG is rooted in the function proposed by Johnson et al.,⁶² which elucidates the distribution of electron densities around molecules. Employing this approach allows for the discernment of weak interactions, including hydrogen bonds, van der Waals contacts, and repulsive steric interactions. These interactions are differentiated using distinct color codes on both the scatter plot and the isosurface map. To identify the existence of a non-covalent interaction in the P-O bond axis, the isosurface map for the original crystallographic structure (Figure S4) was plotted. The regions indicated by the topological parameters, where the interactions transition from a covalent bond to a non-covalent interaction (Figure 8), encompass a distance increase of 3 Å (Figure 9) and involve structures with a P-O distance 4 Å larger than the initial configuration (Figure 10). It is evident that in the original crystallographic structure, there are no Non-Covalent Interactions (NCI) along the P-O bond axis, which is an expected outcome due to the covalent bonding between these two atoms. Figure 8 presents a distinct scenario where an interaction within this region becomes apparent. Blue surfaces depict robust attractive interactions, green surfaces signify van der Waals interactions, and red surfaces denote substantial repulsion. The depiction in Figure 8 indicates a minor attractive interaction between the phosphorus of the OP and the oxygen of serine residue, with the strongest occurrence observed in system **4**, followed by systems **3**, **1**, and **2**.

An essential point to highlight is the presence of a void, where there is a lack of interaction signal, encompassed by a zone featuring prominently attractive and repulsive interactions. This pattern

aligns with the prevalent explanation for this interaction type, known as the σ -hole. Similar to NCI, the σ -hole explanation solely accounts for electron density factors.^{15, 63}

Maps in Figures 9 and 10 indicate a different scenario, with a moderate to strong interaction in the P-O bond axis. In Figure 8, the distance of P-O is around 3 Å, demonstrating that both the energetic and topological analyses align, indicating the presence of a non-covalent interaction. In contrast to the shorter distance, the interaction between VX and serine (system **1**) emerges as the most potent, followed by systems **3**, **2**, and **4**.

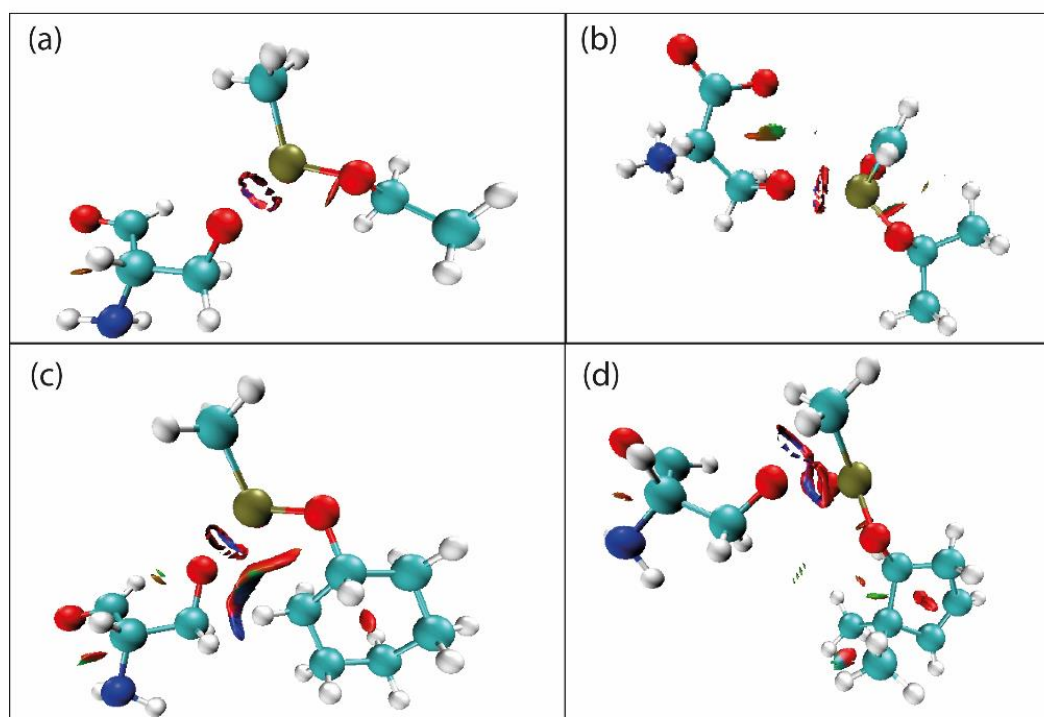


Figure 8. NCI plot (isovalue= 0.5 au) for the system (a) **1**, (b) **2**, (c) **3**, and (d) **4** at 1 Å P—O distance.

H= white, C=light blue, N=dark blue, O=red, P=yellow.

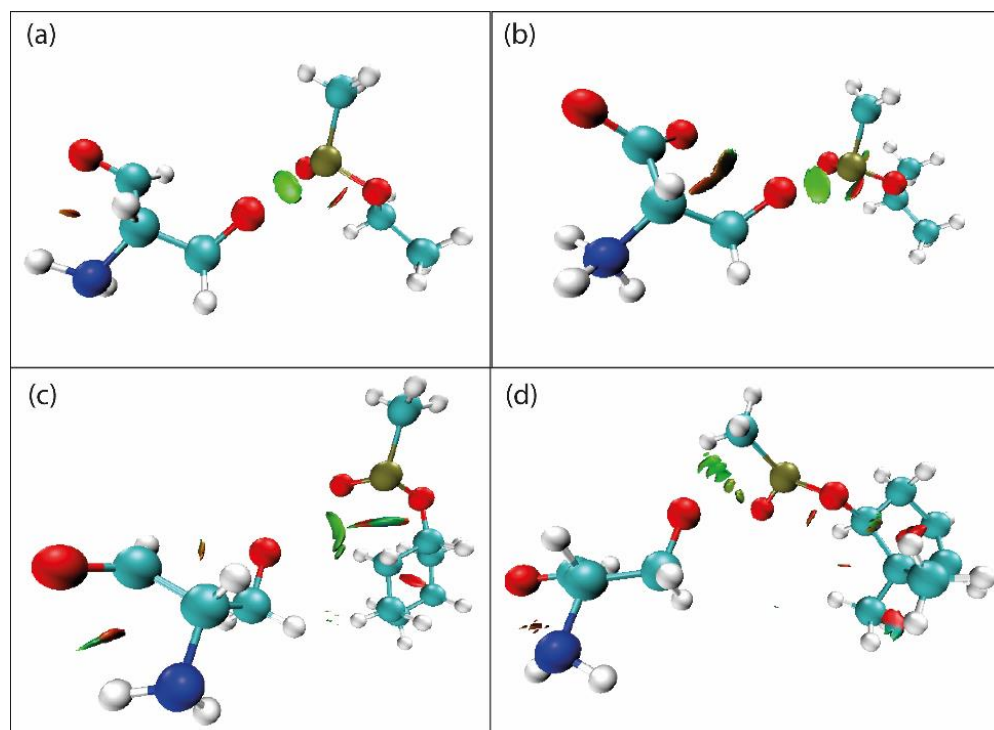


Figure 9. NCI plot (isovalue= 0.5 au) for the system (a) **1**, (b) **2**, (c) **3**, and (d) **4** at 3Å P—O distance.

H= white, C=light blue, N=dark blue, O=red, P=yellow.

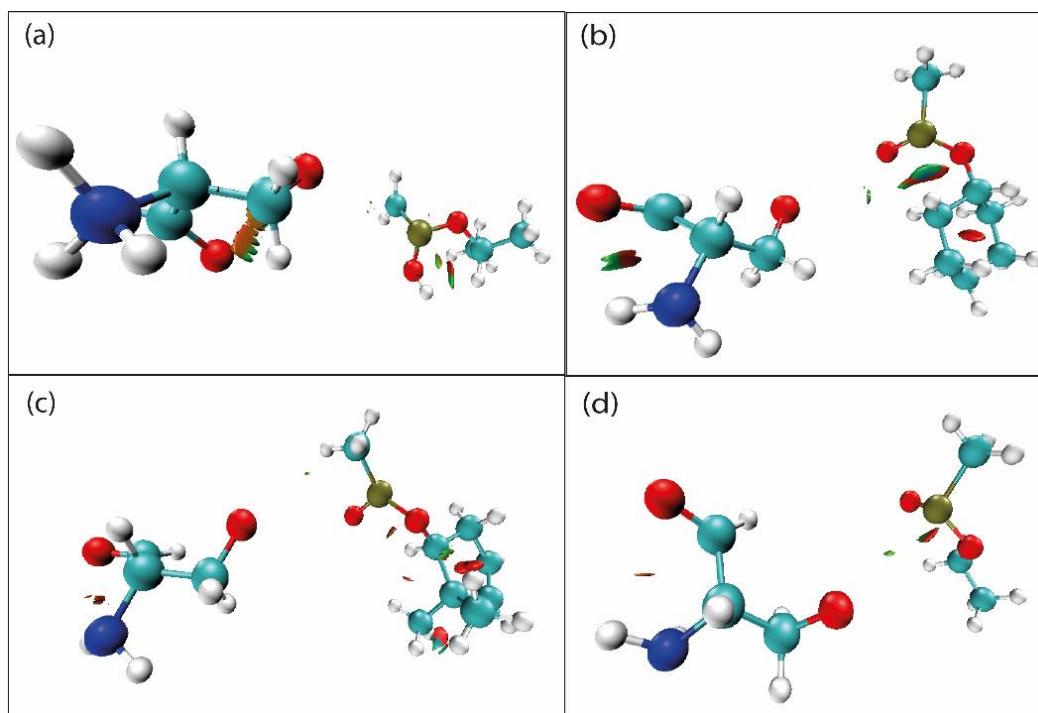


Figure 10. NCI plot (isovalue= 0.5 au) for the system (a) **1**, (b) **2**, (c) **3**, and (d) **4** at 4Å P—O distance.

H= white, C=light blue, N=dark blue, O=red, P=yellow.

When the OP and serine residue are separated by a distance of 4Å from their initial configuration, a subtle interaction continues to exist. This interaction is identified as attractive in a van der Waals (VdW) manner across all four systems. However, this increased distance renders the interaction in system **3** comparatively weaker, followed by systems **1**, **2**, and **4**.

Once we ascertain the persistence of the interaction over the entire OP-Serine distance, it becomes essential to study its nature in depth at the point where PnB begins to exist, i.e., at distances where there is no longer a chemical bond between the organophosphorus and the serine oxygen. For this, we have used the Energy decomposition Analysis (EDA)^{50, 51}, implemented in AMS2022 package⁴⁹ and computed at B3LYP/TZ2P level, that describes the interaction energy as a sum of three terms with physical meaning (Eq. S1).

These results are shown in Table S7 and point out that the pnictogen bond mechanism is not purely electrostatic, having a large covalent component (ΔE_{OI}), correspondent to 70.32% for system **1**, 70.29% for system **2**, 62.11% for system **3** and 81.98% for system **4** of the total bonding interactions, i.e., $\Delta E_{OI} + \Delta V_{elstat}$.

These findings are in line with the results obtained by Azevedo et al., in 2021, where they showed that the pnictogen bond is governed not only by electrostatic interactions, as the σ -hole indicates, but also by an orbital component.¹² The findings demonstrated that, in the case of charged Lewis acids and bases, the orbital contribution to the overall energy of the pnictogen bond spans from 33% to 65%.¹²

In this context, our results for the four systems illustrate the proportion of the energy derived from orbital interactions. Based on this outcome, we intend to demonstrate that even for a real system, with no charges, the orbital component persists.

A factor that may influence this difference in percentage contribution for our results and the ones found by Azevedo's, is the fact that the model systems presented in the literature are charged, while the systems involved in the pnictogen bond studied in the current work are neutral. Therefore, it is to be expected that the electrostatic contribution to the interaction energy will be greater.

With this, it is possible to observe that the Pnictogen Bond, although commonly categorized as a non-covalent interaction, displays a notable orbital, i.e., covalent, contribution.

Conclusions

This paper investigated interactions that transpire between a range of organophosphorus chemical warfare agents and their biological target, acetylcholinesterase. Of particular focus was the interaction between the phosphorus of the organophosphorus (OP) and the oxygen of the serine residue within the catalytic triad at the active site of AChE. Our investigation entailed EDA calculations, revealing that over than 60 percent of the overall system energy originates from orbital contributions. This finding implies that the energy associated with the pnictogen bond potentially incorporates a significant orbital factor.

Moreover, the NBO calculations illustrated an anticipated pattern: the energy associated with the transfer of a lone electron pair from the serine oxygen to the σ^* orbital of the OP P-O bond escalates in direct correlation with the OP's proximity to the serine residue.

The isosurface maps reveal that just before the establishment of the P-O-Ser bond, there exists a region within the bond path devoid of electronic density. This region shows an absence of interaction-related electronic density, forming what could be termed a "hole" in terms of interaction indication via electronic density. Even as the OP is distanced from the serine, a distinct region persists—often resembling a substantial disk—where an interaction between P and O can be identified. This interaction varies from strong to intermediate as the OP's distance increases.

Finally, the topological parameters confirm the existence of a Pnictogen bond between the phosphorus and the oxygen of the serine residue. Furthermore, this constitutes the primary interaction occurring between the oxygen and phosphorus (OP) and the catalytic triad of the AChE active site. Eventually, this molecular interaction leads to the formation of a chemical bond responsible for the enzyme's deactivation.

This pattern is observed for the systems containing the chemical warfare agents GB, GF, GP, and VX interacting both with the enzyme's active site and only with the serine residue participating in the bond.

All these results collectively emphasize the significant role of pnictogen bonding in AChE inactivation. Understanding how this interaction occurs and its nature is essential in order to be able to use it to maximize the power of agents capable of preventing the formation of the bond between an organophosphorus compound and AChE. This optimization can greatly enhance

responses to poisoning by compounds of this category. Although the most commonly used explanation for this type of interaction is the sigma-hole model, results from the literature and some of our findings highlight the substantial orbital component within this phenomenon.

Acknowledgments

The authors are thankful to Fundação de Amparo à Pesquisa de Minas Gerais (FAPEMIG), Coordenação de Aperfeiçoamento de Pessoal de Nível Superior (CAPES), Conselho Nacional de Desenvolvimento Científico e Tecnológico (CNPq) for financial support of this research. This study was supported by Excellence Project UHK.

Keywords: Chemical warfare agents; AIM analysis; NBO analysis; P-O Bonding; Pnictogen-bond interaction

Additional Supporting Information may be found in the online version of this article.

References and Notes

- (1) de Oliveira, O. V.; Cuya, T.; Ferreira, E. C.; da Silva Gonçalves, A. Theoretical investigations of human acetylcholinesterase inhibition efficiency by neurotoxic organophosphorus compounds. *Chemical Physics Letters* **2018**, *706*, 82-86. DOI: <https://doi.org/10.1016/j.cplett.2018.05.072>.
- (2) Figueroa-Villar, J. D.; Petronilho, E. C.; Kuca, K.; Franca, T. C. C. Review about structure and evaluation of reactivators of Acetylcholinesterase inhibited with neurotoxic organophosphorus compounds. *Current medicinal chemistry* **2021**, *28* (7), 1422-1442.
- (3) Delfino, R. T.; Ribeiro, T. S.; Figueroa-Villar, J. D. Organophosphorus compounds as chemical warfare agents: a review. *Journal of the Brazilian Chemical Society* **2009**, *20*, 407-428.
- (4) Soreq, H.; Seidman, S. Acetylcholinesterase—new roles for an old actor. *Nature Reviews Neuroscience* **2001**, *2* (4), 294-302.
- (5) Gifford, R. M.; Chathuranga, U.; Lamb, T.; Verma, V.; Sattar, M. A.; Thompson, A.; Siribaddana, S.; Ghose, A.; Forbes, S.; Reynolds, R. M.; et al. Short-term glucose dysregulation following acute poisoning with organophosphorus insecticides but not herbicides, carbamate or pyrethroid insecticides in South Asia. *Clinical Toxicology* **2019**, *57* (4), 254-264. DOI: 10.1080/15563650.2018.1515438.
- (6) Joshi, A. K. R.; Rajini, P. S. Reversible hyperglycemia in rats following acute exposure to acephate, an organophosphorus insecticide: Role of gluconeogenesis. *Toxicology* **2009**, *257* (1), 40-45. DOI: <https://doi.org/10.1016/j.tox.2008.12.006>.

- (7) Joshi, A. K. R.; Rajini, P. S. Hyperglycemic and stressogenic effects of monocrotophos in rats: Evidence for the involvement of acetylcholinesterase inhibition. *Experimental and Toxicologic Pathology* **2012**, *64* (1), 115-120. DOI: <https://doi.org/10.1016/j.etp.2010.07.003>.
- (8) Lasram, M. M.; Annabi, A. B.; Rezg, R.; Elj, N.; Slimen, S.; Kamoun, A.; El-Fazaa, S.; Gharbi, N. Effect of short-time malathion administration on glucose homeostasis in Wistar rat. *Pesticide Biochemistry and Physiology* **2008**, *92* (3), 114-119. DOI: <https://doi.org/10.1016/j.pestbp.2008.06.006>.
- (9) Possamai, F. P.; Fortunato, J. J.; Feier, G.; Agostinho, F. R.; Quevedo, J.; Wilhelm Filho, D.; Dal-Pizzol, F. Oxidative stress after acute and sub-chronic malathion intoxication in Wistar rats. *Environmental Toxicology and Pharmacology* **2007**, *23* (2), 198-204. DOI: <https://doi.org/10.1016/j.etap.2006.09.003>.
- (10) Selmi, S.; Rtibi, K.; Grami, D.; Sebai, H.; Marzouki, L. Malathion, an organophosphate insecticide, provokes metabolic, histopathologic and molecular disorders in liver and kidney in prepubertal male mice. *Toxicology Reports* **2018**, *5*, 189-195. DOI: <https://doi.org/10.1016/j.toxrep.2017.12.021>.
- (11) Teimouri, F.; Amirkabirian, N.; Esmaily, H.; Mohammadirad, A.; Aliahmadi, A.; Abdollahi, M. Alteration of hepatic cells glucose metabolism as a non-cholinergic detoxication mechanism in counteracting diazinon-induced oxidative stress. *Human & Experimental Toxicology* **2006**, *25* (12), 697-703. DOI: 10.1177/0960327106075064 (accessed 2023/02/24).
- (12) de Azevedo Santos, L.; Hamlin, T. A.; Ramalho, T. C.; Bickelhaupt, F. M. The pnicogen bond: A quantitative molecular orbital picture. *Physical Chemistry Chemical Physics* **2021**, *23* (25), 13842-13852.
- (13) de Azevedo Santos, L.; Ramalho, T. C.; Hamlin, T. A.; Bickelhaupt, F. M. Intermolecular Covalent Interactions: Nature and Directionality. *Chemistry—A European Journal* **2023**, *29* (14), e202203791.
- (14) Politzer, P.; Murray, J. S.; Clark, T. Halogen bonding and other σ -hole interactions: A perspective. *Physical Chemistry Chemical Physics* **2013**, *15* (27), 11178-11189.
- (15) Politzer, P.; Murray, J. S.; Concha, M. C. σ -hole bonding between like atoms; a fallacy of atomic charges. *Journal of molecular modeling* **2008**, *14*, 659-665.
- (16) Politzer, P.; Murray, J. S.; Clark, T. Explicit inclusion of polarizing electric fields in σ - and π -hole interactions. *The Journal of Physical Chemistry A* **2019**, *123* (46), 10123-10130.
- (17) Bauzá, A.; Mooibroek, T. J.; Frontera, A. The bright future of unconventional σ/π -hole interactions. *ChemPhysChem* **2015**, *16* (12), 2496-2517.
- (18) Shukla, R.; Chopra, D. "Pnicogen bonds" or "chalcogen bonds": exploiting the effect of substitution on the formation of $P \cdots Se$ noncovalent bonds. *Physical Chemistry Chemical Physics* **2016**, *18* (20), 13820-13829.
- (19) Zierkiewicz, W.; Michalczyk, M.; Wysokiński, R.; Scheiner, S. On the ability of pnicogen atoms to engage in both σ and π -hole complexes. Heterodimers of $ZF_2C_6H_5$ ($Z = P, As, Sb, Bi$) and NH_3 . *Journal of Molecular Modeling* **2019**, *25*, 1-13.
- (20) Alkorta, I.; Elguero, J.; Del Bene, J. E. Pnicogen bonded complexes of PO_2X ($X = F, Cl$) with nitrogen bases. *The Journal of Physical Chemistry A* **2013**, *117* (40), 10497-10503.

- (21) Del Bene, J. E.; Alkorta, I.; Elguero, J. Influence of substituent effects on the formation of P... Cl pnictogen bonds or halogen bonds. *The Journal of Physical Chemistry A* **2014**, *118* (12), 2360-2366.
- (22) Del Bene, J. E.; Alkorta, I.; Elguero, J. Pnictogen-bonded anionic complexes. *The Journal of Physical Chemistry A* **2014**, *118* (18), 3386-3392.
- (23) Wolters, L. P.; Bickelhaupt, F. M. Halogen bonding versus hydrogen bonding: a molecular orbital perspective. *ChemistryOpen* **2012**, *1* (2), 96-105.
- (24) de Azevedo Santos, L.; van Der Lubbe, S. C. C.; Hamlin, T. A.; Ramalho, T. C.; Matthias Bickelhaupt, F. A Quantitative Molecular Orbital Perspective of the Chalcogen Bond. *ChemistryOpen* **2021**, *10* (4), 391-401.
- (25) Larrañaga, O.; Arrieta, A.; Fonseca Guerra, C.; Bickelhaupt, F. M.; de Cózar, A. Nature of Alkali-and Coinage-Metal Bonds versus Hydrogen Bonds. *Chemistry—An Asian Journal* **2021**, *16* (4), 315-321.
- (26) Scheiner, S. Detailed comparison of the pnictogen bond with chalcogen, halogen, and hydrogen bonds. *International Journal of Quantum Chemistry* **2013**, *113* (11), 1609-1620.
- (27) McGuire, J. R.; Bester, S. M.; Guelta, M. A.; Cheung, J.; Langley, C.; Winemiller, M. D.; Bae, S. Y.; Funk, V.; Myslinski, J. M.; Pegan, S. D.; et al. Structural and Biochemical Insights into the Inhibition of Human Acetylcholinesterase by G-Series Nerve Agents and Subsequent Reactivation by HI-6. *Chemical Research in Toxicology* **2021**, *34* (3), 804-816. DOI: 10.1021/acs.chemrestox.0c00406.
- (28) Thomsen, R.; Christensen, M. H. MolDock: a new technique for high-accuracy molecular docking. *Journal of medicinal chemistry* **2006**, *49* (11), 3315-3321.
- (29) Hörnberg, A.; Tunemalm, A.-K.; Ekström, F. Crystal structures of acetylcholinesterase in complex with organophosphorus compounds suggest that the acyl pocket modulates the aging reaction by precluding the formation of the trigonal bipyramidal transition state. *Biochemistry* **2007**, *46* (16), 4815-4825.
- (30) Shafferman, A.; Kronman, C.; Flashner, Y.; Leitner, M.; Grosfeld, H.; Ordentlich, A.; Gozes, Y.; Cohen, S.; Ariel, N.; Barak, D. Mutagenesis of human acetylcholinesterase. Identification of residues involved in catalytic activity and in polypeptide folding. *Journal of Biological Chemistry* **1992**, *267* (25), 17640-17648.
- (31) Dvir, H.; Silman, I.; Harel, M.; Rosenberry, T. L.; Sussman, J. L. Acetylcholinesterase: From 3D structure to function. *Chemico-Biological Interactions* **2010**, *187* (1), 10-22. DOI: <https://doi.org/10.1016/j.cbi.2010.01.042>.
- (32) Zhuang, Q.; Young, A.; Callam, C. S.; McElroy, C. A.; Ekici, Ö. D.; Yoder, R. J.; Hadad, C. M. Efforts toward treatments against aging of organophosphorus-inhibited acetylcholinesterase. *Annals of the New York Academy of Sciences* **2016**, *1374* (1), 94-104. DOI: <https://doi.org/10.1111/nyas.13124> (accessed 2023/08/24).
- (33) Franjesevic, A. J.; Sillart, S. B.; Beck, J. M.; Vyas, S.; Callam, C. S.; Hadad, C. M. Resurrection and Reactivation of Acetylcholinesterase and Butyrylcholinesterase. *Chemistry – A European Journal* **2019**, *25* (21), 5337-5371. DOI: <https://doi.org/10.1002/chem.201805075> (accessed 2023/08/24).

- (34) SystÈMes, D. BIOVIA Discovery Studio. Dassault Syst mes: 2016.
- (35) Neese, F. Software update: The ORCA program system—Version 5.0. *WIREs Computational Molecular Science* **2022**, *12* (5), e1606. DOI: <https://doi.org/10.1002/wcms.1606> (accessed 2023/08/24).
- (36) Boraiei, A. T. A.; Haukka, M.; Sarhan, A. A. M.; Soliman, S. M.; Barakat, A. Intramolecular Hydrogen Bond, Hirshfeld Analysis, AIM; DFT Studies of Pyran-2,4-dione Derivatives. In *Crystals*, 2021; Vol. 11.
- (37) Tripathi, M. K.; Ramanathan, V. Nature and Strength of Sulfur-Centered Hydrogen Bond in Methanethiol Aqueous Solutions. *The Journal of Physical Chemistry A* **2023**, *127* (10), 2265-2273. DOI: 10.1021/acs.jpca.2c08314.
- (38) Hamlin, T. A.; van Beek, B.; Wolters, L. P.; Bickelhaupt, F. M. Nucleophilic Substitution in Solution: Activation Strain Analysis of Weak and Strong Solvent Effects. *Chemistry – A European Journal* **2018**, *24* (22), 5927-5938. DOI: <https://doi.org/10.1002/chem.201706075> (accessed 2023/11/27).
- (39) Zijlstra, H.; León, T.; de Cózar, A.; Guerra, C. F.; Byrom, D.; Riera, A.; Verdaguer, X.; Bickelhaupt, F. M. Stereodivergent SN2@P Reactions of Borane Oxazaphospholidines: Experimental and Theoretical Studies. *Journal of the American Chemical Society* **2013**, *135* (11), 4483-4491. DOI: 10.1021/ja400208t.
- (40) van Bochove, M. A.; Bickelhaupt, F. M. Nucleophilic Substitution at C, Si and P: How Solvation Affects the Shape of Reaction Profiles (Eur. J. Org. Chem. 4/2008). *European Journal of Organic Chemistry* **2008**, *2008* (4), 587-587. DOI: <https://doi.org/10.1002/ejoc.200890003> (accessed 2023/11/27).
- (41) van Bochove, M. A.; Swart, M.; Bickelhaupt, F. M. Nucleophilic Substitution at Phosphorus Centers (SN2@P). *ChemPhysChem* **2007**, *8* (17), 2452-2463. DOI: <https://doi.org/10.1002/cphc.200700488> (accessed 2023/11/27).
- (42) van Bochove, M. A.; Swart, M.; Bickelhaupt, F. M. Nucleophilic Substitution at Phosphorus (SN2@P): Disappearance and Reappearance of Reaction Barriers. *Journal of the American Chemical Society* **2006**, *128* (33), 10738-10744. DOI: 10.1021/ja0606529.
- (43) Lu, T.; Chen, F. Multiwfn: A multifunctional wavefunction analyzer. *Journal of computational chemistry* **2012**, *33* (5), 580-592.
- (44) Bader, R. F. W. Atoms in molecules. *Accounts of chemical research* **1985**, *18* (1), 9-15.
- (45) Laplaza, R.; Peccati, F.; A. Boto, R.; Quan, C.; Carbone, A.; Piquemal, J.-P.; Maday, Y.; Contreras-García, J. NCIPLLOT and the analysis of noncovalent interactions using the reduced density gradient. *WIREs Computational Molecular Science* **2021**, *11* (2), e1497. DOI: <https://doi.org/10.1002/wcms.1497> (accessed 2023/08/24).
- (46) Humphrey, W.; Dalke, A.; Schulten, K. VMD: visual molecular dynamics. *Journal of molecular graphics* **1996**, *14* (1), 33-38.
- (47) Glendening, E. D.; Landis, C. R.; Weinhold, F. NBO 6.0: Natural bond orbital analysis program. *Journal of computational chemistry* **2013**, *34* (16), 1429-1437.

- (48) Frisch, M. J.; Trucks, G. W.; Schlegel, H. B.; Scuseria, G. E.; Robb, M. A.; Cheeseman, J. R.; Scalmani, G.; Barone, V.; Mennucci, B.; Petersson, G. A.; et al. Gaussian 09 Revision E.1. 2009.
- (49) Te Velde, G. t.; Bickelhaupt, F. M.; Baerends, E. J.; Fonseca Guerra, C.; van Gisbergen, S. J. A.; Snijders, J. G.; Ziegler, T. Chemistry with ADF. *Journal of Computational Chemistry* **2001**, *22* (9), 931-967.
- (50) Bickelhaupt, F. M. Understanding reactivity with Kohn–Sham molecular orbital theory: E2–SN2 mechanistic spectrum and other concepts. *Journal of computational chemistry* **1999**, *20* (1), 114-128.
- (51) Bickelhaupt, F. M.; Baerends, E. J. Kohn-Sham density functional theory: predicting and understanding chemistry. *Reviews in computational chemistry* **2000**, 1-86.
- (52) Zhang, Y.; Kua, J.; McCammon, J. A. Role of the catalytic triad and oxyanion hole in acetylcholinesterase catalysis: an ab initio QM/MM study. *Journal of the American Chemical Society* **2002**, *124* (35), 10572-10577.
- (53) Silman, I. The multiple biological roles of the cholinesterases. *Progress in biophysics and molecular biology* **2021**, *162*, 41-56.
- (54) Thomas, J. M.; Thomas, R. Study of Non-Covalent Interactions Present in the Tapinarof–Ethanol System with Special Emphasis on Hydrogen-Bonding Interactions. *The Journal of Physical Chemistry B* **2023**, *127* (26), 5933-5940. DOI: 10.1021/acs.jpccb.3c03152.
- (55) Koch, U.; Popelier, P. L. A. Characterization of CHO hydrogen bonds on the basis of the charge density. *The Journal of Physical Chemistry* **1995**, *99* (24), 9747-9754.
- (56) Popelier, P. L. A. Characterization of a dihydrogen bond on the basis of the electron density. *The Journal of Physical Chemistry A* **1998**, *102* (10), 1873-1878.
- (57) Mary, Y. S.; Mary, Y. S.; Rad, A. S.; Yadav, R.; Celik, I.; Sarala, S. Theoretical investigation on the reactive and interaction properties of sorafenib–DFT, AIM, spectroscopic and Hirshfeld analysis, docking and dynamics simulation. *Journal of Molecular Liquids* **2021**, *330*, 115652.
- (58) Scheiner, S. Transition between the Noncovalency and Covalency of σ -Hole Bonds. *The Journal of Physical Chemistry A* **2023**, *127* (46), 9760-9770. DOI: 10.1021/acs.jpca.3c06093.
- (59) Garazade, I. M.; Gurbanov, A. V.; Gomila, R. M.; Frontera, A.; Nunes, A. V. M.; Mahmudov, K. T.; Pombeiro, A. J. L. Spodium, halogen and hydrogen bonds in the reactivity of bis(2,4-bis(trichloromethyl)-1,3,5-triazapentadienato)-Zn(II). *New Journal of Chemistry* **2023**, *47* (34), 15856-15861, 10.1039/D3NJ02994H. DOI: 10.1039/D3NJ02994H.
- (60) Silva, D. R.; Silla, J. M.; Santos, L. A.; da Cunha, E. F. F.; Freitas, M. P. The Role of Intramolecular Interactions on the Bioactive Conformation of Epinephrine. *Molecular Informatics* **2019**, *38* (6), 1800167. DOI: <https://doi.org/10.1002/minf.201800167> (accessed 2023/08/24).
- (61) Toledo, E. J. L.; Ramalho, T. C. Controversies about hydrogen bonds in water molecules on the influence of high magnetic fields: implications on structural and electronic parameters. *Molecular Simulation* **2021**, *47* (14), 1159-1167. DOI: 10.1080/08927022.2021.1957883.

(62) Johnson, E. R.; Keinan, S.; Mori-Sánchez, P.; Contreras-García, J.; Cohen, A. J.; Yang, W. Revealing Noncovalent Interactions. *Journal of the American Chemical Society* **2010**, *132* (18), 6498-6506. DOI: 10.1021/ja100936w.

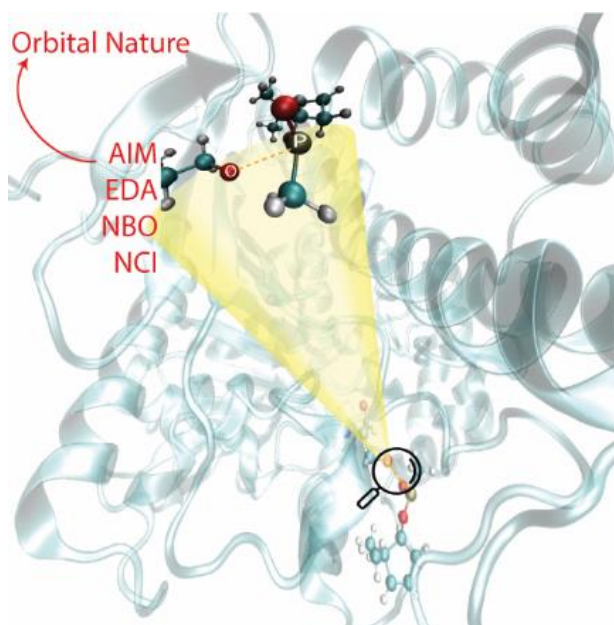
(63) Politzer, P.; Murray, J. S.; Clark, T.; Resnati, G. The σ -hole revisited. *Physical Chemistry Chemical Physics* **2017**, *19* (48), 32166-32178.

GRAPHICAL ABSTRACT

Gustavo A. Andolpho and Teodorico C. Ramalho

Pnictogen Bond-Driven Control of the Molecular Interaction Between Organophosphorus and Acetylcholinesterase Enzyme

Understanding the factors that lead to the formation of the bond between an organophosphorus, specifically chemical warfare agents, and AChE is essential for understanding these systems. This work used DFT techniques, such as AIM, NBO, and EDA, finding indications that this bond is driven by the pnictogen bond and, unlike the usual explanation that considers only electrostatic factors, orbital factors are important for this interaction.



Article 2 - Written in accordance with journal standards - Published version	
Article Title:	Intramolecular Pnictogen Bonds as Key Determinants for NMR Quantum Computation Parameters
Autors:	Gustavo A. Andolpho Teodorico C. Ramalho
Journal:	ACS Omega
ISSN	2470-1343
DOI	https://doi.org/10.1021/acsomega.5c05640

Intramolecular Pnictogen Bonds as Key Determinants for NMR Quantum Computation Parameters

Gustavo A. Andolpho¹ and Teodorico C. Ramalho^{1,2}*

¹Chemistry Department, Institute of Natural Sciences, Lavras Federal University, 37200-900, Lavras, MG, Brazil.

²Center for Basic and Applied Research, University Hradec Kralove, Hradec Kralove 500 03, Czech Republic.

ABSTRACT

In this work, four molecules, two naphthalene derivatives, and two acenaphthene derivatives were studied via DFT for their ability to act as a quantum bit (qubit) for transferring information for NMR Quantum Computational Information (QIP). NMR calculations indicate that all four molecules are suitable as qubits. Additionally, AIM, NBO, and EDA analyses provided insights into the presence and nature of intramolecular interactions between key atoms relevant to NMR-QIP. The results suggest that these P—P or P—Se interactions correspond to Pnictogen Bonds (PnB) in three compounds and to Chalcogen Bond in the other compound, with most of their interaction energy originating from orbital interactions. To investigate the role of PnB in NMR parameters, the P—P interaction was modified to either increase or decrease its interaction energy. AIM and EDA analyses, combined with NMR calculations, reveal that as the interaction strengthens, the NMR parameters become more suitable for NMR-QIP. Additionally, the results confirm that orbital interactions remain the primary contributor to the interaction energy. In summary, the findings of this study highlight the relationship between intramolecular pnictogen interactions and NMR parameters in four compounds with potential applications in quantum information processing.

INTRODUCTION

In recent years, the demand for quantum computers has been steadily rising, as they have the potential to solve complex problems that have challenged society for decades. At the same time, artificial intelligence is becoming an integral part of our daily lives, further driving the need for advanced computing power. This ongoing technological evolution is shaping the future in ways we are only beginning to understand¹. To meet this demand, many studies have emerged on

quantum information processing (QIP)¹⁻¹⁰. One of the main techniques for QIP is nuclear magnetic resonance (NMR)^{6-8,10}, which uses quantum bits (qubits) as the basis for transferring information⁷. To do this, qubits need to have spin 1/2, so nuclei such as ¹H, ¹³C, ¹⁹F, and ³¹P are some of the most common nuclei for this application^{4,5}. Other nuclei that also have this spin can be used for this purpose, such as ¹¹³Cd, ¹⁹⁹Hg or ⁷⁷Se^{4,5}.

One of the main challenges of Quantum Information Processing is its scalability. As a result, research on building large-scale quantum processors using NMR has become increasingly intense. Scientists are continuously exploring more efficient ways to control quantum states while also striving to accommodate a greater number of qubits within the system⁴. A good candidate for a qubit must be capable of implementing quantum gates, as well as being able to be put together in an organized and scalable way^{3,6,7,11}.

To be applicable for this use, a molecule must fulfill the so-called DiVincenzo criteria^{5,12}, having a large difference between the chemical shifts of the nuclei involved and a high value of spin-spin coupling between these nuclei³⁻⁵. Some studies have reported molecules that meet these criteria and can therefore be applied as qubits^{1,3-5}. Among these studies, it was possible to observe the use of molecules with naphthalene in their structure³, as well as the use of P and Se atoms as the nuclei of interest for NMR^{3,5}.

Therefore, the NMR parameters of these interest atoms are of great importance for a molecule to be applicable as a qubit. It is also well known that these parameters are sensitive to intermolecular or intramolecular interactions that can occur in the molecule^{6,7,10,13-15}. Given that some of the good qubit molecules contain the P nucleus as the atom of interest for the NMR values, it is crucial to relate the NMR parameters to the interactions that occur with this atom, in particular the so-called pnictogen bond (PnB)^{16,17}.

Recently, this interaction has attracted a lot of attention in the literature due to its importance in various types of systems¹⁷⁻²¹. Beyond pnictogen bonds, other types of directional interactions involving elements from groups 12 to 17 have also been widely explored. These include spodium, halogen, chalcogen, and tetrel bonds, which, despite involving different atomic centers, share key features with pnictogen bonds, such as their highly directional nature and dependence on electrostatic regions like σ -holes or π -hole^{19,22-26}. These regions act as localized sites of positive electrostatic potential that can engage in attractive interactions with electron-rich atoms or lone pairs. The comparative analysis of these interactions, both experimentally

and through DFT-based methods, has contributed to a broader understanding of how orbital and electrostatic effects combine to determine interaction strength and spectroscopic behavior^{13–15,22,23,27}. This broader framework reinforces the relevance of studying PnB not only as an isolated phenomenon but as part of a general class of interactions that can impact molecular design and function.

In addition, new findings have emerged that point to doubt regarding the explanation of the nature of the PnB^{16,17,19,20}, where the σ -hole, *i.e.*, the electrostatic factor, is used to justify the interaction between the atoms involved in the interaction²⁴. This doubt arises from studies that show that, not only in PnB but in other so-called non-covalent interactions, a large part of the interaction energy comes from the interaction between the Lewis orbitals of the acid and the base^{17,20}. Therefore, the strength and nature of the interactions that take place in molecules are important factors in understanding the behavior of these molecules in NMR and, consequently, their use for qubits.

The compounds investigated in this study were selected based on the presence of well-defined spin-active nuclei and well-characterized NMR behavior, as well as the occurrence of intramolecular interactions involving P and Se atoms, which can be analyzed in terms of pnictogen and chalcogen bonding. In this line, two compounds with substituted Naphthalene^{28,29} and two with substituted Acenaphthene^{30,31} that are suitable for QIP and present the PnB are shown in Figure 1. These four compounds were selected for this study to investigate, via DFT³², the influence of the Pnictogen Bond on the spin-spin coupling constants (SSCC) and the chemical shift (δ) values, which are essential parameters for the QIP^{1,8,10}.

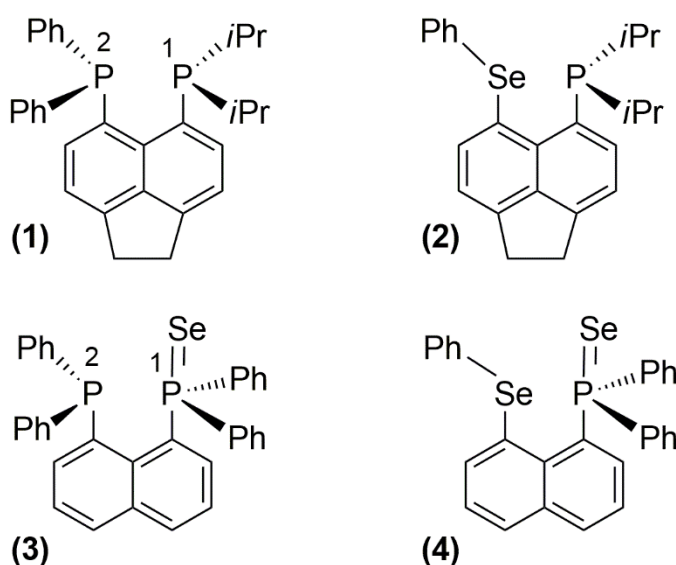


Figure 1. (1) Acenaphthene(PPh₂)(P*i*Pr₂); (2) Acenaphthene(SePh)(P*i*Pr₂); (3) Naphthalene(PPh₂Se)(PPh₂); (4) Naphthalene(PPh₂Se)(SePh).

METHODS

The crystallographic structures of compounds **1-4** were obtained from the Cambridge Crystallographic Data Base (CCDC codes= 1009481; 2278201; 145354 and 766926, respectively). These structures were optimized using density functional theory (DFT) with the PBE0 functional³³ including relativistic effects (ZORA), ZORA-TZVP basis set³⁴, and D4 dispersion corrections. Optimized geometries were confirmed as minimum by frequency analysis. This protocol was reported as an efficient methodology for the geometry optimization of similar compounds⁵.

NMR parameters, namely chemical shifts (δ) and spin-spin coupling constants (SSCC or J), were calculated using B3LYP|aug-cc-pVTZ-J and PBE0-ZORA|pcJ-2 level of theory, respectively. These protocols showed a successful performance for these parameters in these types of compounds^{3,35}. To obtain the δ , PH₃ and SeC₂H₆ were used as reference⁵, for P and Se, with chloroform as solvent using the CPCM solvation model.

Intramolecular interactions were characterized through atoms-in-molecules (AIM) analysis, performed using Multiwfn 3.7 software³⁶. The wfn-files were obtained through DFT calculations under B3LYP-ZORA|ZORA-TZVP theory level^{34,37}. In the sequence, the NBO 6.0 program³⁸ in the Gaussian09 package, using B3LYP functional and def2-TZVP basis set, was used to perform the natural bond orbital (NBO) analysis. Finally, the AMS2022 package³⁹ was used to perform the energy decomposition analysis (EDA) at the B3LYP|TZ2P theory level. These methods were selected due to their suitability for describing weak directional interactions such as PnB and ChB, allowing the assessment of their electronic nature and energetic contributions^{16-18,40}. To investigate the influence of these interactions on NMR parameters, internuclear distances were systematically varied at 0.1 Å intervals²⁰, with single-point calculations performed at each step. Unless otherwise specified, all DFT calculations were performed using the ORCA 5.0.4 package⁴¹.

RESULTS AND DISCUSSION

Validation of NMR Calculations

The first step is to validate our methodology for obtaining the NMR parameters. Table 1 presents J_{PP} , $\delta(P1)$, and $\delta(P2)$ values, for compounds **1** and **3** and J_{PSe} , $\delta(Se)$, and $\delta(P)$ values for compounds **2** and **4**, calculated, along with experimental values for these parameters, used as reference.

Table 1. Experimental and Theoretical NMR parameters, J_{PP} , $\delta(P1)$, and $\delta(P2)$, for compounds **1** and **3** and J_{PSe} , $\delta(Se)$, and $\delta(P)$ for compounds **2** and **4**.

Compound	Spin-Spin Coupling Constant (Hz)		Chemical Shifts (ppm)					
	Experimental ¹	Theoretical (Δ)	Experimental ¹		Theoretical (Δ)	Experimental ¹		Theoretical (Δ)
1	160	163.99 (3.99)	P(1)	-11.3	2.61 (13.91)	P(2)	-12.8	-23.71 (10.91)
2	452.2	408.567 (43.63)	Se	425.3	540.00 (114.70)	P	-6.0	5.05 (11.05)
3	53	48.318 (4.68)	P(1)	42.8	72.99 (30.19)	P(2)	-8.7	1.57 (10.27)
4	715	766.288 (51.29)	Se	451.4	449.62 (1.78)	P	40.5	90.03 (49.53)

¹ Experimental values from references 26, 25, 23, and 24, for compounds **1-4**, respectively.

These values point out that our theoretical approach is suitable for obtaining the NMR parameters for compounds **1-4**. For the δ values, the error is, in general, smaller for phosphorus, especially when the scale for this parameter is considered⁴²⁻⁴⁷. The error percentage related to the scale ranges from 1.8% for the P2 atom in compound **3** to 8.6% for the P atom in compound **4**. For the selenium atom, the error related to the scale is smaller than 0.5% for compound **4**, and around 4.4% for compound **2**.

The SSCC values present a similar behavior, with the calculated J_{PP} with smaller errors than J_{PSe} . Reported values for similar compounds point out that this error ranges from around 28 to 67 Hz for J_{PSe} ^{4,48} and 9 to 71 Hz for J_{PP} ^{3,49}. So, errors of around 4 Hz for compounds **1** and **3** J_{PP} and around 43 Hz for compound **2** and 51 Hz for compound **4** J_{PSe} are in agreement with the

reported values and, therefore, show the effectiveness of the theoretical methodology chosen to obtain the SSCC values^{3,4,48,49}.

The existence and nature of Intramolecular Interactions and their relationship with NMR quantum computation parameters

Intra(inter)molecular interactions are the name given to interactions similar to the hydrogen bond (HB), in which a Lewis acid interacts with a Lewis base, forming the interaction, which is classified according to the family of the atom in the periodic table^{14,24,50}. These include halogen (XB), chalcogen (ChB), pnictogen (PnB), and tetrel (TB) bonds^{14,19,50,51}. Understanding the nature of these interactions has attracted a lot of interest from the academic community in recent years^{14,16–20,24,50,51}, as controversies about the energy governing these interactions have arisen in recent years^{16–20,50}. Recent studies point out that the interaction energy between the σ^* orbital of the covalent bond from the Lewis acid and the HOMO of the Lewis base is the main factor in the interaction energy between these fragments, *i.e.*, a covalent component^{16,17}.

Studying the nature of intramolecular interactions is a crucial factor when considering molecules for qubits, as the literature suggests that these interactions significantly influence the NMR parameters of the atoms involved^{14,51}. The relationship between the strength of the interaction and the NMR parameters is well defined when related to Lewis bases; however, this correlation, although it exists, does not play a quantitative role in Lewis's acid analysis^{14,51}.

Recently, two studies have made a direct correlation between the NMR parameters and the interaction data provided by AIM calculations, for systems where there is HB, XB, ChB, PnB, or TB, occurring between Me₂CO and 20 different Lewis acids in one study¹⁴ and another study with (CH₃)₃PSe interacting with the same 20 Lewis acids⁵¹, pointing to a high correlation between the interaction energy and variation of shield tensor ($\Delta\sigma$) parameters for C and O in the first study, and the second study for the ΔJ_{PSe} value and some correlation with the $\Delta\delta(\text{P})$ and $\Delta\delta(\text{Se})$ values.

Also, the Pnictogen Bond has been investigated in several chemical phenomena showing its importance, however, there is a lack of NMR studies that consider how this type of interaction affects the NMR parameters. With this in mind, it is important to understand the molecular interaction, likely a pnictogen bond (PnB) formation, that occurs between the phosphorus atoms in compounds **1** and **3**, where one P could act as the Lewis Basis and the other as the Lewis

Acid, or for compounds **2** and **4**, between P and Se, where the Se atom could act as the donor atom and the P as the receiving atom.

Employing computational techniques can aid in understanding the intramolecular interactions that occur in the selected compounds. Methods such as the molecular electrostatic potential (MEP)¹⁴ and the non-covalent interaction (NCI) index⁵² are powerful tools for visualizing regions prone to interactions and highlighting weak contacts in molecular systems. However, in the present study, our main objective was to establish a direct correlation between specific molecular interactions, particularly intramolecular pnictogen bonds, and the NMR parameters of interest. To this end, we employed AIM, NBO, and EDA analyses, as these techniques offer a more detailed and quantitative assessment of molecular interactions. These methods enable a comprehensive evaluation of interaction topology, orbital contributions, and energy decomposition, providing insights that go beyond those afforded by MEP and NCI analyses. Accordingly, AIM, NBO, and EDA are particularly well-suited for elucidating the electronic nature of the interactions under investigation, as well as their influence on the associated NMR parameters.

The topological parameters obtained from the atoms-in-molecules (AIM) analysis at the bond critical points (BCP) offer valuable insights into the existence, nature, and strength of the interaction. Figure 2 brings information about the location of the BCP related to the intramolecular interaction on the four select compounds.

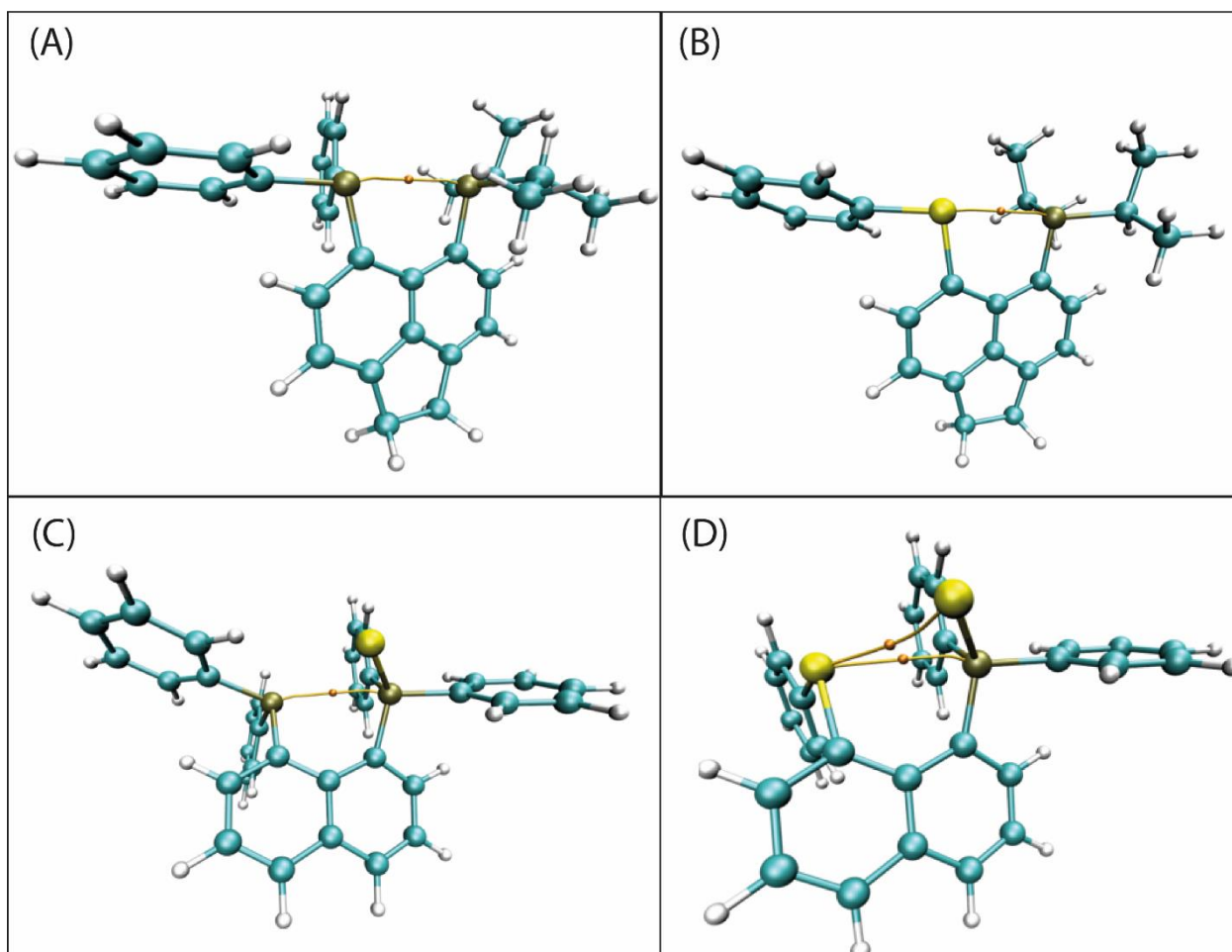


Figure 2. Bond Critical Points related to the intramolecular interactions for compounds **1** (A), **2** (B), **3** (C), and **4** (D).

The presence of a BCP between the P—P, compounds **1** and **3**, or P—Se, compounds **2** and **4**, axis evidence of the existence of an intramolecular interaction between these atoms. For compounds **1** and **3**, this interaction may be characterized as a pnictogen bond, since the interaction occurs between two pnictogen atoms. On the other hand, for compounds **2** and **4**, both pnictogen and chalcogen bonds can occur. Also, in Figure 2, part D, it is possible to observe a BCP in the axis of the Se—Se, pointing out an interaction between these atoms, i.e., a possible chalcogen bond. Then, it is necessary to understand the nature of this interaction.

Table 2 presents the values for the AIM parameters for the selected compounds. It is possible to compare the interaction of compounds **1** and **3**, with **2** and **4**, respectively. The values indicate that for both pairs of compounds, *i.e.*, **1** and **2**, and **3** and **4**, the intramolecular contact has similar characteristics. Similar values of ρ and $\nabla^2\rho$ are observed for both pairs at the BCP that correspond to the PnB, indicating that both compounds present a similar strength.

Table 2. Topological parameters (a.u.) at the Bond Critical Point (BCP) that correspond to the intramolecular interactions.

Compound	ρ	$\nabla^2\rho$	V	G	$-G/V$	E_{int}
1	0.0216	0.0358	-0.0109	0.0099	0.9095	-0.0055
2	0.0244	0.0447	-0.0134	0.0123	0.9169	-0.0067
3	0.0164	0.0372	-0.0089	0.0091	1.0203	-0.0045
4	0.0173	0.0387	-0.0095	0.0096	1.0073	-0.0048

* ρ =electron density; $\nabla^2\rho$ =Laplacian of the electron density; V =Potential energy; G =Kinetic energy.

To better understand the nature of these interactions, the natural bond orbital (NBO) analysis can provide insights into the orbitals involved in the interaction and the associated energy. In Figure 3, it is possible to observe the donating orbitals, corresponding to the lone pair of P or Se, and the receiving orbitals, *i.e.*, the $\sigma^*(P-C)$. Table S1 brings the main orbital contributions.

The most stabilizing donor-acceptor interaction is the one that is responsible for the intramolecular interaction, and, where applicable, the definition of the presence of a pnictogen or chalcogen bond. For compound **1**, the energy related to the interaction is around 2.56 kcal/mol. For compound **2**, the most significant interaction presents an energy of 7.76 kcal/mol between the P lone pair and the $\sigma^*(Se-C)$, indicating the presence of a chalcogen bond. Compounds **3** and **4**, like compound **1**, exhibit a PnB interaction, with slightly higher stabilization energies of 3.94 and 4.23 kcal/mol, respectively. These values suggest that the electronic features of these systems are very similar in nature.

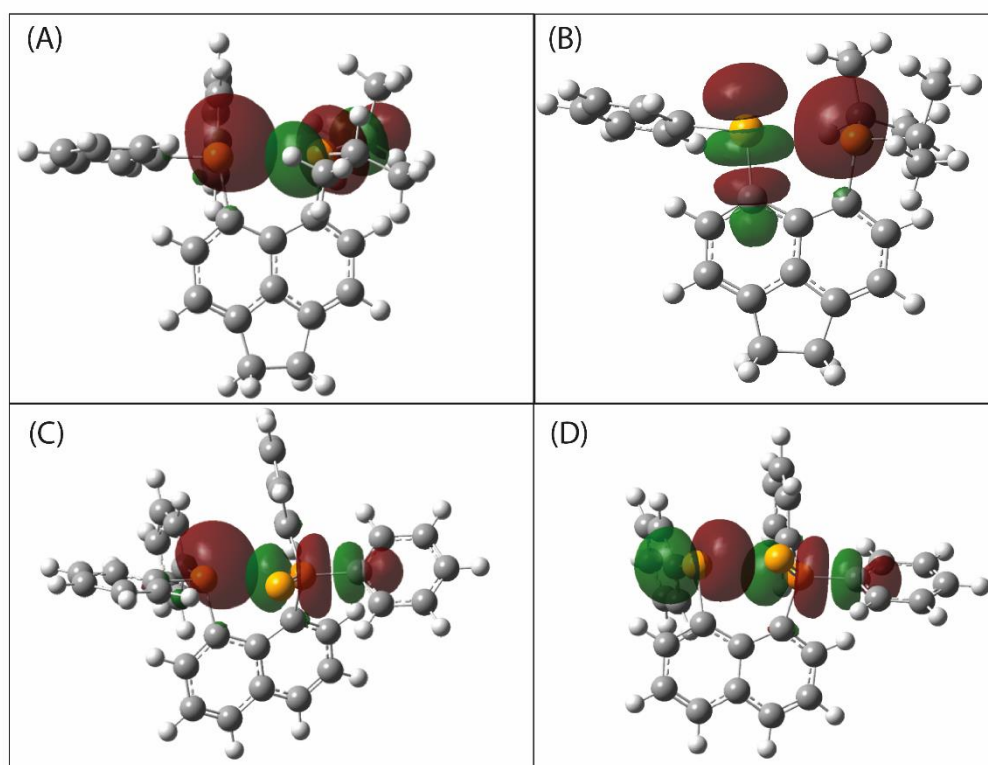


Figure 3. NBOs involved in the interaction of P—P, for compounds **1** (A) and **3** (C), or P—Se, for compounds **2** (B) and **4** (D).

Recent findings point out that intramolecular interactions, like the pnictogen bond and chalcogen bond, show an important covalent factor in the interaction energy.^{16,17,20} In this sense, performing an energy decomposition analysis (EDA) is essential to understand which contributions are most relevant.

The decomposition used in this work splits the interaction energy in three terms (Equation S1), the Pauli repulsion energy, the Coulomb interaction, *i.e.*, the electrostatic interaction, and the orbital-interaction energy (E_{OI}). Our EDA calculations point out that the E_{OI} is the most important factor in the total interaction of energy. For compounds **1**, **3**, and **4** this factor represents 72.10, 70.47, and 70.43%, respectively, and for compound **2**, this percentage corresponds to 71.99%. This additional perspective confirms the similarity between PnB that occurs in compounds **1**, **3**, and **4**. These results are in agreement with values reported in the literature, where the orbital contribution to the interaction energy for the pnictogen bond ranges from around 62 to 82% for organophosphorus compounds²⁰ and 33 to 65% for model structures¹⁷, and 37 to 72% for model structures that present the chalcogen bond¹⁸. These findings reinforce the thesis that these interactions are not electrostatic, but rather covalent.

In short, the AIM, NBO, and EDA results indicate that the nature of the pnictogen bond is similar for compounds **3** and **4**. Also, compound **1** presents an intramolecular PnB, while in compound **2** displays a chalcogen bond. Therefore, these parameters are not the main values that govern the NMR parameters in the compounds studied. Considering the potential of these molecules as qubit candidates, they should exhibit a high SSCC value and a significant difference between the δ values of the nuclei involved¹.

Our goal in this work is to study the influence of the pnictogen bond in the NMR parameters. In this context, compounds **1** and **3** were selected for the next stage of the study, aiming to better understand the role of the interactions between phosphorus atoms—specifically the pnictogen bond—in influencing the NMR parameters, and to enable comparison of this effect across similar molecular structures.

Influence of the Pnictogen Bond in the NMR parameters

As mentioned earlier, compounds **1** and **3** were selected for this step of the work. In addition to the facts already described another factor that influenced the choice of these compounds was the guarantee that the interaction between the nuclei involved in the NMR parameters will be a pnictogen bond, since we have two phosphorus atoms, so surely one will act as the Lewis acid and the other as the Lewis basis.

The distance between the phosphorus atoms was changed from the crystallographic structure and increased until the AIM analysis showed that there is no more BCP between the phosphorus, *i.e.*, the pnictogen bond no longer exists and decreased until around 2.20 Å, that is the P—P bond distance. For compound **1**, the original distance between phosphorus is 3.09 Å and they have been moved away from each other to 4.39 Å and closer together to 2.19 Å. These distances for compound **3** have a smaller range, going from 2.20 Å to 3.40 Å, with the crystallographic structure showing the distance between P of 3.20 Å.

The chemical shift values can be obtained in Tables S2 and S3. For compound **1**, it is possible to observe that the chemical shifts for P1 are higher when the phosphorus are closer to each other and closer to zero when the distance is the maximum. For P2, the behavior is the opposite, with the δ showing the lowest values with the phosphorus closer to each other, and the maximum value with the distance between the P equal to 4.39 Å. In this scenario, the interaction energy and the electron density have the highest values with the lower P—P distance (Figure

5-A), so the phosphorus that acts as a donor, P1, has a negative $\Delta\delta$ along the distance and, for the Lewis base, P2, the $\Delta\delta$ is positive, with negative δ values.

For compound **3**, the behavior is quite similar, with the values of δ for P1 decreasing when the atoms come closer and increasing for P2. However, the values of δ for compound **3** are always positive. As seen in compound **1**, the $\Delta\delta(\text{P1})$ is negative, however, the variation of the chemical shift of P2, *i.e.*, the phosphorus which receives electron density, is also negative. An interesting behavior can be observed for the two phosphorus atoms in both compounds, where when these atoms are brought closer together, thus increasing the interaction energy and the electron density (Figure 5), the shift values move away from zero, becoming larger for both P in compound **3** and P1 in compound **1**, and decreasing for P2 in compound **1**.

This behavior between donor and acceptor atoms can be interpreted through Ramsey's theory of nuclear shielding, in which the chemical shift arises from the sum of diamagnetic and paramagnetic contributions to the shielding tensor^{53,54}. The paramagnetic term, in particular, is sensitive to changes in orbital occupancy and electron delocalization caused by intramolecular interactions such as pnictogen bonding^{53,54}. As the interaction strengthens and the atoms move closer, the electronic coupling between donor and acceptor orbitals alters its energy, enhancing or suppressing paramagnetic deshielding depending on the electronic role of each phosphorus atom. Therefore, the observed trends in $\Delta\delta$ reflect not only the proximity or electron density variations, but also orbital effects that modulate shielding via the paramagnetic term of Ramsey's framework.

In Figure 4, the relation between the distance and the spin-spin coupling constant can be observed. Part A is related to compound **1**, while part B shows the results for compound **3**. The shape of the curve for these compounds is very similar, with higher values when the phosphorus atoms are closer. For compound **3**, the higher values of J are around 500 Hz, almost three times smaller than the higher values of compound **1**. Therefore, for both compounds, the increase in the strength of the PnB causes an increase in the values of the SSCC.

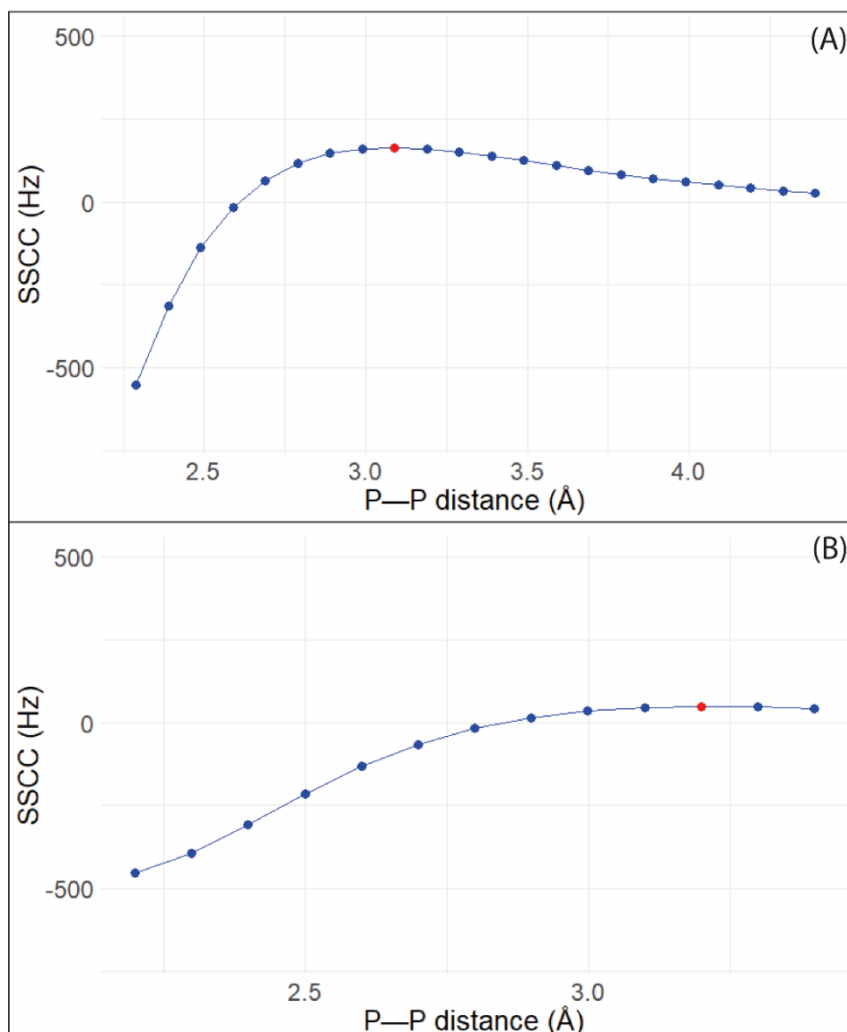


Figure 4. SSCC for compounds **1** (part A) and **3** (part B). The red point is the value for the original P—P distance.

This effect can be primarily attributed to changes in the Fermi Contact (FC) term, which is the dominant contribution to the spin-spin coupling constants^{53,55,56}. As the pnictogen bond becomes stronger and the atoms come closer, the spin density at the phosphorus nuclei increases. This modulation of the electronic structure leads to an increase in the FC term and, consequently, in the observed J values. The sign inversion of the SSCC as the P—P distance changes is an intriguing characteristic seen in both compounds. Longer distances result in a positive coupling, while smaller distances yield negative values. This behavior may result from the competition between different Ramsey contributions to the total J coupling. At shorter distances, the spin-dipole or paramagnetic spin-orbit terms may contribute more significantly and negatively, while at longer distances, the FC term becomes dominant and positive. The SSCC's sensitivity to structural changes is further supported by the change in the balance

between contributions, which reflects alterations in the electronic environment and orbital interactions as a function of distance.

To help in understanding the behavior of the NMR parameters for both compounds, the nature of the P—P interaction was analyzed through its topological parameters and the decomposition of the energy related to the interaction. Figure 5 brings this information for compounds **1** and **3**, the topological parameters, ρ and the E_{int} , related to the P—P distance, the interaction energy (E_{int}) values were obtained from the AIM parameters, specifically as half the potential energy value ($E_{int} = \frac{1}{2}V$), as described by Espinosa et al.⁵⁷. This definition, initially established for hydrogen bonds, can be extended to other intermolecular interactions, such as the pnictogen bond, due to their similar nature. Values of $\nabla^2\rho$ and V for the BCP of each P—P distance can be found in Tables S3 and S4. A similar behavior can be observed for both compounds, where the interaction energy is higher when the distance between the P comes closer to each other, the same occurs with the electronic density related to the BCP correspondent to the PnB.

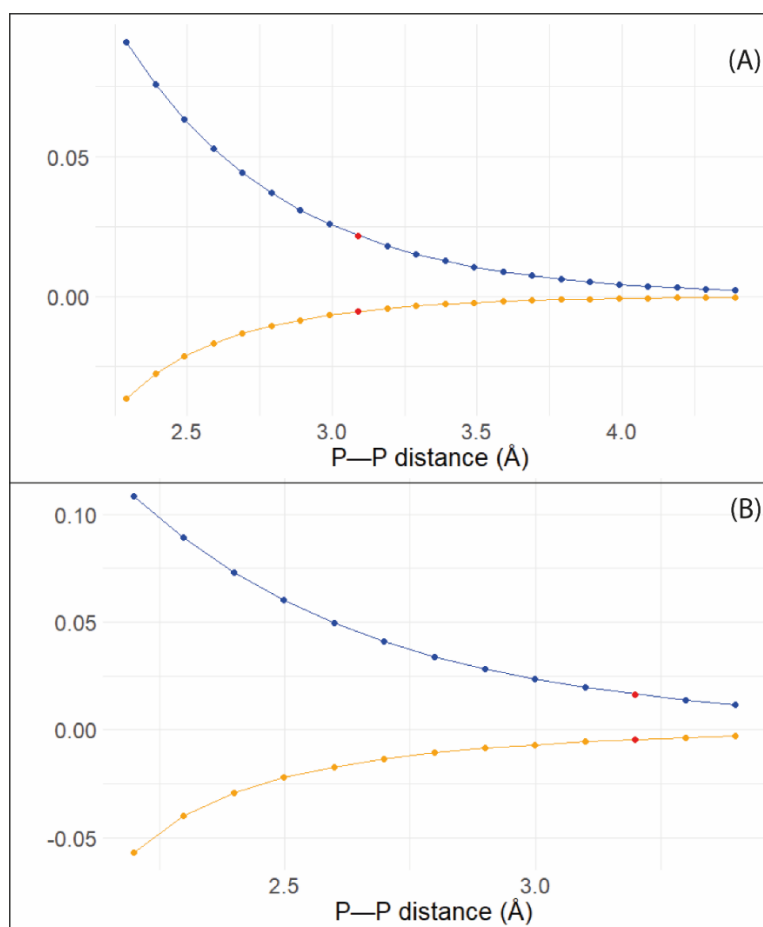


Figure 5. Topological parameters, ρ (blue, a.u.), and E_{int} (orange, kcal/mol) for compounds **1** (part A) and **3** (part B). The red point is the value for the original P—P distance.

The AIM analysis shows that, for compound **3**, the interaction between the phosphorus ends with just 0.2 Å further away from the crystallographic structure, for compound **1**, this distance was increased by 1.3 Å. When these distances were increased by another 0.1 Å, the AIM analysis no longer showed a BCP between the P atoms, indicating that the pnictogen bond no longer existed. For the scenario where the phosphorus atoms came closer to each other, for compound **1** the distance of the P atoms decreased by 0.9 Å, and 1.0 Å for compound **3**, reaching around 2.2 Å, the distance where a P—P bond is observed, so the intramolecular interaction does not exist.

Figure 6 provides information about the interaction energy, specifically the portion of this energy that came from the interaction between the phosphorus orbitals, provided by the energy decomposition analysis (EDA). It is possible to observe that, as expected, the orbital interaction became stronger as the P—P distance became smaller. As seen for the crystallographic structure of compounds **1-4**, the contribution of the orbital interaction for the total interaction energy is the main factor and is primarily responsible for the interaction between the phosphorus atoms. The percentage of the orbital energy in the total interaction energy stays around 70% for compounds **1** and **3**. These values are in line with reported values for other Pnictogen Bond.^{17,20}

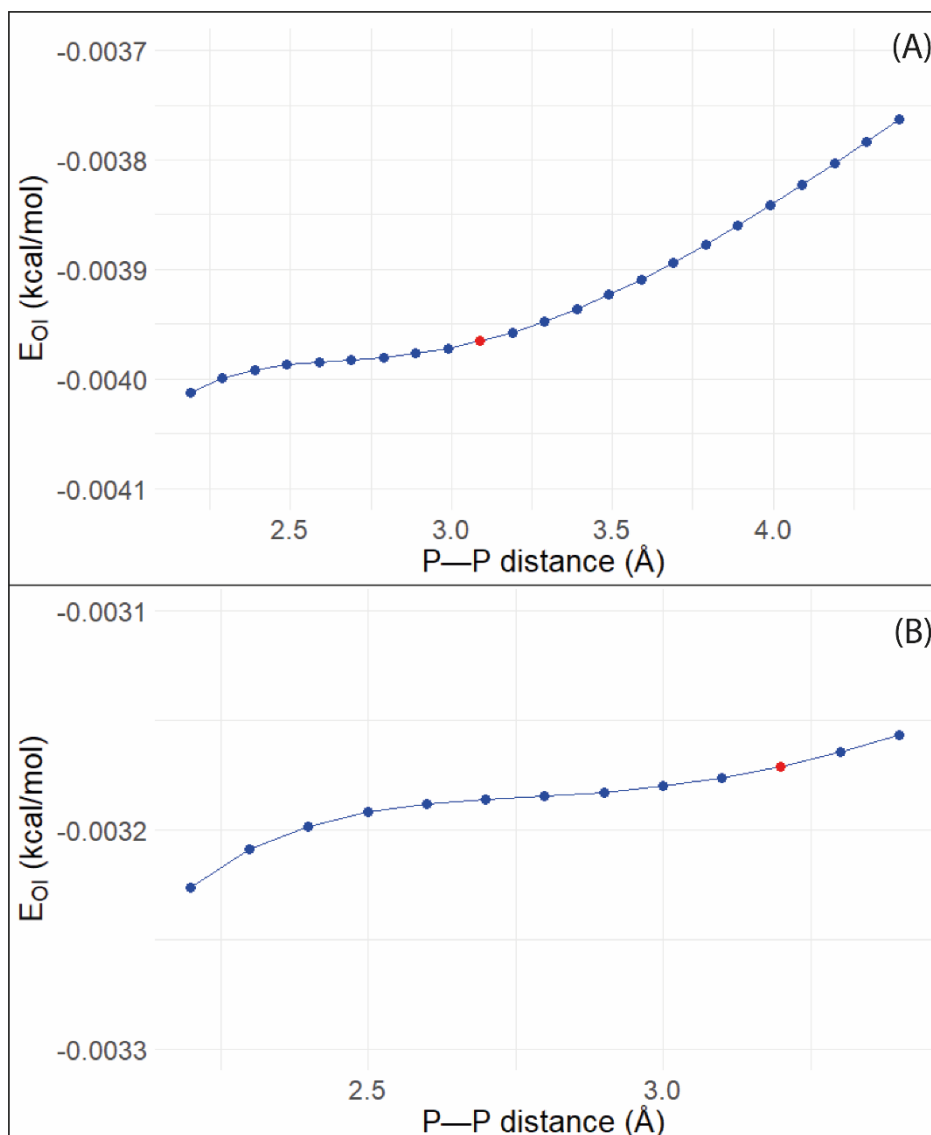


Figure 6. Orbital interaction energy for compounds **1** (part A) and **3** (part B). The red point is the value for the original P—P distance.

Thus, these results indicate that the interaction became stronger when the phosphorus atoms came closer to each other. Aligned with this, the difference between the δ for the two phosphorus atoms increases and the J_{PP} reaches the highest value when the interaction energy reaches the highest values. As a result, as the interaction became stronger, the NMR parameters reached values that make these compounds more promising for use as a QIP molecule.

These results reinforce that the strength and nature of the intramolecular interaction are directly related to the NMR parameters of interest for qubit applications. As the interaction energy increases, the spin–spin coupling constants become larger and the chemical shifts more differentiated, which improves the ability of the molecule to act as a qubit. Therefore,

modulating these interactions through molecular design may serve as an effective strategy to enhance the NMR properties of these systems for quantum information processing (QIP).

CONCLUSIONS

The importance of NMR parameters for a molecule to act as a quantum bit (qubit) in Quantum Information Processing (QIP) is evident, highlighting the necessity for these molecules to meet specific criteria. The results in this work point that the four selected molecules meet those criteria. The AIM analysis points out the existence of intramolecular interactions occurring between the phosphorus atoms, for compounds **1** and **3**, and phosphorus and selenium for compounds **2** and **4**, and the NBO analysis indicates that these interactions can be characterized as a Pnictogen Bond (PnB) for compound **1**, **3**, and **4**, and a Chalcogen Bond in compound **2**. Allied with these findings, an energy decomposition analysis (EDA) of the interaction energy (E_{int}) shows that the main component of the E_{int} is the orbital interaction energy, with around 70% of the total energy contribution.

In the sequence, the relationship between the strength of the PnB and the NMR parameters was studied for compounds **1** and **3**. This current study demonstrates that, as the interaction energy of the PnB increases, the spin-spin coupling constant reaches higher values and the chemical shifts for the phosphorus involved in the interaction are more distant from each other. The EDA analysis confirms that orbital interaction is the main factor for the interaction energy during the variation of distance analyzed. These behaviors increase the ability of the molecule to act as a qubit, *i.e.*, as the energy of the PnB interaction between the two atoms relevant to the NMR parameters for qubits increases, the molecule aligns more closely with the required NMR parameters, enhancing its potential as a qubit in QIP. Furthermore, the use of those methods was essential to access interaction energies, topological properties, and orbital contributions, allowing for a detailed characterization of the bonding nature and its direct influence on spectroscopic parameters. These findings reinforce the role of theoretical approaches in understanding and predicting how specific intramolecular interactions can be employed to tune properties relevant to quantum applications.

ASSOCIATED CONTENT

Supplementary Material

Energy Decomposition equation, Cartesian coordinates, AIM parameters, NBO parameters, and calculated chemical shifts.

AUTHOR INFORMATION

Corresponding Author

Teodorico Castro Ramalho – Department of Chemistry, Natural Sciences Institute, Federal University of Lavras, 37200-900 Lavras, Minas Gerais, Brazil; Center for Basic and Applied Research, Faculty of Informatics and Management, University Hradec Kralove, 50003 Hradec Kralove, Czech Republic; orcid.org/0000-0002-7324-1353; Phone: +55 35 3829-1522; Email: teodorico.ramalho@gmail.com; Fax: +55 35 3829-1271

Author

Gustavo de Almeida Andolpho - Department of Chemistry, Natural Sciences Institute, Federal University of Lavras, 37200-900 Lavras, Minas Gerais, Brazil. orcid.org/0000-0002-0104-7420

ACKNOWLEDGMENT

The authors are thankful to Coordenação de Aperfeiçoamento de Pessoal de Nível Superior (CAPES) grant number 88887.999494/2024-0, Fundação de Amparo à Pesquisa de Minas Gerais (FAPEMIG), Conselho Nacional de Desenvolvimento Científico e Tecnológico (CNPq) for financial support of this research, Financiadora de Estudos e Projetos (FINEP) and INCT Defesa. This study was supported by Excellence Project UHK.

REFERENCES

- (1) Lino, J. B. R.; Rocha, E. P.; Ramalho, T. C. Value of NMR Parameters and DFT Calculations for Quantum Information Processing Utilizing Phosphorus Heterocycles. *Journal of Physical Chemistry A* **2017**, *121* (23), 4486–4495. <https://doi.org/10.1021/acs.jpca.6b12728>.

- (2) Lino; Ramalho, J. B. R.; *Informação Quântica e Parâmetros de Ressonância Magnética Nuclear Quantum Information and Nuclear Magnetic Resonance Parameters*; **2018**; Vol. 10. <http://rvq.s bq.org.br>.
- (3) Lino, J. B. D. R.; Ramalho, T. C. Exploring Through-Space Spin-Spin Couplings for Quantum Information Processing: Facing the Challenge of Coherence Time and Control Quantum States. *Journal of Physical Chemistry A* **2019**, *123* (7), 1372–1379. <https://doi.org/10.1021/acs.jpca.8b09425>.
- (4) Lino, J. B. D. R.; Sauer, S. P. A.; Ramalho, T. C. Enhancing NMR Quantum Computation by Exploring Heavy Metal Complexes as Multiqubit Systems: A Theoretical Investigation. *Journal of Physical Chemistry A* **2020**, *124* (24), 4946–4955. <https://doi.org/10.1021/acs.jpca.0c01607>.
- (5) Lino, J. B. dos R.; Gonçalves, M. A.; Sauer, S. P. A.; Ramalho, T. C. Extending NMR Quantum Computation Systems by Employing Compounds with Several Heavy Metals as Qubits. *Magnetochemistry* **2022**, *8* (5). <https://doi.org/10.3390/magnetochemistry8050047>.
- (6) Jones, J. A. *NMR Quantum Computation*. www.elsevier.nl/locate/pnmrs.
- (7) Jones, J. A. Quantum Computing with NMR. *Progress in Nuclear Magnetic Resonance Spectroscopy*. Elsevier B.V. **2011**, pp 91–120. <https://doi.org/10.1016/j.pnmrs.2010.11.001>.
- (8) Jones, J. A. Controlling NMR Spin Systems for Quantum Computation. *Progress in Nuclear Magnetic Resonance Spectroscopy*. **2024**, pp 49–85. <https://doi.org/10.1016/j.pnmrs.2024.02.002>.
- (9) Ramanathan, C.; Boulant, N.; Chen, Z.; Cory, D. G.; Chuang, I.; Steffen, M. *NMR Quantum Information Processing*; **2004**; Vol. 3.
- (10) Criger, B.; Passante, G.; Park, D.; Laflamme, R. Recent Advances in Nuclear Magnetic Resonance Quantum Information Processing. *Philosophical Transactions of the Royal Society A: Mathematical, Physical and Engineering Sciences*. **2012**, pp 4620–4635. <https://doi.org/10.1098/rsta.2011.0352>.
- (11) Ryan, C. A.; Laforest, M.; Boileau, J. C.; Laflamme, R. Experimental Implementation of a Discrete-Time Quantum Random Walk on an NMR Quantum-Information Processor. *Phys Rev A* **2005**, *72* (6). <https://doi.org/10.1103/PhysRevA.72.062317>.

- (12) DiVincenzo, D. P. The Physical Implementation of Quantum Computation. *Fortschritte der Physik*. Wiley-VCH Verlag **2000**, pp 771–783. [https://doi.org/10.1002/1521-3978\(200009\)48:9/11](https://doi.org/10.1002/1521-3978(200009)48:9/11).
- (13) Viesser, V. R.; Ducati, L. C.; Tormena, C. F.; Autschbach, J. The Halogen Effect on the ¹³C NMR Chemical Shift in Substituted Benzenes. *Physical Chemistry Chemical Physics* **2018**, *20* (16), 11247–11259. <https://doi.org/10.1039/c8cp01249k>.
- (14) Scheiner, S.; Michalczyk, M.; Zierkiewicz, W. Correlation between Noncovalent Bond Strength and Spectroscopic Perturbations within the Lewis Base. *Journal of Physical Chemistry A* **2024**. <https://doi.org/10.1021/acs.jpca.4c07382>.
- (15) Jimmink, B.; Sethio, D.; Turunen, L.; Von Der Heiden, D.; Erdélyi, M. Probing Halogen Bonds by Scalar Couplings. *J Am Chem Soc* **2021**, *143* (28), 10695–10699. <https://doi.org/10.1021/jacs.1c04477>.
- (16) de Azevedo Santos, L.; Ramalho, T. C.; Hamlin, T. A.; Bickelhaupt, F. M. Intermolecular Covalent Interactions: Nature and Directionality. *Chemistry - A European Journal* **2023**, *29* (14). <https://doi.org/10.1002/chem.202203791>.
- (17) de Azevedo Santos, L.; Hamlin, T. A.; Ramalho, T. C.; Bickelhaupt, F. M. The Pnictogen Bond: A Quantitative Molecular Orbital Picture. *Physical Chemistry Chemical Physics* **2021**, *23* (25), 13842–13852. <https://doi.org/10.1039/d1cp01571k>.
- (18) de Azevedo Santos, L.; van der Lubbe, S. C. C.; Hamlin, T. A.; Ramalho, T. C.; Matthias Bickelhaupt, F. A Quantitative Molecular Orbital Perspective of the Chalcogen Bond. *ChemistryOpen* **2021**, *10* (4), 391–401. <https://doi.org/10.1002/open.202000323>.
- (19) Alkorta, I.; Elguero, J.; Frontera, A. Not Only Hydrogen Bonds: Other Noncovalent Interactions. *Crystals*. **2020**. <https://doi.org/10.3390/cryst10030180>.
- (20) Andolpho, G. A.; Ramalho, T. C. Pnictogen Bond-Driven Control of the Molecular Interaction between Organophosphorus and Acetylcholinesterase Enzyme. *J Comput Chem* **2024**, *45* (15), 1303–1315. <https://doi.org/10.1002/jcc.27328>.
- (21) Zahn, S.; Frank, R.; Hey-Hawkins, E.; Kirchner, B. Pnictogen Bonds: A New Molecular Linker? *Chemistry - A European Journal* **2011**, *17* (22), 6034–6038. <https://doi.org/10.1002/chem.201002146>.

- (22) Hazra, S.; Majumdar, D.; Frontera, A.; Roy, S.; Gassoumi, B.; Ghalla, H.; Dalai, S. On the Significant Importance of Hg \cdots Cl Spodium Bonding/ σ/π -Hole/Noncovalent Interactions and Nanoelectronic/Conductivity Applications in Mercury Complexes: Insights from DFT Spectrum. *Cryst Growth Des* **2024**, *24* (17), 7246–7261. <https://doi.org/10.1021/acs.cgd.4c00893>.
- (23) Majumdar, D.; Frontera, A.; Roy, S.; Sutradhar, D. Experimental and Theoretical Survey of Intramolecular Spodium Bonds/ σ/π -Holes and Noncovalent Interactions in Trinuclear Zn(II)-Salen Type Complex with OCN $^-$ Ions: A Holistic View in Crystal Engineering. *ACS Omega* **2024**, *9* (1), 1786–1797. <https://doi.org/10.1021/acsomega.3c08422>.
- (24) Politzer, P.; Murray, J. S.; Clark, T.; Resnati, G. The σ -Hole Revisited. *Physical Chemistry Chemical Physics* **2017**, pp 32166–32178. <https://doi.org/10.1039/c7cp06793c>.
- (25) Hupf, E.; Lork, E.; Mebs, S.; Chęcińska, L.; Beckmann, J. Probing Donor-Acceptor Interactions in Peri-Substituted Diphenylphosphinoacenaphthyl-Element Dichlorides of Group 13 and 15 Elements. *Organometallics* **2014**, *33* (24), 7247–7259. <https://doi.org/10.1021/om501036c>.
- (26) Tripathi, M. K.; Ramanathan, V. Nature and Strength of Sulfur-Centered Hydrogen Bond in Methanethiol Aqueous Solutions. *Journal of Physical Chemistry A* **2023**, *127* (10), 2265–2273. <https://doi.org/10.1021/acs.jpca.2c08314>.
- (27) Braga, L. S.; Leal, D. H. S.; Kuca, K.; Ramalho, T. C. Perspectives on the Role of the Frontier Effective-for-Reaction Molecular Orbital (FERMO) in the Study of Chemical Reactivity: An Updated Review. *Curr Org Chem* **2020**, *24* (3), 314–331. <https://doi.org/https://doi.org/10.2174/1385272824666200204121044>.
- (28) Karaçar, A.; Freytag, M.; Thönnessen, H.; Omelanczuk, J.; Jones, P. G.; Bartsch, R.; Schmuitzler, R. Monoxidised Sulfur and Selenium Derivatives of 1,8-Bis(Diphenylphosphino)Naphthalene: Synthesis and Coordination Chemistry. *Z Anorg Allg Chem* **2000**, *626* (11), 2361–2372. <https://doi.org/10.1002/1521-3749>.
- (29) Knight, F. R.; Fuller, A. L.; Bühl, M.; Slawin, A. M. Z.; Woollins, J. D. Sterically Crowded Peri-Substituted Naphthalene Phosphines and Their P v Derivatives. *Chemistry - A European Journal* **2010**, *16* (25), 7617–7634. <https://doi.org/10.1002/chem.201000454>.
- (30) Zhang, L.; Christie, F. A.; Tarcza, A. E.; Lancaster, H. G.; Taylor, L. J.; Bühl, M.; Malkina, O. L.; Woollins, J. D.; Carpenter-Warren, C. L.; Cordes, D. B.; Slawin, A. M. Z.; Chalmers, B. A.;

- Kilian, P. Phosphine and Selenoether Peri-Substituted Acenaphthenes and Their Transition-Metal Complexes: Structural and NMR Investigations. *Inorg Chem* **2023**, *62* (39), 16084–16100. <https://doi.org/10.1021/acs.inorgchem.3c02255>.
- (31) Chalmers, B. A.; Athukorala Arachchige, K. S.; Prentis, J. K. D.; Knight, F. R.; Kilian, P.; Slawin, A. M. Z.; Woollins, J. D. Sterically Encumbered Tin and Phosphorus Peri-Substituted Acenaphthenes. *Inorg Chem* **2014**, *53* (16), 8795–8808. <https://doi.org/10.1021/ic5014768>.
- (32) Ramalho, T. C.; De Alencastro, R. B.; La-Scalea, M. A.; Figueroa-Villar, J. D. Theoretical Evaluation of Adiabatic and Vertical Electron Affinity of Some Radiosensitizers in Solution Using FEP, Ab Initio and DFT Methods. *Biophys Chem* **2004**, *110* (3), 267–279. <https://doi.org/10.1016/j.bpc.2004.03.002>.
- (33) Adamo, C.; Barone, V. Toward Reliable Density Functional Methods without Adjustable Parameters: The PBE0 Model. *Journal of Chemical Physics* **1999**, *110*, 6158–6170. <https://doi.org/10.1063/1.478522>.
- (34) Weigend, F.; Ahlrichs, R. Balanced Basis Sets of Split Valence, Triple Zeta Valence and Quadruple Zeta Valence Quality for H to Rn: Design and Assessment of Accuracy. *Physical Chemistry Chemical Physics* **2005**, *7*, 3297–3305. <https://doi.org/10.1039/b508541a>.
- (35) Pascual-Borràs, M.; López, X.; Poblet, J. M. Accurate Calculation of ³¹P NMR Chemical Shifts in Polyoxometalates. *Physical Chemistry Chemical Physics* **2015**, *17*, 8723–8731. <https://doi.org/10.1039/c4cp05016a>.
- (36) Lu, T.; Chen, F. Multiwfn: A Multifunctional Wavefunction Analyzer. *J Comput Chem* **2012**, *33*, 580–592. <https://doi.org/10.1002/jcc.22885>.
- (37) Becke, A. D. Density-Functional Thermochemistry. III. The Role of Exact Exchange. *J Chem Phys* **1993**, *98*, 5648–5652. <https://doi.org/10.1063/1.464913>.
- (38) Glendening, E. D.; Landis, C. R.; Weinhold, F. NBO 6.0: Natural Bond Orbital Analysis Program. *J Comput Chem* **2013**, *34*, 1429–1437. <https://doi.org/10.1002/jcc.23266>.
- (39) te Velde, G.; Bickelhaupt, F. M.; Baerends, E. J.; Fonseca Guerra, C.; van Gisbergen, S. J. A.; Snijders, J. G.; Ziegler, T. Chemistry with ADF. *J Comput Chem* **2001**, *22*, 931–967. <https://doi.org/10.1002/jcc.1056>.

- (40) Andolpho, G. A.; Ramalho, T. C. Pnictogen Bond-Driven Control of the Molecular Interaction between Organophosphorus and Acetylcholinesterase Enzyme. *J Comput Chem* **2024**, *45* (15), 1303–1315. <https://doi.org/10.1002/jcc.27328>.
- (41) Neese, F. Software Update: The ORCA Program System—Version 5.0. *Wiley Interdisciplinary Reviews: Computational Molecular Science*. **2022**. <https://doi.org/10.1002/wcms.1606>.
- (42) Nielsen, M. L.; Pustinger, J. V; Strobel, J. Phosphorus-31 Nuclear Magnetic Resonance Chemical Shifts of Phosphorus Compounds. *Journal of Chemical & Engineering Data*. **1964**, *9*(2), 167-170. <https://doi.org/10.1021/je60021a003>
- (43) Zheng, A.; Liu, S. Bin; Deng, F. 31P NMR Chemical Shifts of Phosphorus Probes as Reliable and Practical Acidity Scales for Solid and Liquid Catalysts. *Chem Rev* **2017**, *117* (19), 12475–12531. <https://doi.org/10.1021/acs.chemrev.7b00289>.
- (44) Duddeck, H. Selenium-77 Nuclear Magnetic Resonance Spectroscopy. *Prog Nucl Magn Reson Spectrosc* **1995**, *27*, 1–323. [https://doi.org/10.1016/0079-6565\(94\)00005-F](https://doi.org/10.1016/0079-6565(94)00005-F).
- (45) Rusakov, Y. Y.; Rusakova, I. L.; Krivdin, L. B. MP2 Calculation of 77Se NMR Chemical Shifts Taking into Account Relativistic Corrections. *Magnetic Resonance in Chemistry* **2015**, *53*, 485–492. <https://doi.org/10.1002/mrc.4226>.
- (46) Bould, J.; Londesborough, M. G. S.; Tok, O. L. Experimental and Computational 77Se NMR Spectroscopic Study on Selenaborane Cluster Compounds. *Inorg Chem* **2024**, *63*, 16186–16193. <https://doi.org/10.1021/acs.inorgchem.4c01890>.
- (47) Duddeck, H. 77Se NMR Spectroscopy and Its Applications in Chemistry. *Annual Reports on NMR Spectroscopy*. **2004**, pp 105–166. [https://doi.org/10.1016/S0066-4103\(04\)52003-3](https://doi.org/10.1016/S0066-4103(04)52003-3).
- (48) Rusakova, I. L.; Rusakov, Y. Y. Correlated Ab Initio Calculations of One-Bond 31P-77Se and 31P-125Te Spin–Spin Coupling Constants in a Series of P-Se and P-Te Systems Accounting for Relativistic Effects (Part 2). *Magnetic Resonance in Chemistry* **2020**, *58*, 929–940. <https://doi.org/10.1002/mrc.5058>.
- (49) Sanz Camacho, P.; McKay, D.; Dawson, D. M.; Kirst, C.; Yates, J. R.; Green, T. F. G.; Cordes, D. B.; Slawin, A. M. Z.; Woollins, J. D.; Ashbrook, S. E. Investigating Unusual Homonuclear Intermolecular “through-Space” J Couplings in Organochalcogen Systems. *Inorg Chem* **2016**, *55* (21), 10881–10887. <https://doi.org/10.1021/acs.inorgchem.6b01121>.

- (50) Wolters, L. P.; Bickelhaupt, F. M. Halogen Bonding versus Hydrogen Bonding: A Molecular Orbital Perspective. *ChemistryOpen*. **2012**, pp 96–105. <https://doi.org/10.1002/open.201100015>.
- (51) Michalczyk, M.; Zierkiewicz, W.; Scheiner, S. Ability of the Spectroscopic Properties of the P=Se Bond of a Base to Assess Noncovalent Bond Strength. *Journal of Physical Chemistry A* **2025**. <https://doi.org/10.1021/acs.jpca.4c08283>.
- (52) Furan, S.; Vogt, M.; Winkels, K.; Lork, E.; Mebs, S.; Hupf, E.; Beckmann, J. (6-Diphenylphosphinoacenaphth-5-Yl)Indium and -Nickel Compounds: Synthesis, Structure, Transmetalation, and Cross-Coupling Reactions. *Organometallics* **2021**, *40* (9), 1284–1295. <https://doi.org/10.1021/acs.organomet.1c00078>.
- (53) Ramsz, N. F. *MAGNETIC SHIELDING OF NUCLEI IN MOLECULES*; **1950**; Vol. 78.
- (54) Krivdin, L. B. Recent Advances in Computational ³¹P NMR: Part 1. Chemical Shifts. *Magnetic Resonance in Chemistry*. **2020**, pp 478–499. <https://doi.org/10.1002/mrc.4965>.
- (55) Alkorta, I.; Popelier, P. L. A. Linking the Interatomic Exchange-Correlation Energy to Experimental J-Coupling Constants. *Journal of Physical Chemistry A* **2023**, *127* (2), 468–476. <https://doi.org/10.1021/acs.jpca.2c07693>.
- (56) Dračinský, M.; Buchta, M.; Buděšínský, M.; Vacek-Chocholoušová, J.; Stará, I. G.; Starý, I.; Malkina, O. L. Dihydrogen Contacts Observed by Through-Space Indirect NMR Coupling. *Chem Sci* **2018**, *9* (38), 7437–7446. <https://doi.org/10.1039/c8sc02859a>.
- (57) Espinosa, E.; Molins, E.; Lecomte, C. *Hydrogen Bond Strengths Revealed by Topological Analyses of Experimentally Observed Electron Densities*; **1998**; Vol. 285.

3 THIRD PART

3.1 FINAL REMARKS

This thesis aimed to investigate the fundamental nature of pnictogen bonds (PnB) in complex real-world systems, moving beyond the traditional electrostatic σ -hole model to explore the critical role of orbital interactions. The motivation for this study lies in the ambiguity of the non-covalent nomenclature often applied to these interactions, which fails to capture the significant covalent character that drives their stability and functionality. By addressing two distinct yet impactful scenarios, the inhibition of the acetylcholinesterase (AChE) enzyme by organophosphorus compounds and the design of molecular qubits for quantum computing, this work sought to establish a direct correlation between the orbital nature of PnBs and macroscopic properties of interest, such as biological activity and magnetic resonance parameters.

Regarding the biological context, presented in Article 1, the computational results demonstrated that the interaction between organophosphorus agents (such as Sarin, Soman, and VX) and the serine residue in the active site of AChE is not merely an electrostatic attraction. The analysis revealed that the formation of the PnB is a key step in the inhibition mechanism, where charge transfer effects and orbital mixing play a dominant role in stabilizing the transition states. This challenges the purely electrostatic view and suggests that the efficacy of these nerve agents, and potentially the design of more effective reactivators (oximes), depends on fine-tuning these orbital interactions. The study successfully linked the electronic nature of the $P\cdots O$ bond to the inhibition potential, fulfilling the specific objective of elucidating the role of PnBs in enzymatic systems.

In the context of quantum technologies, discussed in Article 2, the investigation focused on intramolecular interactions in naphthalene and acenaphthene derivatives. The results confirmed that intramolecular pnictogen and chalcogen bonds are powerful tools for modulating Nuclear Magnetic Resonance (NMR) parameters. It was observed that the magnitude of the spin-spin coupling constant (J) and the chemical shift difference ($\Delta\delta$) are strictly dependent on the strength of the orbital interaction (specifically the overlap between lone pairs and antibonding orbitals), rather than just spatial proximity or electrostatic forces. By manipulating these interactions, it was possible to design molecules that satisfy the DiVincenzo criteria for qubits, exhibiting large coupling constants that enable faster quantum gate operations. This finding validates the hypothesis that through-space couplings are, in essence,

manifestations of through-orbital communication, offering a rational chemical strategy for qubit engineering.

Critically, the findings from both parts of this thesis converge to support the re-evaluation of the nomenclature for these interactions. The significant orbital energy contributions identified via Energy Decomposition Analysis (EDA) and Natural Bond Orbital (NBO) methods in both biological and materials systems reinforce the proposal that these interactions are better described as "intermolecular (or intramolecular) covalent interactions" rather than non-covalent bonds. This shift in perspective is not merely semantic but has practical implications for molecular design, suggesting that chemists should look for ways to maximize orbital overlap rather than just optimizing electrostatic potentials.

However, this research is not without limitations. The studies relied primarily on Density Functional Theory (DFT), which, while robust, involves approximations in the exchange-correlation functionals that may affect the precise quantification of dispersion and weak interactions. Furthermore, the biological study considered a static model of the enzyme active site, potentially underestimating dynamic effects such as protein flexibility and solvent fluctuations. Future research should therefore focus on incorporating molecular dynamics simulations (QM/MM) to capture the time-evolution of these PnBs in the enzymatic pocket. Additionally, regarding the quantum computing aspect, experimental synthesis and NMR characterization of the proposed qubit candidates are necessary steps to validate the theoretical predictions. Investigating other pnictogen derivatives (e.g., involving Arsenic or Antimony) could also reveal new regimes of coupling strength, further expanding the library of available molecular quantum processors.

In conclusion, this work contributes to the advancement of chemical knowledge by demonstrating that the pnictogen bond is a versatile and chemically tunable interaction whose orbital nature dictates function across disparate fields. Whether in the lethal mechanism of chemical warfare agents or in the delicate quantum states of a computer, the covalent character of these interactions proves to be a determining factor, paving the way for new applications in drug discovery and materials science.

REFERENCES

- Adhav, V. A., & Saikrishnan, K. (2023). The Realm of Unconventional Noncovalent Interactions in Proteins: Their Significance in Structure and Function. In *ACS Omega* (Vol. 8, Number 25, pp. 22268–22284). American Chemical Society. <https://doi.org/10.1021/acsomega.3c00205>
- Alkorta, I., Elguero, J., & Frontera, A. (2020). Not only hydrogen bonds: Other noncovalent interactions. In *Crystals* (Vol. 10, Number 3). MDPI AG. <https://doi.org/10.3390/cryst10030180>
- Alkorta, I., & Popelier, P. L. A. (2023). Linking the Interatomic Exchange-Correlation Energy to Experimental J-Coupling Constants. *Journal of Physical Chemistry A*, 127(2), 468–476. <https://doi.org/10.1021/acs.jpca.2c07693>
- Anwar, M. S., Blazina, D., Carteret, H. A., Duckett, S. B., & Jones, J. A. (2004). Implementing Grover's quantum search on a para-hydrogen based pure state NMR quantum computer. *Chemical Physics Letters*, 400(1), 94–97. <https://doi.org/https://doi.org/10.1016/j.cplett.2004.10.078>
- Atkinson, B. E., Hu, H.-S., & Kaltsoyannis, N. (2018). Post Hartree–Fock calculations of pnictogen–uranium bonding in EUF3 (E = N–Bi). *Chemical Communications*, 54(79), 11100–11103. <https://doi.org/10.1039/C8CC05581E>
- Bader, R. F. W. (1985). Atoms in molecules. *Accounts of Chemical Research*, 18(1), 9–15.
- Bagno, A., & Saielli, G. (2007). Computational NMR spectroscopy: Reversing the information flow. *Theoretical Chemistry Accounts*, 117(5–6), 603–619. <https://doi.org/10.1007/s00214-006-0196-z>
- Balali-Mood, M., & Abdollahi, M. (2014). *Basic and clinical toxicology of organophosphorus compounds*.
- Bauzá, A., Mooibroek, T. J., & Frontera, A. (2015). The bright future of unconventional σ/π -hole interactions. *ChemPhysChem*, 16(12), 2496–2517.
- Bickelhaupt, F. M. (1999). Understanding reactivity with Kohn–Sham molecular orbital theory: E2–SN2 mechanistic spectrum and other concepts. *Journal of Computational Chemistry*, 20(1), 114–128.
- Bickelhaupt, F. M., & Baerends, E. J. (2000). Kohn-Sham density functional theory: predicting and understanding chemistry. *Reviews in Computational Chemistry*, 1–86.
- Bickelhaupt, F. M., & Houk, K. N. (2017). Analyzing reaction rates with the distortion/interaction-activation strain model. *Angewandte Chemie International Edition*, 56(34), 10070–10086.

- Boraei, A. T. A., Haukka, M., Sarhan, A. A. M., Soliman, S. M., & Barakat, A. (2021). *Intramolecular Hydrogen Bond, Hirshfeld Analysis, AIM; DFT Studies of Pyran-2,4-dione Derivatives* (Vol. 11, Number 8). <https://doi.org/10.3390/cryst11080896>
- Bursch, M., Kunze, L., Vibhute, A. M., Hansen, A., Sureshan, K. M., Jones, P. G., Grimme, S., & Werz, D. B. (2021). Quantification of Noncovalent Interactions in Azide–Pnictogen, –Chalcogen, and –Halogen Contacts. *Chemistry – A European Journal*, 27(14), 4627–4639. <https://doi.org/https://doi.org/10.1002/chem.202004525>
- Cai, W., Li, Z., Zhou, W., Chen, H., Xu, Y., Zhu, Q., & Zou, Y. (2025). Characterization of Protein–Ligand Chalcogen Bonds: Insights from Database Survey and Quantum Mechanics Calculations. *Journal of Chemical Information and Modeling*, 65(18), 9610–9622. <https://doi.org/10.1021/acs.jcim.5c01492>
- Caldeweyher, E., Mewes, J.-M., Ehlert, S., & Grimme, S. (2020). Extension and evaluation of the D4 London-dispersion model for periodic systems. *Physical Chemistry Chemical Physics*, 22(16), 8499–8512. <https://doi.org/10.1039/D0CP00502A>
- Černý, J., & Hobza, P. (2007). Non-covalent interactions in biomacromolecules. *Physical Chemistry Chemical Physics*, 9(39), 5291–5303.
- Chae, E., Choi, J., & Kim, J. (2024). An elementary review on basic principles and developments of qubits for quantum computing. *Nano Convergence*, 11(1), 11. <https://doi.org/10.1186/s40580-024-00418-5>
- Cheeseman, J., Keith, T. A., & Bader, R. F. W. (1992). AIMPAC program package. *McMaster University, Hamilton, Ontario*, 18.
- Contreras-García, J., Johnson, E. R., Keinan, S., Chaudret, R., Piquemal, J.-P., Beratan, D. N., & Yang, W. (2011). NCIPLLOT: A Program for Plotting Noncovalent Interaction Regions. *Journal of Chemical Theory and Computation*, 7(3), 625–632. <https://doi.org/10.1021/ct100641a>
- Corrêa, S., Rosa, I. A., Andolpho, G. A., de Assis, L. C., Pires, M. D. S., Lacerda, L. C. T., Nogueira, F. G. E., da Cunha, E. F. F., Nepovimova, E., Kuca, K., & Ramalho, T. C. (2021). Hybrid materials based on magnetic iron oxides with benzothiazole derivatives: A plausible potential spectroscopy probe. *International Journal of Molecular Sciences*, 22(8). <https://doi.org/10.3390/ijms22083980>
- Costa, L. G. (2018). Organophosphorus compounds at 80: some old and new issues. *Toxicological Sciences*, 162(1), 24–35.
- Cramer, C. J. (2013). *Essentials of computational chemistry: theories and models*. John Wiley & Sons.
- Criger, B., Passante, G., Park, D., & Laflamme, R. (2012). Recent advances in nuclear magnetic resonance quantum information processing. In *Philosophical Transactions of the Royal Society A: Mathematical, Physical and Engineering Sciences* (Vol. 370, Number 1976, pp. 4620–4635). Royal Society. <https://doi.org/10.1098/rsta.2011.0352>

Das, S., & Merz, K. M. (2025). Exploring the Frontiers of Computational NMR: Methods, Applications, and Challenges. In *Chemical Reviews* (Vol. 125, Number 19, pp. 9256–9295). American Chemical Society. <https://doi.org/10.1021/acs.chemrev.5c00259>

de Azevedo Santos, L., Hamlin, T. A., Ramalho, T. C., & Bickelhaupt, F. M. (2021a). The pnictogen bond: a quantitative molecular orbital picture. *Physical Chemistry Chemical Physics*, 23(25), 13842–13852. <https://doi.org/10.1039/d1cp01571k>

de Azevedo Santos, L., Hamlin, T. A., Ramalho, T. C., & Bickelhaupt, F. M. (2021b). The pnictogen bond: a quantitative molecular orbital picture. *Physical Chemistry Chemical Physics*, 23(25), 13842–13852.

de Azevedo Santos, L., Ramalho, T. C., Hamlin, T. A., & Bickelhaupt, F. M. (2023). Intermolecular Covalent Interactions: Nature and Directionality. *Chemistry - A European Journal*, 29(14). <https://doi.org/10.1002/chem.202203791>

de Azevedo Santos, L., van der Lubbe, S. C. C., Hamlin, T. A., Ramalho, T. C., & Matthias Bickelhaupt, F. (2021). A Quantitative Molecular Orbital Perspective of the Chalcogen Bond. *ChemistryOpen*, 10(4), 391–401. <https://doi.org/10.1002/open.202000323>

De Castro, A. A., Prandi, I. G., Kuca, K., & Ramalho, T. C. (2017). Organophosphorus degrading enzymes: Molecular basis and perspectives for enzymatic bioremediation of agrochemicals. *Ciencia e Agrotecnologia*, 41(5), 471–482.

De Vleeschouwer, F., De Proft, F., Ergün, Ö., Herrebout, W., & Geerlings, P. (2021). A Combined Experimental/Quantum-Chemical Study of Tetrel, Pnictogen, and Chalcogen Bonds of Linear Triatomic Molecules. *Molecules*, 26(22). <https://doi.org/10.3390/molecules26226767>

Delfino, R. T., Ribeiro, T. S., & Figueroa-Villar, J. D. (2009). Organophosphorus compounds as chemical warfare agents: a review. *Journal of the Brazilian Chemical Society*, 20, 407–428.

DiVincenzo, D. P. (2000). The physical implementation of quantum computation. In *Fortschritte der Physik* (Vol. 48, Numbers 9–11, pp. 771–783). Wiley-VCH Verlag. [https://doi.org/10.1002/1521-3978\(200009\)48:9/11<771::AID-PROP771>3.0.CO;2-E](https://doi.org/10.1002/1521-3978(200009)48:9/11<771::AID-PROP771>3.0.CO;2-E)

Dračinský, M., Buchta, M., Buděšínský, M., Vacek-Chocholoušová, J., Stará, I. G., Starý, I., & Malkina, O. L. (2018). Dihydrogen contacts observed by through-space indirect NMR coupling. *Chemical Science*, 9(38), 7437–7446. <https://doi.org/10.1039/c8sc02859a>

Duarte, H. A. (2001). Índices de reatividade química a partir da teoria do funcional de densidade: formalismo e perspectivas. *Química Nova*, 24(4), 501–508.

Dube, J. W., Hänninen, M. M., Dutton, J. L., Tuononen, H. M., & Ragoona, P. J. (2012). Homoleptic Pnictogen–Chalcogen Coordination Complexes. *Inorganic Chemistry*, 51(16), 8897–8903. <https://doi.org/10.1021/ic300892p>

Duddeck, H. (1995). Selenium-77 nuclear magnetic resonance spectroscopy. *Progress in Nuclear Magnetic Resonance Spectroscopy*, 27, 1–323. [https://doi.org/10.1016/0079-6565\(94\)00005-F](https://doi.org/10.1016/0079-6565(94)00005-F)

Esrafilı, M. D., Mohammadian-Sabet, F., & Baneshi, M. M. (2015). The dual role of halogen, chalcogen, and pnictogen atoms as Lewis acid and base: Triangular XBr:SHX:PH₂X complexes (X = F, Cl, Br, CN, NC, OH, NH₂, and OCH₃). *International Journal of Quantum Chemistry*, 115(22), 1580–1586. <https://doi.org/https://doi.org/10.1002/qua.24987>

Fanfrlík, J., & Hnyk, D. (2018). Dihalogen and Pnictogen Bonding in Crystalline Icosahedral Phosphaboranes. *Crystals*, 8(10). <https://doi.org/10.3390/cryst8100390>

Fernández, I., & Bickelhaupt, F. M. (2014). The activation strain model and molecular orbital theory: understanding and designing chemical reactions. *Chemical Society Reviews*, 43(14), 4953–4967.

Figueroa-Villar, J. D., Petronilho, E. C., Kuca, K., & Franca, T. C. C. (2021). Review about structure and evaluation of reactivators of Acetylcholinesterase inhibited with neurotoxic organophosphorus compounds. *Current Medicinal Chemistry*, 28(7), 1422–1442.

Frisch, M. J., Trucks, G. W., Schlegel, H. B., Scuseria, G. E., Robb, M. A., Cheeseman, J. R., Scalmani, G., Barone, V., Mennucci, B., Petersson, G. A., Nakatsuji, H., Caricato, M., Li, X., Hratchian, H. P., Izmaylov, A. F., Bloino, J., Zheng, G., Sonnenberg, J. L., Hada, M., ... Fox, D. J. (2009). *Gaussian 09 Revision E.1*.

Ganesan, K., Raza, S. K., & Vijayaraghavan, R. (2010). Chemical warfare agents. *Journal of Pharmacy and Bioallied Sciences*, 2(3), 166–178.

Gehlhaar, A., Schiavo, E., Wölper, C., Schulte, Y., Auer, A. A., & Schulz, S. (2022). Comparing London dispersion pnictogen– π interactions in naphthyl-substituted dipnictanes. *Dalton Transactions*, 51(13), 5016–5023. <https://doi.org/10.1039/D2DT00477A>

George, J., Deringer, V. L., & Dronskowski, R. (2014). Cooperativity of Halogen, Chalcogen, and Pnictogen Bonds in Infinite Molecular Chains by Electronic Structure Theory. *The Journal of Physical Chemistry A*, 118(17), 3193–3200. <https://doi.org/10.1021/jp5015302>

Gini, A., Paraja, M., Galmés, B., Besnard, C., Poblador-Bahamonde, A. I., Sakai, N., Frontera, A., & Matile, S. (2020). Pnictogen-bonding catalysis: brevetoxin-type polyether cyclizations. *Chemical Science*, 11(27), 7086–7091. <https://doi.org/10.1039/D0SC02551H>

Girolami, G. S. (2009). Origin of the Terms Pnictogen and Pnictide. *Journal of Chemical Education*, 86(10), 1200. <https://doi.org/10.1021/ed086p1200>

Glendening, E. D., Landis, C. R., & Weinhold, F. (2013). NBO 6.0: Natural bond orbital analysis program. *Journal of Computational Chemistry*, *34*, 1429–1437. <https://doi.org/10.1002/jcc.23266>

Gomila, R. M., & Frontera, A. (2021). Metalloid Chalcogen–pnictogen σ -hole bonding competition in stibanyl telluranes. *Journal of Organometallic Chemistry*, *954–955*, 122092. <https://doi.org/10.1016/j.jorganchem.2021.122092>

Grabowski, S. J., Alkorta, I., & Elguero, J. (2013). Complexes between Dihydrogen and Amine, Phosphine, and Arsine Derivatives. Hydrogen Bond versus Pnictogen Interaction. *The Journal of Physical Chemistry A*, *117*(15), 3243–3251. <https://doi.org/10.1021/jp4016933>

Grimme, S., Hansen, A., Brandenburg, J. G., & Bannwarth, C. (2016). Dispersion-Corrected Mean-Field Electronic Structure Methods. *Chemical Reviews*, *116*(9), 5105–5154. <https://doi.org/10.1021/acs.chemrev.5b00533>

Grunenberg, J. (2010). *Computational spectroscopy: methods, experiments and applications*. Wiley-VCH.

Hashemi, B., Assadpour, E., & Jafari, S. M. (2026). Recent advances in protein modification strategies to enhance their gel formation capability and stability: Principles, mechanisms, and techniques. In *Advances in Colloid and Interface Science* (Vol. 351). Elsevier B.V. <https://doi.org/10.1016/j.cis.2026.103790>

Heinig, R., Zimmer, D., Yeh, S., & Krol, G. J. (2000). Development, validation and application of assays to quantify metrifonate and 2, 2-dichlorovinyl dimethylphosphate in human body fluids. *Journal of Chromatography B: Biomedical Sciences and Applications*, *741*(2), 257–269.

Hill, W. E., & Silva-Trivino, L. M. (1978). Preparation and characterization of di (tertiary phosphines) with electronegative substituents. 1. Symmetrical derivatives. *Inorganic Chemistry*, *17*(9), 2495–2498.

Hörnberg, A., Tunemalm, A.-K., & Ekström, F. (2007). Crystal structures of acetylcholinesterase in complex with organophosphorus compounds suggest that the acyl pocket modulates the aging reaction by precluding the formation of the trigonal bipyramidal transition state. *Biochemistry*, *46*(16), 4815–4825.

Hosseini Faradonbeh, S. M., Seyedalipour, B., Keivan Behjou, N., Rezaei, K., Baziyar, P., & Hosseinkhani, S. (2025). Structural insights into SOD1: from in silico and molecular dynamics to experimental analyses of ALS-associated E49K and R115G mutants. *Frontiers in Molecular Biosciences*, *12*. <https://doi.org/10.3389/fmolb.2025.1532375>

Humeniuk, H. V, Gini, A., Hao, X., Coelho, F., Sakai, N., & Matile, S. (2021). Pnictogen-Bonding Catalysis and Transport Combined: Polyether Transporters Made In Situ. *JACS Au*, *1*(10), 1588–1593. <https://doi.org/10.1021/jacsau.1c00345>

Jacquet, P., Daudé, D., Bzdrenga, J., Masson, P., Elias, M., & Chabrière, E. (2016). Current and emerging strategies for organophosphate decontamination: special focus on

hyperstable enzymes. *Environmental Science and Pollution Research*, 23(9), 8200–8218. <https://doi.org/10.1007/s11356-016-6143-1>

Jayawardane, P., Senanayake, N., & Dawson, A. (2009). Electrophysiological correlates of intermediate syndrome following acute organophosphate poisoning. *Clinical Toxicology*, 47(3), 193–205.

Jensen, F. (2017). *Introduction to computational chemistry*. John Wiley & Sons.

Jimmink, B., Sethio, D., Turunen, L., Von Der Heiden, D., & Erdélyi, M. (2021). Probing Halogen Bonds by Scalar Couplings. *Journal of the American Chemical Society*, 143(28), 10695–10699. <https://doi.org/10.1021/jacs.1c04477>

Jones, J. A. (2011). Quantum computing with NMR. In *Progress in Nuclear Magnetic Resonance Spectroscopy* (Vol. 59, Number 2, pp. 91–120). Elsevier B.V. <https://doi.org/10.1016/j.pnmrs.2010.11.001>

Jones, J. A. (2024). Controlling NMR spin systems for quantum computation. In *Progress in Nuclear Magnetic Resonance Spectroscopy* (Vols. 140–141, pp. 49–85). Elsevier B.V. <https://doi.org/10.1016/j.pnmrs.2024.02.002>

Karabıyık, H., Sevinçek, R., & Karabıyık, H. (2015). Effects of pnictogen and chalcogen bonds on the aromaticities of carbazole-like and dibenzofuran-like molecular skeletons: Cambridge Crystallographic Data Centre (CCDC) Study. *Journal of Physical Organic Chemistry*, 28(7), 490–496. <https://doi.org/https://doi.org/10.1002/poc.3442>

Kaushik, V., & Khaneja, N. (2025). Controlling Ensemble States of a Quantum System. *IEEE Control Systems Letters*, 9, 390–395. <https://doi.org/10.1109/LCSYS.2025.3573242>

Keith, T. A. (2019). AIMAll (Version 19.10. 12). *TK Gristmill Software: Overland Park, KS, USA*.

Klinkhammer, K. W., & Pyykko, P. (1995). Ab Initio Interpretation of the Closed-Shell Intermolecular E. cntdot.. cntdot.. cntdot. E Attraction in Dipnicogen (H₂E-EH₂)₂ and Dichalcogen (HE-EH)₂ Hydride Model Dimers. *Inorganic Chemistry*, 34(16), 4134–4138.

Kohn, W. (1965). Time-dependent Kohn–Sham density-functional theory. *Physical Review A*, 1133, 140–148.

Köppel, H., Domcke, W., & Schleyer, P. V. R. (1998). *Encyclopedia of Computational Chemistry*. Wiley, New York.

Krivdin, L. B. (2020). Recent advances in computational 31P NMR: Part 1. Chemical shifts. In *Magnetic Resonance in Chemistry* (Vol. 58, Number 6, pp. 478–499). John Wiley and Sons Ltd. <https://doi.org/10.1002/mrc.4965>

Kumar, S., Kaushik, G., & Villarreal-Chiu, J. F. (2016). Scenario of organophosphate pollution and toxicity in India: A review. *Environmental Science and Pollution Research*, 23, 9480–9491.

Laplaza, R., Peccati, F., A. Boto, R., Quan, C., Carbone, A., Piquemal, J., Maday, Y., & Contreras-García, J. (2021). NCIPLLOT and the analysis of noncovalent interactions using the reduced density gradient. *Wiley Interdisciplinary Reviews: Computational Molecular Science*, *11*(2), e1497.

Larrañaga, O., Arrieta, A., Fonseca Guerra, C., Bickelhaupt, F. M., & de Cózar, A. (2021). Nature of Alkali-and Coinage-Metal Bonds versus Hydrogen Bonds. *Chemistry—An Asian Journal*, *16*(4), 315–321.

Lee, L. M., Tsemperouli, M., Poblador-Bahamonde, A. I., Benz, S., Sakai, N., Sugihara, K., & Matile, S. (2019). Anion Transport with Pnictogen Bonds in Direct Comparison with Chalcogen and Halogen Bonds. *Journal of the American Chemical Society*, *141*(2), 810–814. <https://doi.org/10.1021/jacs.8b12554>

Legon, A. C. (2017). Tetrel, pnictogen and chalcogen bonds identified in the gas phase before they had names: a systematic look at non-covalent interactions. *Physical Chemistry Chemical Physics*, *19*(23), 14884–14896. <https://doi.org/10.1039/C7CP02518A>

Li, Y., Meng, L., Sun, C., & Zeng, Y. (2020). Organocatalysis by Halogen, Chalcogen, and Pnictogen Bond Donors in Halide Abstraction Reactions: An Alternative to Hydrogen Bond-Based Catalysis. *The Journal of Physical Chemistry A*, *124*(19), 3815–3824. <https://doi.org/10.1021/acs.jpca.0c01060>

Lino, J. B. D. R., & Ramalho, T. C. (2019). Exploring Through-Space Spin-Spin Couplings for Quantum Information Processing: Facing the Challenge of Coherence Time and Control Quantum States. *Journal of Physical Chemistry A*, *123*(7), 1372–1379. <https://doi.org/10.1021/acs.jpca.8b09425>

Lino, J. B. D. R., Sauer, S. P. A., & Ramalho, T. C. (2020). Enhancing NMR Quantum Computation by Exploring Heavy Metal Complexes as Multiqubit Systems: A Theoretical Investigation. *Journal of Physical Chemistry A*, *124*(24), 4946–4955. <https://doi.org/10.1021/acs.jpca.0c01607>

Lino, J. B. dos R., Gonçalves, M. A., Sauer, S. P. A., & Ramalho, T. C. (2022). Extending NMR Quantum Computation Systems by Employing Compounds with Several Heavy Metals as Qubits. *Magnetochemistry*, *8*(5). <https://doi.org/10.3390/magnetochemistry8050047>

Lino, J. B. R., Rocha, E. P., & Ramalho, T. C. (2017). Value of NMR Parameters and DFT Calculations for Quantum Information Processing Utilizing Phosphorus Heterocycles. *Journal of Physical Chemistry A*, *121*(23), 4486–4495. <https://doi.org/10.1021/acs.jpca.6b12728>

Lino, & Ramalho, J. B. R. ; (2018). Informação Quântica e Parâmetros de Ressonância Magnética Nuclear Quantum Information and Nuclear Magnetic Resonance Parameters. In *Rev. Virtual Quim* (Vol. 10, Number 4). <http://rvq.s bq.org.br>

Lu, T., & Chen, F. (2012). Multiwfn: A multifunctional wavefunction analyzer. *Journal of Computational Chemistry*, *33*, 580–592. <https://doi.org/10.1002/jcc.22885>

- Mahmudov, K. T., Gurbanov, A. V., Aliyeva, V. A., Resnati, G., & Pombeiro, A. J. L. (2020). Pnictogen bonding in coordination chemistry. *Coordination Chemistry Reviews*, 418, 213381. <https://doi.org/https://doi.org/10.1016/j.ccr.2020.213381>
- Mahmudov, K. T., Gurbanov, A. V., Guseinov, F. I., & da Silva, M. F. C. (2019). Noncovalent interactions in metal complex catalysis. *Coordination Chemistry Reviews*, 387, 32–46. <https://doi.org/https://doi.org/10.1016/j.ccr.2019.02.011>
- Mahmudov, K. T., Kopylovich, M. N., da Silva, M. F. C. G., & Pombeiro, A. J. L. (2019). *Noncovalent Interactions in Catalysis*. Royal Society of Chemistry.
- Medimagh, M., Issaoui, N., Gatfaoui, S., Antonia Brandán, S., Al-Dossary, O., Marouani, H., & J. Wojcik, M. (2021). Impact of non-covalent interactions on FT-IR spectrum and properties of 4-methylbenzylammonium nitrate. A DFT and molecular docking study. *Heliyon*, 7(10). <https://doi.org/10.1016/j.heliyon.2021.e08204>
- Michalczyk, M., Zierkiewicz, W., & Scheiner, S. (2025). Ability of the Spectroscopic Properties of the P=Se Bond of a Base to Assess Noncovalent Bond Strength. *Journal of Physical Chemistry A*. <https://doi.org/10.1021/acs.jpca.4c08283>
- Moeller, T., Bailar, J. C., Kleinberg, J., Guss, C. O., Castellion, M. E., & Metz, C. (1980). 9 - THE CHEMICAL BOND. In T. Moeller, J. C. Bailar, J. Kleinberg, C. O. Guss, M. E. Castellion, & C. Metz (Eds.), *Chemistry* (pp. 232–272). Academic Press. <https://doi.org/https://doi.org/10.1016/B978-0-12-503350-3.50014-7>
- Moilanen, J., Ganesamoorthy, C., Balakrishna, M. S., & Tuononen, H. M. (2009). Weak interactions between trivalent pnictogen centers: Computational analysis of bonding in dimers X3E...EX3 (E= Pnictogen, X= Halogen). *Inorganic Chemistry*, 48(14), 6740–6747.
- Morgon, N. H. (2007). *Métodos de química teórica e modelagem molecular*. Editora Livraria da Física.
- Mukherjee, S., & Gupta, R. D. (2020). Organophosphorus nerve agents: types, toxicity, and treatments. *Journal of Toxicology*, 2020(1), 3007984.
- Murray, J. S., Lane, P. A. T., & Politzer, P. (2007). A predicted new type of directional noncovalent interaction. *International Journal of Quantum Chemistry*, 107(12), 2286–2292.
- Neese, F. (2022). Software update: The ORCA program system—Version 5.0. In *Wiley Interdisciplinary Reviews: Computational Molecular Science* (Vol. 12). John Wiley and Sons Inc. <https://doi.org/10.1002/wcms.1606>
- Nordheider, A., Hupf, E., Chalmers, B. A., Knight, F. R., Bühl, M., Mebs, S., Checińska, L., Lork, E., Camacho, P. S., Ashbrook, S. E., Athukorala Arachchige, K. S., Cordes, D. B., Slawin, A. M. Z., Beckmann, J., & Woollins, J. D. (2015). Peri -substituted phosphorus-tellurium systems-an experimental and theoretical investigation of the p...te

through-space interaction. *Inorganic Chemistry*, 54(5), 2435–2446. <https://doi.org/10.1021/ic503056z>

Norman, N. C. (1997). *Chemistry of arsenic, antimony and bismuth*. Springer Science & Business Media.

Paraja, M., Gini, A., Sakai, N., & Matile, S. (2020). Pnictogen-Bonding Catalysis: An Interactive Tool to Uncover Unorthodox Mechanisms in Polyether Cascade Cyclizations. *Chemistry – A European Journal*, 26(67), 15471–15476. <https://doi.org/https://doi.org/10.1002/chem.202003426>

Pascual-Borràs, M., López, X., & Poblet, J. M. (2015). Accurate calculation of ³¹P NMR chemical shifts in polyoxometalates. *Physical Chemistry Chemical Physics*, 17, 8723–8731. <https://doi.org/10.1039/c4cp05016a>

Pessôa, K. F., Correia, J. C. G., Carauta, A. N. M., & Silva, F. B. da. (2018). *Revisão de alguns principais métodos utilizados em modelagem molecular. Parte II-Métodos quânticos*.

Pohanka, M. (2011). Cholinesterases, a target of pharmacology and toxicology. *Biomedical Papers of the Medical Faculty of Palacky University in Olomouc*, 155(3).

Politzer, P., & Murray, J. S. (2013). Halogen bonding: an interim discussion. *ChemPhysChem*, 14(2), 278–294.

Politzer, P., Murray, J. S., & Clark, T. (2013). Halogen bonding and other σ -hole interactions: A perspective. *Physical Chemistry Chemical Physics*, 15(27), 11178–11189.

Politzer, P., Murray, J. S., & Clark, T. (2019). Explicit inclusion of polarizing electric fields in σ - and π -hole interactions. *The Journal of Physical Chemistry A*, 123(46), 10123–10130.

Politzer, P., Murray, J. S., Clark, T., & Resnati, G. (2017). The σ -hole revisited. *Physical Chemistry Chemical Physics*, 19(48), 32166–32178.

Politzer, P., Murray, J. S., & Concha, M. C. (2008). σ -hole bonding between like atoms; a fallacy of atomic charges. *Journal of Molecular Modeling*, 14, 659–665.

Pomogaeva, A. V., Khoroshilova, O. V., Davydova, E. I., Suslonov, V. V., & Timoshkin, A. Y. (2021). Antimony(III) Iodide Complexes with Pyridine: Structures and bonding via three pnictogen bonds. *Zeitschrift Für Anorganische Und Allgemeine Chemie*, 647(7), 687–695. <https://doi.org/https://doi.org/10.1002/zaac.202000444>

Radha, A., Kumar, S., Sharma, D., Jassal, A. K., Zaręba, J. K., Franconetti, A., Frontera, A., Sood, P., & Pandey, S. K. (2019). Indirect influence of alkyl substituent on sigma-hole interactions: The case study of antimony(III) diphenyldithiophosphates with covalent Sb-S and non-covalent Sb...S pnictogen bonds. *Polyhedron*, 173, 114126. <https://doi.org/https://doi.org/10.1016/j.poly.2019.114126>

Ramanathan, C., Boulant, N., Chen, Z., Cory, D. G., Chuang, I., & Steffen, M. (2004). *NMR Quantum Information Processing* (Vol. 3, Number 5).

Ramsz, N. F. (1950). MAGNETIC SHIELDING OF NUCLEI IN MOLECULES*. In *JUNE* (Vol. 78, Number 6).

Rasouli, H., Hosseini Ghazvini, S. M. B., Yarani, R., Altıntaş, A., Jooneghani, S. G. N., & Ramalho, T. C. (2022). Deciphering inhibitory activity of flavonoids against tau protein kinases: a coupled molecular docking and quantum chemical study. *Journal of Biomolecular Structure and Dynamics*, 40(1), 411–424. <https://doi.org/10.1080/07391102.2020.1814868>

Rodrigues, R. R., & Gabbai, F. P. (2021). Structural Evidence for Pnictogen-Centered Lewis Acidity in Cationic Platinum-Stibine Complexes Featuring Pendant Amino or Ammonium Groups. *Molecules*, 26(7). <https://doi.org/10.3390/molecules26071985>

Rosli, N. F., Mayorga-Martinez, C. C., Fisher, A. C., Alduhaish, O., Webster, R. D., & Pumera, M. (2020). Arsenene nanomotors as anticancer drug carrier. *Applied Materials Today*, 21, 100819. <https://doi.org/https://doi.org/10.1016/j.apmt.2020.100819>

Rusakov, Y. Y., Rusakova, I. L., & Krivdin, L. B. (2015). MP2 calculation of ⁷⁷Se NMR chemical shifts taking into account relativistic corrections. *Magnetic Resonance in Chemistry*, 53, 485–492. <https://doi.org/10.1002/mrc.4226>

Rusakova, I. L., & Rusakov, Y. Y. (2020). Correlated ab initio calculations of one-bond ³¹P-⁷⁷Se and ³¹P-¹²⁵Te spin-spin coupling constants in a series of P-Se and P-Te systems accounting for relativistic effects (part 2). *Magnetic Resonance in Chemistry*, 58, 929–940. <https://doi.org/10.1002/mrc.5058>

Rusakova, I. L., & Rusakov, Y. Y. (2025). Computational Chemistry in Nuclear Magnetic Resonance. In *Magnetochemistry* (Vol. 11, Number 8). Multidisciplinary Digital Publishing Institute (MDPI). <https://doi.org/10.3390/magnetochemistry11080066>

Saeed, A., Mahesar, P. A., Zaib, S., Khan, M. S., Matin, A., Shahid, M., & Iqbal, J. (2014). Synthesis, cytotoxicity and molecular modelling studies of new phenylcinnamide derivatives as potent inhibitors of cholinesterases. *European Journal of Medicinal Chemistry*, 78, 43–53.

Sanz Camacho, P., McKay, D., Dawson, D. M., Kirst, C., Yates, J. R., Green, T. F. G., Cordes, D. B., Slawin, A. M. Z., Woollins, J. D., & Ashbrook, S. E. (2016). Investigating Unusual Homonuclear Intermolecular “through-Space” J Couplings in Organochalcogen Systems. *Inorganic Chemistry*, 55(21), 10881–10887. <https://doi.org/10.1021/acs.inorgchem.6b01121>

Scheiner, S. (2011a). A new noncovalent force: Comparison of P···N interaction with hydrogen and halogen bonds. *The Journal of Chemical Physics*, 134(9).

Scheiner, S. (2011b). Can two trivalent N atoms engage in a direct N···N noncovalent interaction? *Chemical Physics Letters*, 514(1), 32–35. <https://doi.org/https://doi.org/10.1016/j.cplett.2011.08.028>

Scheiner, S. (2011c). Effects of substituents upon the P \cdots N noncovalent interaction: the limits of its strength. *The Journal of Physical Chemistry A*, 115(41), 11202–11209.

Scheiner, S. (2013). Detailed comparison of the pnictogen bond with chalcogen, halogen, and hydrogen bonds. *International Journal of Quantum Chemistry*, 113(11), 1609–1620.

Scheiner, S. (2023). Transition between the Noncovalency and Covalency of σ -Hole Bonds. *The Journal of Physical Chemistry A*, 127(46), 9760–9770. <https://doi.org/10.1021/acs.jpca.3c06093>

Scheiner, S., & Adhikari, U. (2011). Abilities of different electron donors (D) to engage in a P \cdots D noncovalent interaction. *The Journal of Physical Chemistry A*, 115(40), 11101–11110.

Scheiner, S., Michalczyk, M., & Zierkiewicz, W. (2024). Correlation between Noncovalent Bond Strength and Spectroscopic Perturbations within the Lewis Base. *Journal of Physical Chemistry A*. <https://doi.org/10.1021/acs.jpca.4c07382>

Schiavo, E., Bhattacharyya, K., Mehring, M., & Auer, A. A. (2021). Are Heavy Pnictogen- π Interactions Really “ π Interactions”? *Chemistry – A European Journal*, 27(58), 14520–14526. <https://doi.org/https://doi.org/10.1002/chem.202102418>

Schwarz, S., Lucas, S. D., Sommerwerk, S., & Csuk, R. (2014). Amino derivatives of glycyrrhetic acid as potential inhibitors of cholinesterases. *Bioorganic & Medicinal Chemistry*, 22(13), 3370–3378.

Shieh, M., & Li, Y.-H. (2019). Pnictogen-containing iron and chromium carbonyl complexes: From complexes to semiconducting frameworks. *Journal of the Chinese Chemical Society*, 66(9), 1008–1018. <https://doi.org/https://doi.org/10.1002/jccs.201900119>

Shotonwa, I. O., & Olasunkanmi, L. O. (2023). Insights into non-covalent interactions, molecular and electronic structures of 3-monosubstituted and 3,5-disubstituted 1,2-dithiolium salts: Crystallographic visualization, Hirshfeld surface analysis and DFT Calculations. *Chemical Physics Impact*, 6. <https://doi.org/10.1016/j.chphi.2023.100211>

Smith, R. C., Earl, M. J., & Protasiewicz, J. D. (2004). Synthesis and photoluminescent properties of a series of pnictogen-centered chromophores. *Inorganica Chimica Acta*, 357(14), 4139–4143. <https://doi.org/https://doi.org/10.1016/j.ica.2004.06.051>

Soreq, H., & Seidman, S. (2001). Acetylcholinesterase—new roles for an old actor. *Nature Reviews Neuroscience*, 2(4), 294–302.

Thomas, J. M., & Thomas, R. (2023). Study of Non-Covalent Interactions Present in the Tapinarof–Ethanol System with Special Emphasis on Hydrogen-Bonding Interactions. *The Journal of Physical Chemistry B*, 127(26), 5933–5940. <https://doi.org/10.1021/acs.jpcc.3c03152>

Tondro, T., & Roohi, H. (2019). Substituent effects on the halogen and pnictogen bonds characteristics in ternary complexes 4-YPhNH₂···PH₂F···ClX (Y = H, F, CN, CHO, NH₂, CH₃, NO₂ and OCH₃, and X = F, OH, CN, NC, FCC and NO₂): A theoretical study. *Journal of Chemical Sciences*, 132(1), 18. <https://doi.org/10.1007/s12039-019-1715-5>

Tripathi, G., Badi-uz-zama, K., & Ramanathan, G. (2016). N...N pnictogen bonds in Boc-DOPA-OMe. *Chemical Physics Letters*, 653, 117–121. <https://doi.org/https://doi.org/10.1016/j.cplett.2016.04.076>

Tripathi, M. K., & Ramanathan, V. (2023). Nature and Strength of Sulfur-Centered Hydrogen Bond in Methanethiol Aqueous Solutions. *Journal of Physical Chemistry A*, 127(10), 2265–2273. <https://doi.org/10.1021/acs.jpca.2c08314>

Trujillo, C., Sánchez-Sanz, G., Alkorta, I., & Elguero, J. (2017). An insight on the aromatic changes in closed shell icosagen, tetrel, and pnictogen phenalenyl derivatives. *Structural Chemistry*, 28(2), 345–355. <https://doi.org/10.1007/s11224-016-0882-y>

Vandersypen, L. M. K., Steffen, M., Breyta, G., Yannoni, C. S., Sherwood, M. H., & Chuang, I. L. (2001). Experimental realization of Shor's quantum factoring algorithm using nuclear magnetic resonance. *Nature*, 414(6866), 883–887. <https://doi.org/10.1038/414883a>

Viesser, V. R., Ducati, L. C., Tormena, C. F., & Autschbach, J. (2018). The halogen effect on the ¹³C NMR chemical shift in substituted benzenes. *Physical Chemistry Chemical Physics*, 20(16), 11247–11259. <https://doi.org/10.1039/c8cp01249k>

Watson, A., Opresko, D., Young, R. A., Hauschild, V., King, J., & Bakshi, K. (2015). Organophosphate nerve agents. In *Handbook of toxicology of chemical warfare agents* (pp. 87–109). Elsevier.

Watson, A., Opresko, D., Young, R., Hauschild, V., King, J., & Bakshi, K. (2009). CHAPTER 6 - Organophosphate Nerve Agents. In R. C. Gupta (Ed.), *Handbook of Toxicology of Chemical Warfare Agents* (pp. 43–67). Academic Press. <https://doi.org/https://doi.org/10.1016/B978-0-12-374484-5.00006-7>

Weinhold, F., & Landis, C. R. (2001). Natural bond orbitals and extensions of localized bonding concepts. *Chemistry Education Research and Practice*, 2(2), 91–104.

Weinhold, F., Landis, C. R., & Glendening, E. D. (2016). What is NBO analysis and how is it useful? *International Reviews in Physical Chemistry*, 35(3), 399–440.

Wolters, L. P., & Bickelhaupt, F. M. (2012). Halogen bonding versus hydrogen bonding: a molecular orbital perspective. *ChemistryOpen*, 1(2), 96–105.

Wolters, L. P., & Bickelhaupt, F. M. (2015). The activation strain model and molecular orbital theory. *Wiley Interdisciplinary Reviews: Computational Molecular Science*, 5(4), 324–343.

Worek, F., Thiermann, H., & Wille, T. (2020). Organophosphorus compounds and oximes: a critical review. *Archives of Toxicology*, 94(7), 2275–2292.

Yamauchi, A., & Yanai, N. (2024). Toward Quantum Noses: Quantum Chemosensing Based on Molecular Qubits in Metal–Organic Frameworks. *Accounts of Chemical Research*, 57(20), 2963–2972. <https://doi.org/10.1021/acs.accounts.4c00333>

Yan, Y., & Wei, Z. (2022). Ca₂C MXene monolayer as a superior material for detection of toxic pnictogen hydrides. *Materials Chemistry and Physics*, 281, 125869. <https://doi.org/https://doi.org/10.1016/j.matchemphys.2022.125869>

Youdim, M. B. H., & Buccafusco, J. J. (2005). Multi-functional drugs for various CNS targets in the treatment of neurodegenerative disorders. *Trends in Pharmacological Sciences*, 26(1), 27–35.

Zahn, S., Frank, R., Hey-Hawkins, E., & Kirchner, B. (2011). Pnictogen bonds: A new molecular linker? *Chemistry - A European Journal*, 17(22), 6034–6038. <https://doi.org/10.1002/chem.201002146>

Zhang, J., Wei, J., Ding, W.-Y., Li, S., Xiang, S.-H., & Tan, B. (2021). Asymmetric Pnictogen-Bonding Catalysis: Transfer Hydrogenation by a Chiral Antimony(V) Cation/Anion Pair. *Journal of the American Chemical Society*, 143(17), 6382–6387. <https://doi.org/10.1021/jacs.1c02808>

Zheng, A., Liu, S. Bin, & Deng, F. (2017). ³¹P NMR Chemical Shifts of Phosphorus Probes as Reliable and Practical Acidity Scales for Solid and Liquid Catalysts. *Chemical Reviews*, 117(19), 12475–12531. <https://doi.org/10.1021/acs.chemrev.7b00289>

Ziegler, T., & Rauk, A. (1977). On the calculation of bonding energies by the Hartree Fock Slater method. *Theoretica Chimica Acta*, 46(1), 1–10. <https://doi.org/10.1007/BF00551648>

APPENDIX 1 - LIST OF PUBLICATIONS

1. Intramolecular Pnictogen Bonds as Key Determinants for NMR Quantum Computation Parameters

Gustavo A. Andolpho and Teodorico C. Ramalho

Scientific article published in *ACS Omega*

DOI: 10.1021/acsomega.5c05640

2. Polyethyleneimine-Modified Biosorbent Based on Banana Pseudostem Biomass for Environmental Remediation and Food Analysis

João Antonio Tavares Barboza, Maria Elisa Avila Barboza, Gustavo A. Andolpho, Nathan Patrocínio Viana, Kleryton Luiz Alves de Oliveira, Renata Pereira Lopes Moreira, Júlia Harumi Shinozaki, Letícia Tessaro, Alexandre L. B. Baccaro, Fabiana S. Felix, Teodorico C. Ramalho, and Guilherme Max Dias Ferreira

Scientific article published in *Advanced Sustainable Systems*

DOI: 10.1002/adsu.202500760

3. Solar Cell Innovation: Exploring Third-Generation Photovoltaics Using Compounds from Biomass and Plastic Waste Copyrolysis Analyzed via DFT and TD-DFT Methodologies

Danielle R. Garcia, Gustavo A. Andolpho, Ana Paula Garcia, Tania Maria Basegio, Annelise K. Alves, Hassan Rasouli, Carlos P. Bergmann, and Teodorico C. Ramalho

Scientific article published in *Journal of Chemistry*

DOI: 10.1155/joch/9423342

4. Exploring the potential of vanadium(IV) complex in autophagy activation: structural modifications, NMR calculations, and novel interactions with PI3K γ

Taináh M. R. Santos, Gustavo A. Andolpho, Artur G. Nogueira, Teodorico C. Ramalho

Scientific article published in *Journal of Molecular Modeling*

DOI: 10.1007/s00894-025-06549-8

5. Pnictogen bond-driven control of the molecular interaction between organophosphorus and acetylcholinesterase enzyme.

Gustavo A. Andolpho and Teodorico C. Ramalho

Scientific article published in *Journal of Computational Chemistry*

DOI: 10.1002/jcc.27328

6. Improving the Path to Obtain Spectroscopic Parameters for the PI3K-(Platinum Complex) System: Theoretical Evidences for Using ¹⁹⁵Pt NMR as a Probe

Taináh M. R. Santos, Gustavo A. Andolpho, Camila A. Tavares, Mateus A. Gonçalves, and Teodorico C. Ramalho

Scientific article published in *Magnetochemistry* — Issue Cover

DOI: 10.3390/magnetochemistry9040089

7. Solar-driven CO₂ conversion to methane and methanol using different nanostructured Cu₂O-based catalysts modified with Au nanoparticles

João Angelo Lima Perini, Lilian D. Moura Torquato, Juliana F. de Brito, Gustavo A. Andolpho, Mateus A. Gonçalves, Leonardo D. De Angelis, Lucas D. Germano, Susana I. Córdoba de Torresi, Teodorico C. Ramalho, Maria V. Boldrin Zanoni

Scientific article published in *Journal of Energy Chemistry*

DOI: 10.1016/j.jechem.2023.10.057

8. Insights into the value of statistical models, solvent, and relativistic effects for investigating Re complexes of 2-(4-aminophenyl)benzothiazole: a potential spectroscopic probe

Gustavo A. Andolpho, Elaine F. F. da Cunha, and Teodorico C. Ramalho

Scientific article published in *Journal of Molecular Modeling*

DOI: 10.1007/s00894-022-05146-3

9. Exploring ¹²⁹Xe NMR parameters for structural investigation of biomolecules: relativistic, solvent, and thermal effects

Mateus A. Gonçalves, Gustavo A. Andolpho, Elaine F. F. da Cunha, and Teodorico C. Ramalho

Scientific article published in *Journal of Molecular Modeling*

DOI: 10.1007/s00894-022-05365-8

**10. Exploring EPR Parameters of ^{187}Re Complexes for Designing New MRI Probes:
From the Gas Phase to Solution and a Model Protein Environment**

Gustavo A. Andolpho, Elaine F. F. da Cunha, and Teodorico C. Ramalho

Scientific article published in *Journal of Chemistry*

DOI: 10.1155/2022/7056284

**11. Hybrid Materials Based on Magnetic Iron Oxides with Benzothiazole Derivatives:
A Plausible Potential Spectroscopy Probe**

Silviana Corrêa, Isael Aparecido Rosa, Gustavo A. Andolpho, Leticia Cristina de Assis, Maíra dos S. Pires, Livia C. T. Lacerda, Francisco G. E. Nogueira, Elaine F. F. da Cunha, Eugenie Nepovimova, Kamil Kuca, and Teodorico C. Ramalho

Scientific article published in *International Journal of Molecular Sciences*

DOI: 10.1007/s00894-022-05365-8

APPENDIX 2 – ARTICLE 1 SUPPORTING INFORMATION

Table S1. Topological parameters for System 1. Distance in Angstroms and other parameters in atomic units.

Distance	Electron Densities ($\rho(r)$)	Laplacian Electron Densities ($\nabla^2\rho(r)$)
1.26	0.3821	3.8493
1.36	0.3818	3.8522
1.46	0.2981	1.7356
1.56	0.2409	0.7137
1.66	0.1990	0.2315
1.76	0.1665	0.1723
1.86	0.1410	-0.0613
1.96	0.1205	-0.0707
2.06	0.1038	-0.0513
2.16	0.0897	-0.0231
2.26	0.0774	0.0036
2.36	0.0668	0.0244
2.46	0.0574	0.0383
2.56	0.0493	0.0461
2.66	0.0423	0.0489
2.76	0.0362	0.0483
2.86	0.0310	0.0456
2.96	0.0265	0.0417
3.06	0.0227	0.0373
3.16	0.0167	0.0286
3.26	0.0143	0.0247
3.36	0.0123	0.0214
3.46	0.0105	0.0185
3.56	0.0090	0.0161
3.66	0.0076	0.0141
3.76	0.0065	0.0124
3.86	0.0055	0.0109
3.96	0.0046	0.0095
4.06	0.0039	0.0083
4.16	0.0033	0.0072
4.26	0.0028	0.0062
4.36	0.0027	0.0052

4.46	0.0020	0.0047
4.56	0.0017	0.0040
4.66	0.0017	0.0034
4.76	0.0012	0.0030
4.86	0.0011	0.0025
4.96	0.0009	0.0022
5.06	0.0008	0.0019
5.16	0.0007	0.0017

Table S2. Topological parameters for system **2**. Distance in Angstroms and other parameters in atomic units.

Distance	Electron Densities ($\rho(r)$)	Laplacian Electron Densities ($\nabla^2\rho(r)$)
1.50	0.4353	-0.4818
1.60	0.3910	-0.3432
1.70	0.3486	-0.2262
1.80	0.2767	-0.1732
1.90	0.2200	-0.1012
2.00	0.1754	0.1542
2.10	0.1404	0.1645
2.20	0.1129	0.1518
2.30	0.0913	0.1300
2.40	0.0742	0.1074
2.50	0.0605	0.0875
2.60	0.0496	0.0714
2.70	0.0408	0.0589
2.80	0.0314	0.0340
2.90	0.0263	0.0306
3.00	0.0221	0.0271
3.10	0.0186	0.0237
3.20	0.0157	0.0204
3.30	0.0133	0.0174
3.40	0.0112	0.0115
3.50	0.0095	0.0126
3.60	0.0081	0.0106
3.70	0.0069	0.0090
3.80	0.0058	0.0076
3.90	0.0050	0.0065
4.00	0.0042	0.0055
4.10	0.0036	0.0047

4.20	0.0030	0.0040
4.30	0.0026	0.0035
4.40	0.0022	0.0030
4.50	0.0018	0.0026
4.60	0.0015	0.0022
4.70	0.0012	0.0019
4.80	0.0010	0.0016
4.90	0.0009	0.0014
5.00	0.0007	0.0012
5.10	0.0006	0.0010
5.40	0.0003	0.0007

Table S3. Topological parameters for system **3**. Distance in Angstroms and other parameters in atomic units.

Distance	Electron Densities ($\rho(r)$)	Laplacian Electron Densities ($\nabla^2\rho(r)$)
1.71	0.1391	0.3939
1.81	0.1183	0.1363
1.91	0.1021	0.0291
2.01	0.0888	-0.0031
2.11	0.0770	0.0544
2.21	0.0664	0.0164
2.31	0.0570	0.0327
2.41	0.0488	0.0447
2.51	0.0417	0.0516
2.61	0.0356	0.0542
2.71	0.0304	0.0536
2.81	0.0260	0.0510
2.91	0.0221	0.0472
3.01	0.0189	0.0429
3.11	0.0161	0.0386
3.21	0.0138	0.0344
3.31	0.0117	0.0305
3.41	0.0100	0.0270
3.51	0.0086	0.0239
3.61	0.0073	0.0212
3.71	0.0062	0.0187
3.81	0.0053	0.0166
3.91	0.0045	0.0146
4.01	0.0038	0.0129

4.11	0.0033	0.0114
4.21	0.0028	0.0101
4.31	0.0022	0.0090
4.41	0.0019	0.0079
4.51	0.0016	0.0065
4.61	0.0014	0.0060
4.71	0.0012	0.0051
4.81	0.0010	0.0044
4.91	0.0008	0.0038
5.01	0.0007	0.0033
5.11	0.0006	0.0028
5.21	0.0005	0.0024
5.31	0.0005	0.0021
5.41	0.0004	0.0018
5.51	0.0003	0.0015
5.61	0.0003	0.0013

Table S4. Topological parameters for system 4. Distance in Angstroms and other parameters in atomic units.

Distance	Electron Densities ($\rho(r)$)	Laplacian Electron Densities ($\nabla^2\rho(r)$)
1.40	0.2696	0.2018
1.50	0.2187	0.8133
1.60	0.1796	0.6490
1.70	0.1524	0.1635
1.80	0.1318	-0.4950
1.90	0.1152	-0.1255
2.00	0.1011	-0.1340
2.10	0.0887	-0.1129
2.20	0.0726	-0.0071
2.30	0.0307	-0.0066
2.40	0.0514	0.0269
2.50	0.0432	0.0290
2.60	0.0364	0.0292
2.70	0.0307	0.0280
2.80	0.0260	0.0260
2.90	0.0220	0.0233
3.00	0.0186	0.0205
3.10	0.0158	0.0178
3.20	0.0135	0.0153

3.30	0.0115	0.0131
3.40	0.0098	0.0111
3.50	0.0078	0.0101
3.60	0.0066	0.0083
3.70	0.0056	0.0069
3.80	0.0047	0.0057
3.90	0.0040	0.0048
4.00	0.0034	0.0040
4.10	0.0028	0.0034
4.20	0.0024	0.0028
4.30	0.0020	0.0024
4.40	0.0017	0.0021
4.50	0.0014	0.0017

Figure S1. NBOs involved in the interaction of GF—Serine distance at (a) 1.50 and (b) 2.00Å.

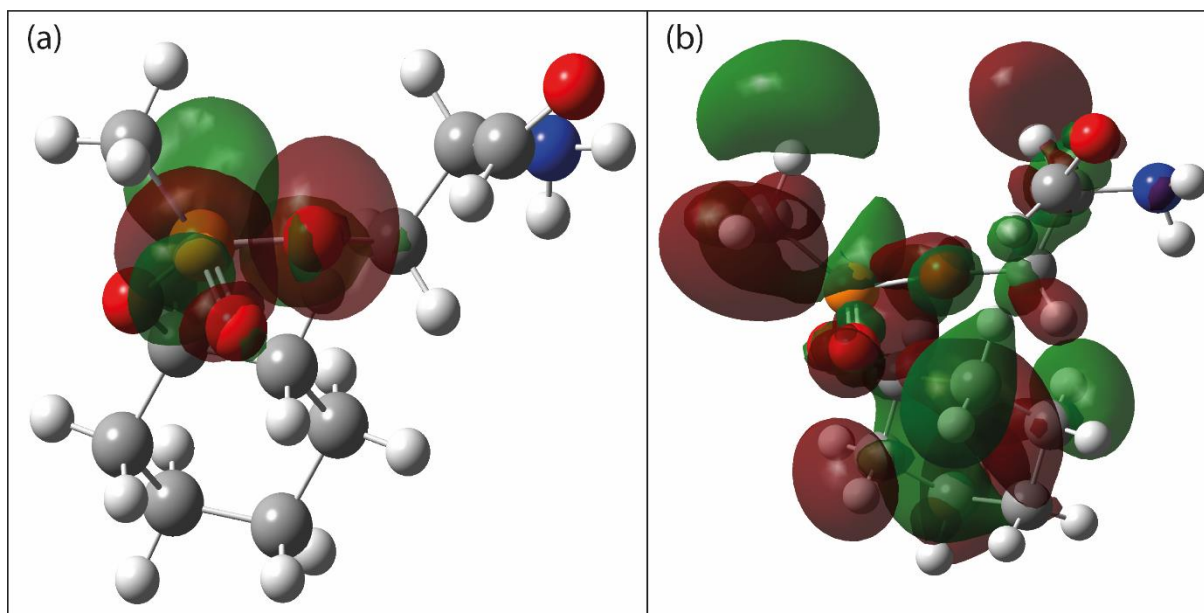


Figure S2. NBOs involved in the interaction of GP—Serine distance at (a) 1.71 and (b) 2.11Å.

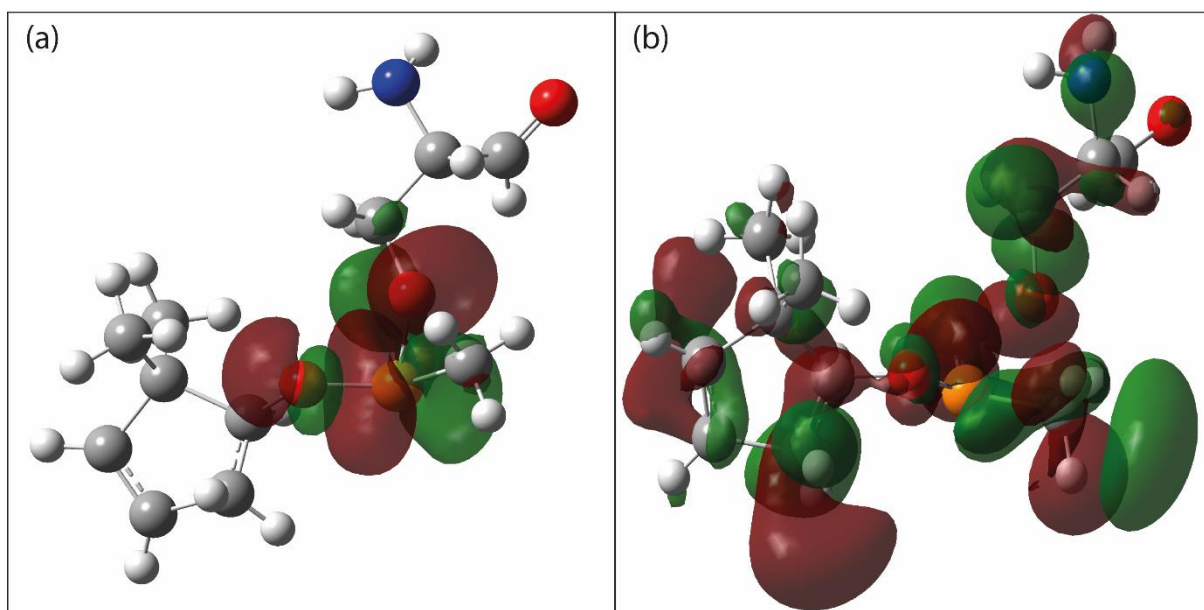


Figure S3. NBOs involved in the interaction of VX—Serine distance at (a) 1.50 and (b) 2.40Å.

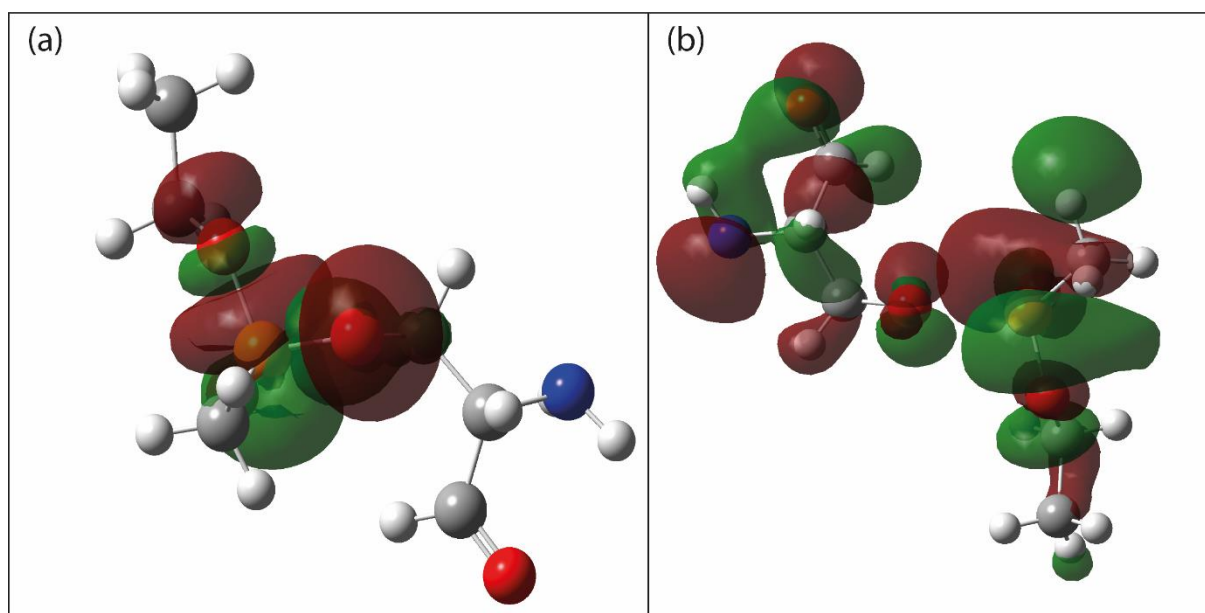
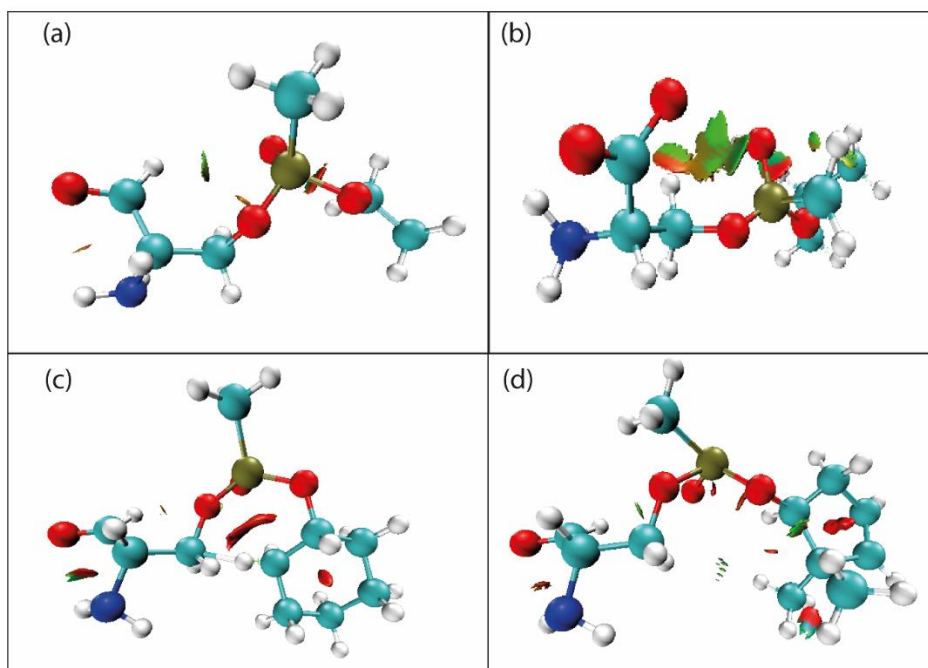


Table S5. NBO analysis of the four systems at the original P-O distance

System	Donor	Acceptor	Energy (kcal.mol ⁻¹)
1	σ_{O6-P13}	$\pi^*_{P13-O14}$	52.69
	$\sigma_{P13-O15}$	$\pi^*_{P13-O14}$	49.51
	$\pi_{P13-O14}$	σ^*_{O6-P13}	26.42
	$\pi_{P13-O14}$	$\sigma^*_{P13-O15}$	26.18
2	n_{O6}	σ^*_{P8-O10}	34.00
	n_{O7}	σ^*_{O6-P8}	20.42
	n_{O7}	σ^*_{P8-O10}	19.95
	n_{O6}	σ^*_{O7-P8}	15.55
3	σ_{O6-P9}	π^*_{O8-P9}	61.71
	π_{O8-P9}	σ^*_{O6-P9}	21.82
	n_{O11}	σ^*_{O8-P9}	15.72
	n_{O8}	σ^*_{P9-C16}	14.33
4	σ_{O6-P8}	π^*_{P8-O9}	56.96
	π_{P8-O9}	σ^*_{O6-P8}	39.19
	σ_{P8-O17}	π^*_{P8-O9}	17.34
	n_{O9}	σ^*_{P8-O17}	16.42

Table S6. NBO analysis of the four systems at the final P-O distance

System	Donor	Acceptor	Energy (kcal.mol ⁻¹)
1	n_{O14}	σ^*_{O6-P13}	59.37
	n_{O14}	$\sigma^*_{P13-O15}$	21.00
	n_{O14}	RY_{P13}	19.90
	n_{O15}	σ^*_{O6-P13}	17.55
2	n_{O7}	σ^*_{P8-O10}	24.11
	n_{P8}	σ^*_{O6-C9}	19.59
	n_{O10}	σ^*_{P8-C9}	9.45
	n_{O7}	RY_{P8}	8.79
3	n_{O8}	σ^*_{O6-P9}	69.37
	n_{O8}	σ^*_{O8-P9}	28.22
	n_{O8}	RY_{P9}	20.17
	n_{O8}	σ^*_{P9-O11}	19.66
4	n_{O9}	σ^*_{O6-P8}	63.95
	n_{O9}	σ^*_{P8-O17}	22.42
	n_{O17}	σ^*_{O6-P8}	17.73
	n_{O9}	RY_{P8}	12.91

Figure S4. NCI plot (isovalue= 0.5 au) for the system (a) **1**, (b) **2**, (c) **3**, and (d) **4** at $r=0\text{\AA}$.

Equation S1. Energy decomposition.

$$\Delta E_{int}(\xi) = \Delta V_{elestat}(\xi) + \Delta E_{Pauli}(\xi) + \Delta E_{OI}(\xi)$$

Table S7. Activation strain analysis and energy decomposition analysis (in kcal mol⁻¹)

System	ΔE_{int}	ΔE_{Pauli}	ΔE_{OI}	$\Delta V_{elestat}$
1	-83.47	125.89	-159.25	-50.11
2	-36.27	281.33	-217.24	-100.37
3	-17.28	226.12	-148.14	-95.26
4	-81.18	84.39	-132.90	-32.67

Table S8. Cartesian coordinates (in Å) for systems 1-4.

System 1			
at 1.26Å P—O distance			
N	-3.48500	60.50500	345.41800
C	-2.38200	61.48300	345.34500
C	-1.23000	61.02600	346.24100
O	-0.62330	59.95300	345.98760
C	-2.95500	62.87200	345.64100
O	-2.03500	63.91800	345.35500
O	-1.67200	64.83000	347.34000
P	-1.74200	64.97300	345.98200
C	-0.04300	65.00400	345.49700
O	-2.12700	66.39600	345.70300
C	-2.69100	67.23400	346.64900
C	-1.60300	68.10300	347.21000
C	-3.71300	68.06800	345.91100
H	-3.12200	62.90480	346.69740
H	-3.77410	63.00480	344.96550
H	-1.94830	61.54710	344.36890
H	-3.23140	59.76220	346.03760
H	-4.30920	60.95700	345.75920
H	-3.66170	60.13320	344.50660
O	-0.84230	61.81790	347.36680
H	0.53410	64.41850	346.18180
H	0.05400	64.59870	344.51150
H	-3.15200	66.70330	347.45570
H	-2.01590	68.76130	347.94560
H	-0.85310	67.48820	347.66230
H	-1.16450	68.67890	346.42200
H	-4.18610	68.74050	346.59570
H	-4.44970	67.42600	345.47520
H	-3.22670	68.62790	345.13970
H	0.31160	66.01350	345.50400
at 2.26Å P—O distance			
N	-3.60100	60.08700	345.17000
C	-2.49800	61.06500	345.09700
C	-1.34600	60.60800	345.99300
O	-0.73930	59.53500	345.73960
C	-3.07100	62.45400	345.39300
O	-2.15100	63.50000	345.10700
O	-1.55600	65.24800	347.58800
P	-1.62600	65.39100	346.23000
C	0.07300	65.42200	345.74500
O	-2.01100	66.81400	345.95100
C	-2.57500	67.65200	346.89700
C	-1.48700	68.52100	347.45800
C	-3.59700	68.48600	346.15900
H	-3.23800	62.48680	346.44940
H	-3.89010	62.58680	344.71750
H	-2.06430	61.12910	344.12090
H	-3.34740	59.34420	345.78960
H	-4.42520	60.53900	345.51120
H	-3.77770	59.71520	344.25860
O	-0.95830	61.39990	347.11880

H	0.65010	64.83650	346.42980
H	0.17000	65.01670	344.75950
H	-3.03600	67.12130	347.70370
H	-1.89990	69.17930	348.19360
H	-0.73710	67.90620	347.91030
H	-1.04850	69.09690	346.67000
H	-4.07010	69.15850	346.84370
H	-4.33370	67.84400	345.72320
H	-3.11070	69.04590	345.38770
H	0.42760	66.43150	345.75200
System 2			
at 1.50Å P—O distance			
N	55.90340	29.92490	22.13000
C	54.85140	28.91390	22.25900
C	53.74440	29.49790	23.13400
O	53.34340	30.64390	22.93200
C	55.40440	27.63290	22.88200
O	54.39240	26.64990	23.01100
C	57.30060	23.20810	23.08900
O	53.85760	25.36710	24.13000
P	54.11060	25.20910	22.68000
C	58.76660	23.53110	23.27400
O	55.15460	24.04410	22.45100
C	58.97260	24.82710	24.03300
C	58.20960	25.97910	23.41000
C	56.74360	25.65610	23.22200
C	56.53860	24.35910	22.46300
C	52.55460	24.79910	21.83800
H	55.62610	30.75750	22.60940
H	56.75120	29.57660	22.52990
H	54.46700	28.66030	21.29310
H	53.31810	28.91190	23.92130
H	55.70820	27.88660	23.87610
H	56.11860	27.24250	22.18750
H	56.89620	23.08110	24.07150
H	57.25840	22.40360	22.38490
H	59.16790	22.75550	23.89230
H	59.16320	23.69270	22.29340
H	58.54690	24.67640	25.00300
H	60.01050	25.06870	23.93590
H	58.25050	26.78140	24.11680
H	58.61500	26.10970	22.42840
H	56.34500	25.49530	24.20180
H	56.34380	26.43140	22.60240
H	56.90900	24.49770	21.46880
H	51.76230	24.75260	22.55560
H	52.65140	23.85100	21.35160
H	52.33350	25.55220	21.11070
at 2.00Å P—O distance			
N	55.95040	30.16440	22.18500
C	54.89840	29.15340	22.31400
C	53.79140	29.73740	23.18900
O	53.39040	30.88340	22.98700
C	55.45140	27.87240	22.93700
O	54.43940	26.88940	23.06600

C	57.25360	22.96860	23.03400
O	53.81060	25.12760	24.07500
P	54.06360	24.96960	22.62500
C	58.71960	23.29160	23.21900
O	55.10760	23.80460	22.39600
C	58.92560	24.58760	23.97800
C	58.16260	25.73960	23.35500
C	56.69660	25.41660	23.16700
C	56.49160	24.11960	22.40800
C	52.50760	24.55960	21.78300
H	55.67310	30.99700	22.66440
H	56.79820	29.81610	22.58490
H	54.51400	28.89980	21.34810
H	53.36510	29.15140	23.97630
H	55.75520	28.12610	23.93110
H	56.16560	27.48200	22.24250
H	56.84920	22.84160	24.01650
H	57.21140	22.16410	22.32990
H	59.12090	22.51600	23.83730
H	59.11620	23.45320	22.23840
H	58.49990	24.43690	24.94800
H	59.96350	24.82920	23.88090
H	58.20350	26.54190	24.06180
H	58.56800	25.87020	22.37340
H	56.29800	25.25580	24.14680
H	56.29680	26.19190	22.54740
H	56.86200	24.25820	21.41380
H	51.71530	24.51310	22.50060
H	52.60440	23.61150	21.29660
H	52.28650	25.31270	21.05570

System 3

 at 1.71 Å P—O distance

N	107.19470	41.92850	29.18580
C	108.27570	41.52350	28.28080
C	108.28570	39.99750	28.20280
O	107.25370	39.41650	27.82480
C	109.56670	42.20650	28.76180
O	110.69170	41.98750	27.91080
C	111.55330	41.83650	26.43320
P	112.37930	41.76650	28.08920
O	112.06830	40.50950	28.80920
C	112.24330	45.25350	31.25020
C	113.06430	43.98150	31.47820
C	112.34030	43.12850	32.50720
C	114.48330	44.38550	32.11720
C	115.46030	43.85950	31.30220
C	114.71730	43.60150	29.82020
C	113.44730	43.13750	30.13320
O	112.54830	43.15850	28.97020
H	106.70290	41.11710	29.50170
H	107.58120	42.41100	29.97180
H	108.14990	41.84440	27.26780
H	109.16090	39.44170	28.46740
H	109.81190	41.74220	29.69410
H	109.37200	43.25790	28.72250

H	110.98510	40.94290	26.28000
H	110.90170	42.68440	26.39520
H	112.29580	41.92270	25.66760
H	111.36900	45.22900	31.86650
H	112.83390	46.10930	31.50290
H	111.95330	45.31130	30.22190
H	111.44350	43.62480	32.81450
H	112.97410	42.97920	33.35620
H	112.09360	42.18120	32.07520
H	114.63910	44.95630	33.00880
H	116.47910	43.65780	31.55970
H	114.60820	44.55170	29.34050
H	115.24110	42.80990	29.32640
H	113.36420	42.09640	30.36570
at 2.11Å P—O distance			
N	106.99750	41.95450	29.16500
C	108.07850	41.54950	28.26000
C	108.08850	40.02350	28.18200
O	107.05650	39.44250	27.80400
C	109.36950	42.23250	28.74100
O	110.49450	42.01350	27.89000
C	111.75050	41.81050	26.45400
P	112.57650	41.74050	28.11000
O	112.26550	40.48350	28.83000
C	112.44050	45.22750	31.27100
C	113.26150	43.95550	31.49900
C	112.53750	43.10250	32.52800
C	114.68050	44.35950	32.13800
C	115.65750	43.83350	31.32300
C	114.91450	43.57550	29.84100
C	113.64450	43.11150	30.15400
O	112.74550	43.13250	28.99100
H	106.50570	41.14310	29.48090
H	107.38400	42.43700	29.95100
H	107.95270	41.87040	27.24700
H	108.96370	39.46770	28.44660
H	109.61470	41.76820	29.67330
H	109.17480	43.28390	28.70170
H	111.18230	40.91690	26.30080
H	111.09890	42.65840	26.41600
H	112.49300	41.89670	25.68840
H	111.56620	45.20300	31.88730
H	113.03110	46.08330	31.52370
H	112.15050	45.28530	30.24270
H	111.64070	43.59880	32.83530
H	113.17130	42.95320	33.37700
H	112.29080	42.15520	32.09600
H	114.83630	44.93030	33.02960
H	116.67630	43.63180	31.58050
H	114.80540	44.52570	29.36130
H	115.43830	42.78390	29.34720
H	113.56140	42.07040	30.38650
System 4			
at 1.50Å P—O distance			
N	50.17500	-29.70540	345.67140

C	50.95500	-28.78640	344.83440
C	52.38300	-28.75440	345.36740
O	53.03500	-29.81340	345.39340
C	50.24100	-27.43640	344.77940
O	50.71700	-26.64640	343.70240
H	50.18200	-29.35940	346.68340
H	50.60700	-30.68340	345.62540
H	50.98300	-29.19440	343.82440
H	52.82400	-27.82140	345.71840
H	49.17100	-27.60540	344.64940
H	50.41400	-26.90440	345.71440
P	51.41000	-25.31160	343.69160
O	51.99700	-24.82560	344.99560
O	50.21600	-24.28960	343.20960
C	52.73800	-25.33660	342.38960
C	49.82600	-23.25860	344.06860
C	48.47700	-22.71160	343.60360
H	53.24800	-24.37260	342.37260
H	52.28900	-25.52660	341.41560
H	53.45600	-26.12360	342.61760
H	49.73500	-23.64260	345.08460
H	50.57000	-22.46260	344.04560
H	48.16300	-21.90560	344.26660
H	47.73500	-23.50960	343.62560
H	48.57000	-22.32960	342.58660
at 2.40Å P—O distance			
N	49.96800	-30.10500	345.67500
C	50.74800	-29.18600	344.83800
C	52.17600	-29.15400	345.37100
O	52.82800	-30.21300	345.39700
C	50.03400	-27.83600	344.78300
O	50.51000	-27.04600	343.70600
H	49.97500	-29.75900	346.68700
H	50.40000	-31.08300	345.62900
H	50.77600	-29.59400	343.82800
H	52.61700	-28.22100	345.72200
H	48.96400	-28.00500	344.65300
H	50.20700	-27.30400	345.71800
P	51.61700	-24.91200	343.68800
O	52.20400	-24.42600	344.99200
O	50.42300	-23.89000	343.20600
C	52.94500	-24.93700	342.38600
C	50.03300	-22.85900	344.06500
C	48.68400	-22.31200	343.60000
H	53.45500	-23.97300	342.36900
H	52.49600	-25.12700	341.41200
H	53.66300	-25.72400	342.61400
H	49.94200	-23.24300	345.08100
H	50.77700	-22.06300	344.04200
H	48.37000	-21.50600	344.26300
H	47.94200	-23.11000	343.62200
H	48.77700	-21.93000	342.58300

APPENDIX 3 – ARTICLE 2 SUPPORTING INFORMATION

Equation S1. Decomposition of the Interaction Energy.

$$\Delta E_{int}(\xi) = \Delta V_{elestat}(\xi) + \Delta E_{Pauli}(\xi) + \Delta E_{OI}(\xi)$$

Table S1. Main results of the NBO analysis of the four compounds. Energy in kcal/mol.
LP=Lone Pair.

Compound	Donor-Acceptor	Energy
1	LP(P1) — $\sigma^*(P2-C)$	5.97
	LP(P2) — $\sigma^*(P1-C)$	2.56
2	LP(Se) — $\sigma^*(P-C)$	2.90
	LP(Se) — $\sigma^*(P-C)$	1.75
	LP(Se) — $\sigma^*(P-C)$	0.58
	LP(P) — $\sigma^*(Se-C)$	7.76
3	LP(P1) — $\sigma^*(P2-C)$	4.23
	LP(P1) — $\sigma^*(P2-C)$	0.56
4	LP(Se) — $\sigma^*(P-C)$	0.88
	LP(Se) — $\sigma^*(P-C)$	3.94
	LP(Se) — $\sigma^*(P-C)$	0.54

Table S2. Chemical Shifts values for compound **1**. Distance in Angstroms and chemical shifts in ppm.

Distance	$\delta(\text{P1})$	$\delta(\text{P2})$
4.39	0.77	-15.74
4.29	1.41	-15.74
4.19	1.81	-16.79
4.09	2.22	-17.87
3.99	2.39	-19.24
3.89	2.23	-20.29
3.79	1.78	-21.27
3.69	1.59	-21.68
3.59	1.76	-22.58
3.49	2.03	-24.11
3.39	2.37	-25.16
3.29	2.60	-25.65
3.19	2.92	-25.04
3.09	2.61	-23.71
2.99	3.34	-23.87
2.89	3.39	-24.57
2.79	3.55	-28.42
2.69	3.57	-29.84
2.59	3.51	-29.48
2.49	3.53	-29.52
2.39	3.57	-30.31
2.29	3.70	-31.07
2.19	4.29	-31.76

Table S3. Chemical Shifts values for compound **3**. Distance in Angstroms and chemical shifts in ppm.

Distance	$\delta(\text{P1})$	$\delta(\text{P2})$
3.40	70.29	2.72
3.30	72.51	2.78
3.20	72.99	1.57
3.10		
3.00	70.81	3.28
2.90	73.80	3.29
2.80	76.09	3.25
2.70	73.47	3.30
2.60	90.06	3.39
2.50	95.00	3.54
2.40	103.04	3.76
2.30	112.64	3.98
2.20	125.06	4.14

Table S4. Topological parameters for compound **1**. Distance in Angstroms and other parameters in atomic units. $\nabla^2\rho$ =Laplacian of the electron density; V=Potential energy.

Distance	$\nabla^2\rho(\mathbf{r})$	V
4.39	0.0058	-0.0007
4.29	0.0066	-0.0008
4.19	0.0077	-0.0010
4.09	0.0089	-0.0012
3.99	0.0105	-0.0015
3.89	0.0122	-0.0019
3.79	0.0143	-0.0023
3.69	0.0166	-0.0029
3.59	0.0192	-0.0036
3.49	0.0221	-0.0045
3.39	0.0252	-0.0056
3.29	0.0287	-0.0070
3.19	0.0320	-0.0088
3.09	0.0358	-0.0109
2.99	0.0392	-0.0136
2.89	0.0418	-0.0170
2.79	0.0431	-0.0213
2.69	0.0419	-0.0267
2.59	0.0364	-0.0337
2.49	0.0240	-0.0430
2.39	0.0011	-0.0555
2.29	-0.0372	-0.0728
2.19	-0.0974	-0.0978

Table S5. Topological parameters for system **3**. Distance in Angstroms and other parameters in atomic units. $\nabla^2\rho$ =Laplacian of the electron density; V=Potential energy.

Distance	$\nabla^2\rho(\mathbf{r})$	V
3.40	0.0287	-0.0059
3.30	0.0328	-0.0072
3.20	0.0372	-0.0089
3.10	0.0416	-0.0110
3.00	0.0459	-0.0137
2.90	0.0494	-0.0170
2.80	0.0514	-0.0213
2.70	0.0503	-0.0268
2.60	0.0442	-0.0342
2.50	0.0298	-0.0443
2.40	0.0025	-0.0586
2.30	-0.0440	-0.0796
2.20	-0.1168	-0.1134

Table S6. Cartesian coordinates (in Å) for compounds **1-4**.

Compound 1			
P	-0.385	7.646	8.023
P	-2.834	8.214	6.223
C	-1.097	8.994	9.037
C	-0.533	9.295	10.264
C	-0.921	10.376	11.072
C	-1.900	11.207	10.603
C	-2.501	10.918	9.366
C	-3.474	11.884	9.051
C	-4.173	11.749	7.888
C	-3.921	10.618	7.088
C	-2.981	9.645	7.376
C	-2.174	9.806	8.555
C	-2.510	12.447	11.190
C	-3.534	12.922	10.134
C	0.285	6.448	9.271
C	1.057	5.366	8.525
C	-0.865	5.847	10.066
C	1.144	8.469	7.336
C	2.194	8.917	8.337
C	0.725	9.625	6.436
C	-4.279	8.487	5.116
C	-4.009	9.085	3.886
C	-5.026	9.330	2.974
C	-6.329	8.958	3.274
C	-6.607	8.345	4.488
C	-5.591	8.114	5.404
C	-3.486	6.841	7.241
C	-3.272	5.546	6.773
C	-3.765	4.452	7.467
C	-4.472	4.640	8.648
C	-4.682	5.925	9.126
C	-4.193	7.019	8.425
H	0.272	8.671	10.632
H	-0.431	10.544	12.024
H	-4.929	12.463	7.581
H	-4.526	10.504	6.199
H	-1.748	13.205	11.391
H	-2.990	12.228	12.147
H	-4.542	13.001	10.549
H	-3.279	13.910	9.742
H	0.974	6.946	9.960
H	0.416	4.861	7.797
H	1.424	4.613	9.229

H	1.920	5.770	7.991
H	-0.489	5.092	10.763
H	-1.588	5.364	9.403
H	-1.397	6.605	10.644
H	1.578	7.687	6.701
H	1.805	9.699	8.994
H	3.057	9.334	7.806
H	2.556	8.097	8.960
H	1.596	10.031	5.912
H	0.284	10.434	7.025
H	-0.011	9.314	5.692
H	-2.988	9.364	3.643
H	-4.799	9.802	2.024
H	-7.125	9.139	2.560
H	-7.623	8.048	4.725
H	-5.823	7.642	6.351
H	-2.706	5.395	5.859
H	-3.591	3.450	7.090
H	-4.852	3.785	9.196
H	-5.231	6.078	10.049
H	-4.366	8.020	8.805
Compound 2			
Se	0.151	5.863	2.040
P	1.637	3.233	1.862
C	1.400	6.301	0.634
C	1.266	7.530	0.022
H	0.452	8.177	0.322
C	2.145	8.005	-0.967
H	1.981	8.987	-1.397
C	3.185	7.207	-1.351
C	3.313	5.940	-0.757
C	4.418	5.250	-1.286
C	4.689	3.991	-0.831
H	5.527	3.413	-1.203
C	3.836	3.438	0.142
H	4.058	2.432	0.473
C	2.739	4.088	0.677
C	2.448	5.417	0.231
C	4.288	7.417	-2.349
H	4.906	8.276	-2.075
H	3.888	7.625	-3.345
C	5.100	6.101	-2.320
H	5.100	5.605	-3.294
H	6.148	6.274	-2.059
C	-0.349	7.659	2.538
C	-1.647	8.091	2.302

H	-2.345	7.446	1.779
C	-2.047	9.352	2.728
H	-3.062	9.686	2.541
C	-1.149	10.183	3.380
H	-1.459	11.168	3.708
C	0.151	9.749	3.615
H	0.854	10.394	4.130
C	0.549	8.487	3.204
H	1.560	8.144	3.395
C	2.531	3.589	3.466
H	2.744	4.659	3.358
C	1.606	3.429	4.665
H	2.097	3.799	5.570
H	1.342	2.383	4.841
H	0.680	3.992	4.527
C	3.848	2.857	3.655
H	3.695	1.782	3.781
H	4.354	3.223	4.554
H	4.522	3.007	2.809
C	1.919	1.433	1.507
H	2.985	1.191	1.560
C	1.191	0.591	2.549
H	1.249	-0.466	2.273
H	0.133	0.863	2.607
H	1.623	0.698	3.544
C	1.396	1.115	0.113
H	0.329	1.345	0.040
H	1.523	0.050	-0.102
H	1.914	1.681	-0.663
Compound 3			
Se	3.037	1.402	1.415
Se	5.059	3.617	2.914
P	4.558	1.999	4.201
C	2.805	1.995	4.720
C	2.606	1.893	6.080
C	1.361	2.128	6.680
C	0.321	2.547	5.908
C	0.458	2.644	4.506
C	-0.652	3.065	3.744
C	-0.589	3.118	2.383
C	0.575	2.676	1.740
C	1.672	2.250	2.448
C	1.690	2.292	3.870
C	5.490	2.205	5.752
C	6.130	1.134	6.368
C	6.837	1.331	7.547

C	6.900	2.590	8.121
C	6.256	3.661	7.511
C	5.560	3.471	6.332
C	5.024	0.337	3.661
C	4.283	-0.767	4.068
C	4.691	-2.042	3.706
C	5.837	-2.216	2.944
C	6.579	-1.111	2.544
C	6.176	0.164	2.903
C	2.267	-0.349	1.337
C	1.240	-0.783	2.164
C	0.821	-2.106	2.108
C	1.424	-3.000	1.235
C	2.449	-2.561	0.406
C	2.870	-1.242	0.454
H	3.440	1.659	6.727
H	1.256	2.024	7.753
H	-0.636	2.803	6.349
H	-1.560	3.338	4.271
H	-1.438	3.451	1.797
H	0.600	2.630	0.658
H	6.083	0.144	5.933
H	7.340	0.492	8.015
H	7.452	2.741	9.042
H	6.303	4.649	7.956
H	5.071	4.309	5.847
H	3.384	-0.634	4.657
H	4.105	-2.900	4.014
H	6.150	-3.213	2.657
H	7.474	-1.244	1.947
H	6.743	1.032	2.583
H	0.765	-0.101	2.858
H	0.019	-2.437	2.758
H	1.095	-4.032	1.197
H	2.925	-3.249	0.283
H	3.675	-0.909	0.193
Compound 4			
Se	6.748	1.029	2.650
P	6.116	2.770	3.690
P	3.445	2.012	2.101
C	5.729	4.205	2.620
C	6.311	5.389	3.019
H	6.769	5.461	3.996
C	6.395	6.507	2.175
H	6.850	7.419	2.541
C	5.981	6.394	0.882

H	6.118	7.209	0.179
C	4.929	5.131	-0.914
H	5.152	5.961	-1.576
C	4.254	4.034	-1.366
H	3.946	3.959	-2.402
C	3.879	3.040	-0.451
H	3.227	2.241	-0.786
C	4.256	3.087	0.871
C	5.111	4.131	1.328
C	5.348	5.216	0.431
C	7.536	3.338	4.681
C	7.426	3.612	6.039
H	6.474	3.509	6.544
C	8.542	4.019	6.760
H	8.447	4.223	7.821
C	9.765	4.164	6.128
H	10.634	4.484	6.692
C	9.878	3.896	4.768
H	10.833	4.006	4.268
C	8.772	3.479	4.050
H	8.864	3.253	2.994
C	4.811	2.563	4.925
C	4.691	1.350	5.592
H	5.317	0.514	5.299
C	3.762	1.213	6.610
H	3.665	0.264	7.126
C	2.956	2.287	6.968
H	2.227	2.176	7.762
C	3.081	3.498	6.304
H	2.448	4.336	6.574
C	4.009	3.641	5.284
H	4.097	4.587	4.762
C	1.936	2.980	2.452
C	1.138	2.525	3.503
H	1.424	1.627	4.042
C	-0.009	3.209	3.870
H	-0.621	2.837	4.684
C	-0.361	4.379	3.209
H	-1.252	4.923	3.503
C	0.435	4.851	2.177
H	0.168	5.765	1.658
C	1.574	4.154	1.796
H	2.179	4.530	0.981
C	2.817	0.647	1.067
C	1.470	0.470	0.758
H	0.736	1.187	1.105

C	1.058	-0.618	0.000
H	0.006	-0.741	-0.233
C	1.986	-1.539	-0.465
H	1.663	-2.385	-1.061
C	3.331	-1.369	-0.163
H	4.064	-2.084	-0.521
C	3.742	-0.291	0.603
H	4.793	-0.165	0.845
